THERMODYNAMIC AND ECONOMIC CONSIDERATIONS FOR LOW-TEMPERATURE ELECTROCHEMICAL NITROGEN FIXATION TECHNOLOGIES

A Thesis
Presented to
The Academic Faculty

By

Carlos A. Fernández

In Partial Fulfillment
of the Requirements for the Degree
Master of Science in the
Woodruff School of Mechanical Engineering

Georgia Institute of Technology

August 2020

THERMODYNAMIC AND ECONOMIC CONSIDERATIONS FOR LOW-TEMPERATURE ELECTROCHEMICAL NITROGEN FIXATION TECHNOLOGIES

Approved by:

Dr. Marta C. Hatzell, Advisor
School of Mechanical Engineering
Georgia Institute of Technology

Dr. Peter Loutzenhiser
School of Mechanical Engineering
Georgia Institute of Technology

Dr. Andrew J. Medford
School of Chemical and Biomolecular Engineering
Georgia Institute of Technology

Date Approved: July 16, 2020

El arte de vencer se aprende en las derrotas.

Simón Bolívar

Le dedico esta tesis a mi familia. Su amor y apoyo me motiva a seguir adelante. Gracias por todo.

I dedicate this thesis to my family. Their love and support motivate me to keep going. Thanks for everything.

ACKNOWLEDGEMENTS

Firstly, I would like to express my sincere gratitude to my advisor, Dr. Marta Hatzell, for the continuous support and guidance that she provided me through my Master's study and research. I am very grateful for the motivation and advice that she provided which enabled me to work at my fullest potential. I want to thank her for her guidance and words of encouragement, especially when my experiments were not going as planned, and for guiding me to explore electrochemical modeling.

Secondly, I would like to thank my committee members, Dr. Peter Loutzenhiser and Dr. Andrew Medford, for taking the time to review and evaluate my Master's work.

Thirdly, I would like to thank my colleagues in the WATER Lab who have provided me with support and encouragement in and outside the lab. In particular, I would like to thank my fellow graduate students Carol (Yu-Hsuan) Liu, Yousuf Bootwala, Jeonghoon Lim, and Rodrigo Caceres.

Finally, I would like to thank my family. Even though we are thousands of miles away, their love is always present. Their love keeps me motivated, especially during the tougher moments of graduate school. I would like to especially thank my parents, who have encouraged me to pursue my passions my whole life. I want to thank them for their patience and support. I would also like to thank my sister for being here to support me during my thesis defense and for always being there for me. I hope this thesis helps bring them closer to my work and life at Georgia Tech.

TABLE OF CONTENTS

LIST OF TABLES

LIST OF FIGURES

SUMMARY

State-of-the-art ammonia synthesis plants (Haber-Bosch process) achieve high energy efficiencies and low product cost through the use of high temperature/pressure thermocatalytic process. The process is responsible for feeding half of the global population, but also emits 450 million tons CO_2 per year. Thus, while this process is often deemed effective, there are many environmental concerns regarding the sustainability of the Haber-Bosch process. Furthermore, the scale that these facilities must operate at to achieve these performance metrics, limit the location where a Haber-Bosch plants are built. For instance, there are only around 70 Haber-Bosch plants globally, which are located in 21 countries [1, 2]. Of these countries only 40% are located in countries deemed developing. However, most of the plants in countries deemed developing are located in China, India, and Russia, which are considered developing countries with well established economies. Only 6% of the plants are located in developing countries (excluding China, India, and Russia) [1, 2]. Centralized manufacturing of ammonia indirectly impacts developing countries ability to access fertilizers. With the strong correlation between fertilizer usages and agricultural yield, access to fertilizers is essential to mitigate global hunger. This has motivated a strong interest in rethinking how we manufacture fertilizer-based feedstocks such as ammonia.

Electrochemical manufacturing of ammonia is one approach being explored for ammonia production, as electrochemical systems can operate a relatively low temperature and pressure (near ambient conditions). Additionally, electrochemical technologies can be scaled to various sizes. This may enable manufacturing to occur at a range of scales to meet large and small agricultural demands. However, there are significant challenges associated with electrochemical manufacturing. First, electrocatalyst suffer from poor nitrogen reduction selectivity. This results in systems which have low product yield and low energy efficiency, both of which contribute to high capitol and operational cost. Since cost ultimately will be the primary driver for technology adoption, it is critical to begin

to determine what role system and catalyst design plays in reducing the cost of ammonia to meet Haber-Bosch parity. Here, we perform a theoretical analyses of low-temperature ammonia electrosynthesis. The primary aim of this thesis is to identify the electrochemical system performance targets may enable Haber-Bosch parity, and to assess the feasibility of attaining these targets.

Chapter 1 will provide an introduction and background. In the introduction chapter, I motivate the need for low-temperature electrochemical ammonia synthesis by introducing the challenges with the Haber-Bosch process and the existing nitrogen stress in the developing world. I also introduce the need for comprehensive models that describe the economics of low-temperature ammonia synthesis.

Chapter 2 will provide a literature review. Emphasis is placed on literature which describes the performance and system operation of the Haber-Bosch process, and on literature motivating renewable alternatives for ammonia synthesis.

In Chapter 3, the thermodynamic and kinetic consideration for ammonia electrosynthesis will be compared with thermochemical approaches. We investigate the impact of operational temperature and discuss the trade-off which may exist at high temperatures.

In Chapter 4, we will introduce the system and techno-economic model used throughout the thesis. We introduce the electrochemical equations used to model the reaction inside the electrolysis cell. We also introduce thermodynamic concepts used to evaluate the energy efficiency of the system and economic concepts used to predict the levelized cost of ammonia.

Finally, in Chapter 5, we discuss the techno-economic considerations of low-temperature ammonia electrosynthesis. We also evaluate the viability of low-temperature electrochemical ammonia synthesis through the techno-economic model. We set performance targets and we highlight a pathway for sequential improvement of the technology.

CHAPTER 1
THESIS MOTIVATION AND INTRODUCTION

The continuous and rapid expansion of society has created increasing stress in global resources such as water, nutrients, and minerals. The development of technologies that aid in the industrialized production of these resources has been of growing importance for nearly a century. In modern history, thermocatalytic processes have been a pillar for the centralized production of fuels, chemicals, and fertilizers. The fertilizer industry relies on a thermochemical process, the Haber-Bosch process, to produce around 150 million tons of ammonia per year at an efficiency of up to $70\ \%$ [3]. However, this process utilizes high temperatures (700 K) and pressures (100 bar) to achieve high production rates and designed catalyst to achieve high product selectivity. These elevated operating conditions mean that the Haber-Bosch process is only economically viable on the production scale of thousands of metric tons per day [4]. Furthermore, due to the Haber-Bosch process reliance on fossil fuels, the production of ammonia accounts for 2% of the total global energy consumption and 1.2% of the greenhouse gas emissions worldwide [5, 6]. Growing concerns regarding the environmental impact of the Haber-Bosch process have encouraged the development of alternative technologies for renewable ammonia. The electrochemical production of ammonia from water and air at near ambient conditions using renewable energy is a possible solution to reduce the CO_2 footprint of the fertilizer industry.

According to the Department of Energy (DOE), electrochemical technologies for carbon neutral fuel production have to achieve energy efficiencies higher than 60% while operating at current densities above 300 mA/cm^2 in order to meet viability requirements [7]. These analyses provides general targets for electrochemical fuels. However, a specific techno-economic analysis for electrochemical nitrogen reduction will yield more accurate performance targets. The reported energy efficiencies for low-temperature electrocatalysts

are typically in the order of 0.1% to 10% and the reported current densities do not surpass 10 mA/cm^2 (Fig. 1.1). However, energy efficiencies above 10% have been reported at low current densities or with the aid of highly expensive ionic liquids and non-aqueous electrolytes [8]. Operating at small current densities (< 1 mA/cm^2) minimizes the energy losses in the electrolysis cell. However, operating at these current densities is impractical from an economic point of view as the reactor size and capital cost see an exponential increase with a decrease in the current density [9]. Additionally, even though ionic liquid and non-aqueous electrolytes enhance the reaction selectivity and efficiency, their elevated costs and toxicity might hinder their application at industrial scales [10]. Hence, practical reactor and system design is of extreme importance to advance the electrochemical production of ammonia. There is still a large room for improvement of both the energy efficiency and achievable current density before low-temperature electrochemical ammonia synthesis meets the DOE practicality requirements.

As economic considerations drive technology adoption, a more accurate representation of the practicality of low-temperature electrochemical ammonia synthesis is the levelized cost of the ammonia (LCOA). Furthermore, there is a growing need to connect cost to system properties, such as operating temperature and pressure and catalyst activity and selectivity. These models ultimately may better guide the direction of future research in electrochemical nitrogen fixation and speed the advancement of useful electrochemical technologies.

Herein, we present a techno-economic model to evaluate the feasibility of electrochemical ammonia synthesis technologies. The model integrates electrochemical, thermodynamic, and cost analyses to predict price targets based on the catalyst and system properties. Finally, we outline a path to improve the performance of electrochemical system to reach Haber-Bosch parity.

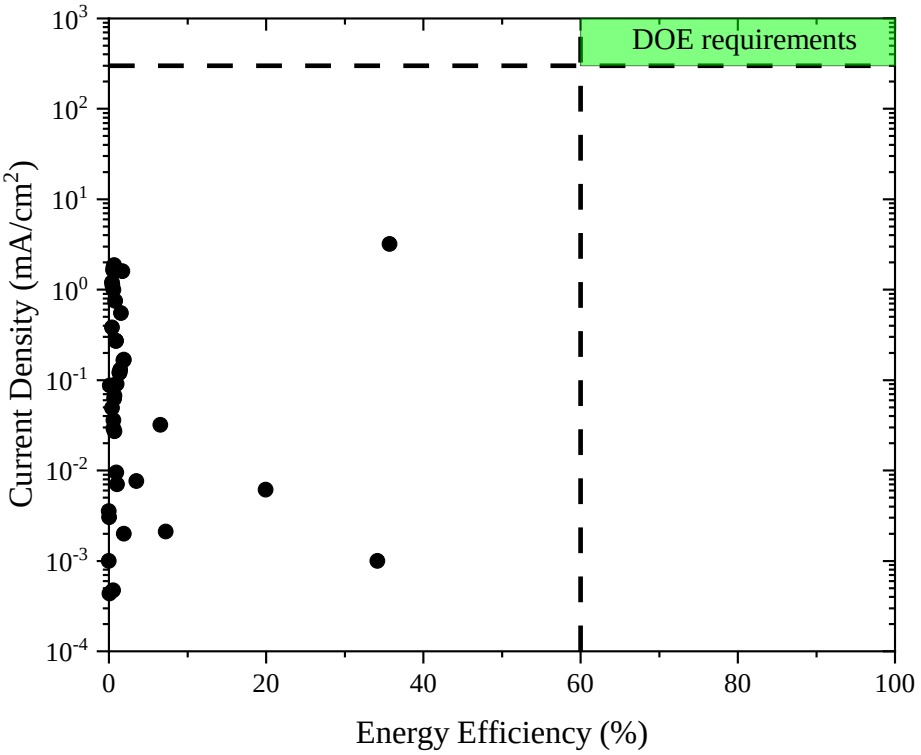

Figure 1.1: Experimental performance of electrochemical ammonia synthesis technologies. Department of Energy targets highlighted in green (data from [8])

CHAPTER 2

BACKGROUND AND LITERATURE REVIEW

2.1 Global Nitrogen Usage

Fixed nitrogen distribution is disproportional, with rich and developed countries having a nitrogen surplus and most developing countries experiencing nitrogen stress or scarcity (Fig. 2.1).

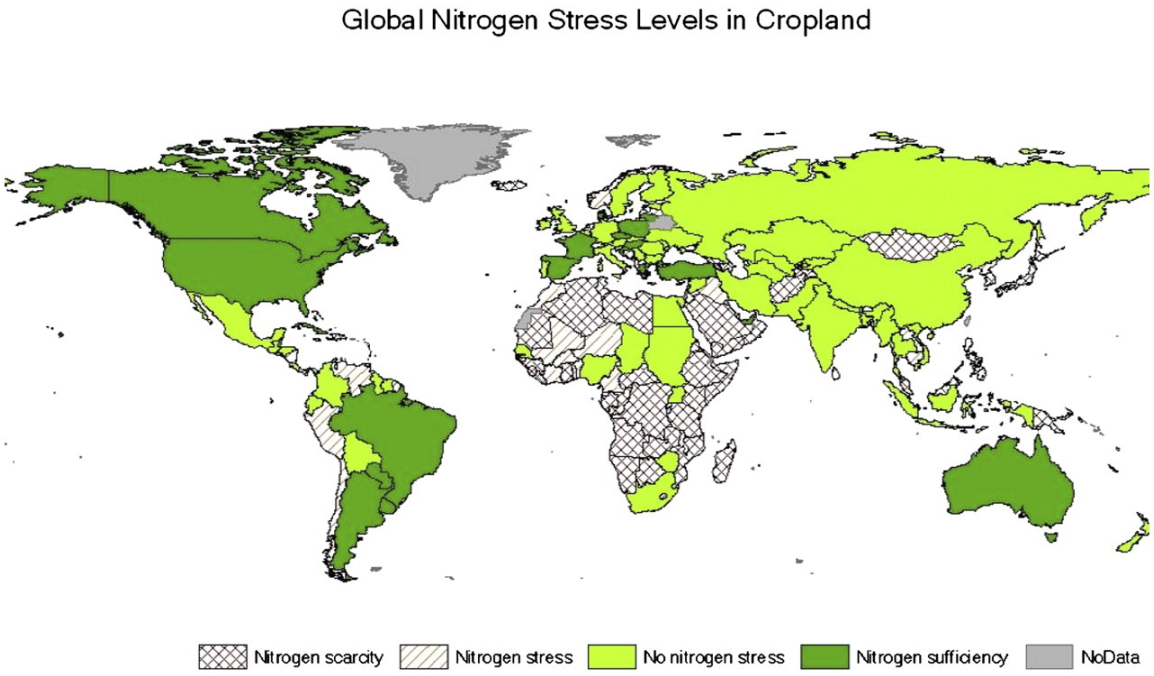

Figure 2.1: Nitrogen stress levels in cropland on national average. [11]

Africa has the lowest nitrogen input of all continents with the per capita nitrogen input at 11 $\frac{Kg}{Capita*year}$, which is 55% times less than the global average. Nitrogen scarcity in Africa correlates with malnutrition rates which are ≈30%. The poor infrastructure in rural areas in Africa largely reduces the ability for nitrogen fertilizers to be transported to these regions. Thus combination of low fertilizer supply and excess transportation and storage costs, results in an increase in fertilizer price[12]. In fact, the farm-gate value of

fertilizers in the Sub-Saharan African region is often two to six times that of the rest of the world [13]. The elevated investment required by farmers to purchase fertilizers and the diminished returns due to the lack of infrastructure to transport their products discourages the farmers in rural areas to purchase and use fertilizers. This has led to a decrease in the use of fertilizers in the last decades [14]. Without the use of nitrogen fertilizers, Africa is not capable of producing enough food to feed Africa's growing population. Additionally, poverty limits Africa's ability to import sufficient food from international suppliers. As a result, Africa has made little to no progress in mitigating the malnutrition problems in the last decades. In fact, malnutrition has been rising in certain regions in Africa despite the global decline of malnutrition rates. A decentralized approach to produce fertilizer might prove advantageous in developing regions to overcome these challenges.

2.2 Current Global Food Nitrogen Supply Chain

Thermochemical ammonia synthesis through the Haber-Bosch process is only economically feasible at large scales, resulting in a centralized scheme for ammonia production. Due to the required capital investment on the order of billions of dollars [15], the production facilities are concentrated in regions with stable access to natural gas, reliable infrastructure, and developed financial systems [1]. Most of the Haber-Bosch plants are located in developed regions (Fig. 2.2). The fertilizer use is highly decentralized, as fewer than 100 Haber-Bosch plants produce fertilizers for 1.55 billion hectares of arable land [16]. The discrepancy between a highly centralized production scheme and highly decentralized use of the fertilizers means that the fertilizer produced in the centralized Haber-Bosch plants (Fig. 2.2 black dots) must be transported and globally dispersed to the agricultural production centers (Fig. 2.2 green dots).

The fertilizer retail cost can be broken down into production, transportation, and storage costs [17]. The production cost of ammonia is low due to the large scales of the Haber-Bosch plants . However, the production cost also depends on the natural gas price, which

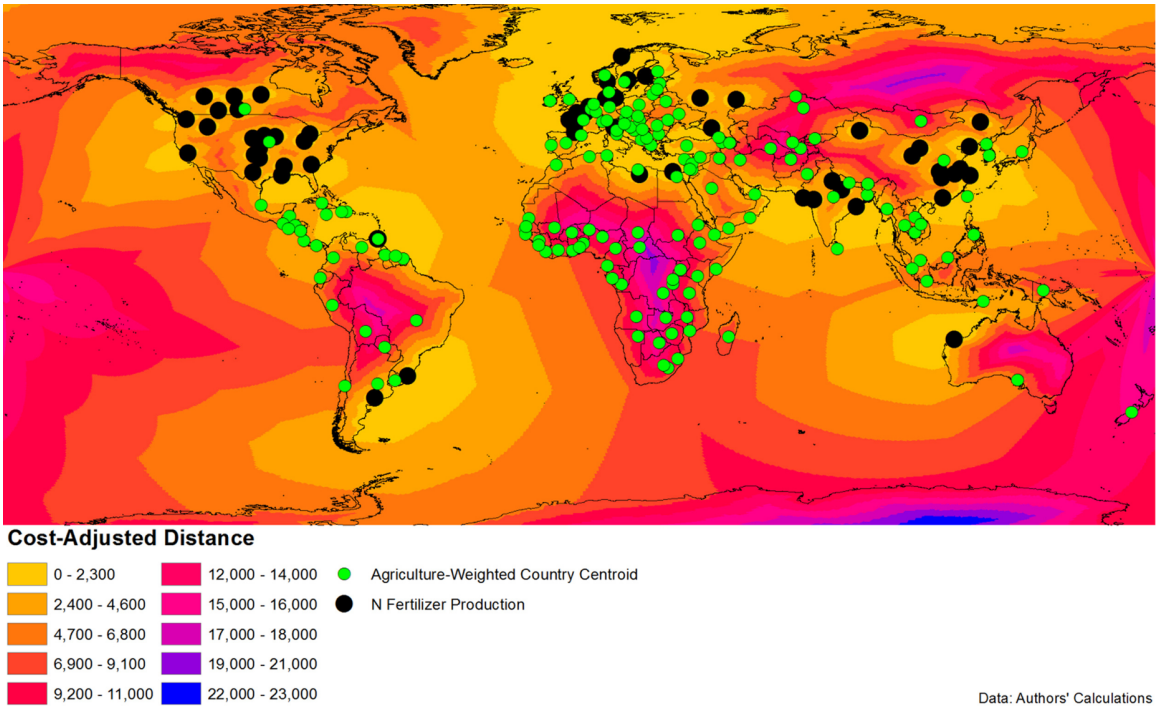

Figure 2.2: Cost-adjusted distance to major fertilizer production sites. [1]

depends on the location of the Haber-Bosch plant [18, 19]. Furthermore, the cost of transportation depends on the location of use, transportation method, and the distance to the nearest production facility [17]. Usually, the transportation method depends on the distance; with barges, pipelines, and trains are used to transport anhydrous ammonia through long distances and trucks can be used for shorter distances [17]. Transportation costs depend on the availability of the transportation infrastructure and transportation to rural areas tends to be harder due to the limited infrastructure. Additionally, roughly 75% of the fertilizer produced is sold in the spring during the planting season [20]. For these reasons, the ammonia must be stored in large refrigerated containers to be able to meet the seasonal demand. Additionally, safely transporting and storing ammonia represents a serious infrastructure challenge due to the dangerous nature of anhydrous ammonia. Evidently, these challenges are intensified in zones with poor infrastructure. Finally, developing countries tend to purchase fertilizers in smaller quantities due to their limited economic power, leading to higher prices when compared to the nation able to purchase higher quantities of

fertilizers at bargain prices [21]. These factors lead to a situation in which fertilizers are significantly more expensive in the poorest regions where they are needed the most. Many of these issues can be mitigated by the decentralized production of fertilizers using renewable resources. Producing fertilizers near the location of use would eliminate transportation and storage costs and make fertilizers more accessible for the regions that need it most.

2.3 Ammonia Synthesis Technologies

Thermochemical approaches for ammonia synthesis (Haber-Bosch) have been used for nearly a century to produce most of the ammonia needed in the world (Fig. 2.3a). However, the Haber-Bosch process uses natural gas as a hydrogen source and emits 1.5 tons of carbon dioxide for every ton of ammonia produced. There are other approaches for the synthesis of ammonia that are scalable and can be integrated with renewable energy. One proposed alternative approach is a thermochemical process integrated with water electrolysis (Fig. 2.3b). This is a hybrid electrochemical-thermochemical synthesis process. Therefore, there are still challenges with scalability, but most carbon emissions can be mitigated through the use of an water instead of methane as the source of hydrogen. A third approach is to directly reduce nitrogen through nitrogen electrolysis (ammonia electrosynthesis – Fig. 2.3c).

2.3.1 Haber-Bosch Process: Current Practice

Current thermochemical approaches for ammonia synthesis (Haber-Bosch process) rely on the use elevated temperature and pressure to drive the chemical reaction. The schematics of the conventional methane-fed Haber-Bosch process is shown in Figure 2.3a. In the first stage of the Haber-Bosch process, the reactants (H_2 and N_2) are purified. High purity hydrogen is produced through reacting steam and methane at high temperature (1,120–1,170 K) and pressure (25-35 atm) on a nickel-based catalyst (primary steam methane reforming process) [23]. High purity nitrogen is produced by separating the oxygen from the air

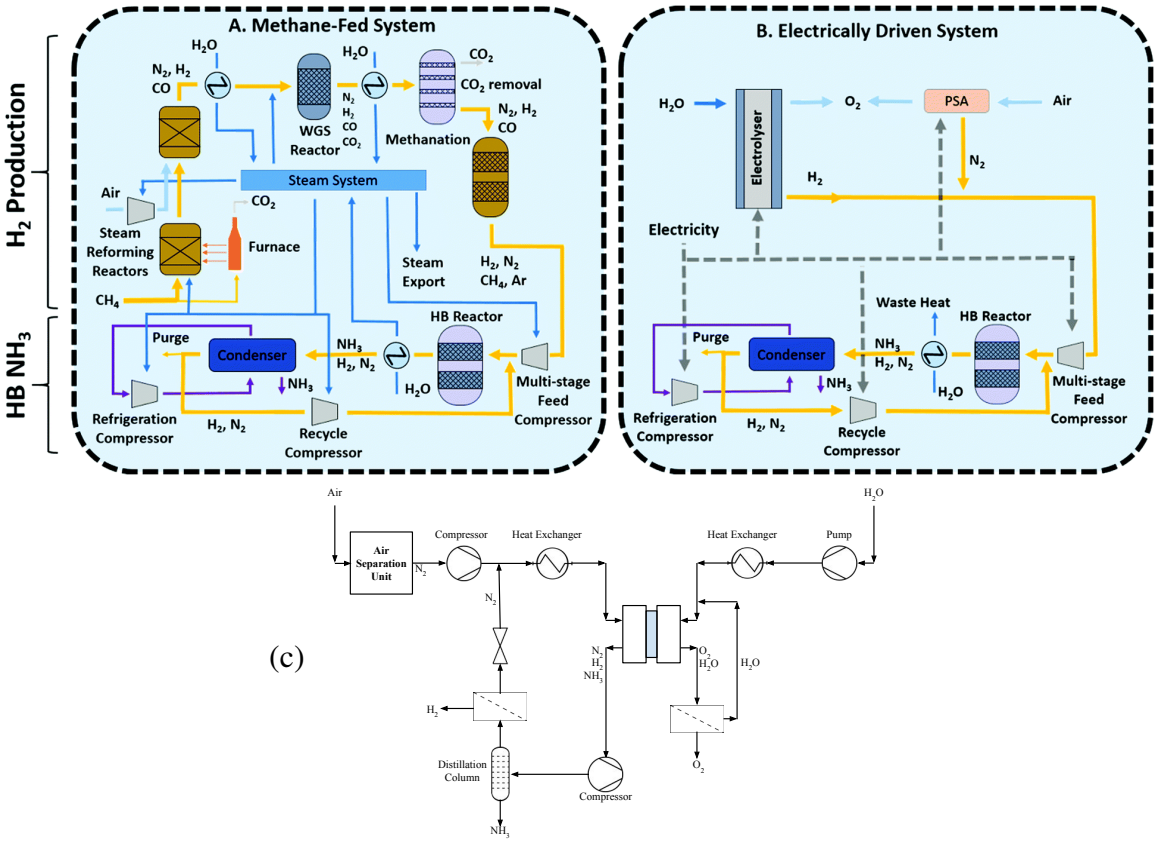

Figure 2.3: Ammonia synthesis using the Haber-Bosch process with natural gas as a hydrogen source (a), and water as a hydrogen source (b) [22]. And direct ammonia electrosynthesis (c).

through a reactive process in the second stage of steam reforming [22]. Oxygen can easily react with methane through a combustion reaction, resulting in the formation of more hydrogen and carbon monoxide. The steam reforming process accounts for 75% of the energy used within the entire Haber-Bosch process [24]. Alternatively, pure nitrogen can be directly supplied, if a cryogenic air separation unit is economically feasible. The cryogenic air separation has a similar energy expenditure to the CO_2 removal in the methane-fed Haber-Bosch process [24]. If cryogenic air separation would be used, it would not require additional energy as it could replace the energy requirements of CO_2 removal. After steam reforming, carbon monoxide is transformed to carbon dioxide through the water-gas shift reaction. The carbon dioxide then is removed through the Benfield or Selexol process, resulting in a pure mixture of the hydrogen and nitrogen [22]. Finally, ammonia is synthe-

sized through reacting nitrogen and hydrogen at high temperature and pressure (723-823 K and 250-350 bar) on an Fe-based catalyst. The elevated temperatures facilitate the kinetics of the reaction. However, an increase in temperature also favors the backwards reaction of decomposition of ammonia to nitrogen and hydrogen. For this reason, if the temperatures are increased, the pressure of the system also has to be increased to shift the reaction towards the forward path of ammonia synthesis from hydrogen and nitrogen [25]. Ammonia is separated from reactants (H_2 and N_2) by compressing and cooling the products. This allows for liquefied ammonia to be easily separated from gaseous nitrogen and hydrogen which are recycled.

The Haber-Bosch process emits 1.5 to 1.6 tons of carbon dioxide for every ton of ammonia that is produced (Fig. 2.4) [26]. Around 76% (1.22 t_{CO2}/t_{NH3}) of the CO_2 emitted by the process is associated with the steam methane reforming (SMR) reaction [22]. Hence, the minimum CO_2 emissions possible through a methane-fed Haber-Bosch process are 1.22 t_{CO2}/t_{NH3}. The remaining 24% of the CO_2 emitted is used to raise the temperatures in the catalyst bed and to provide power to the turbines. All these sum up to 1.6 t_{CO2}/t_{NH3}. However, if we add the emissions associated to the extraction and transportation of the methane, the total emissions of the Haber-Bosch process increase to 1.7 t_{CO2}/t_{NH3}.

Energy Requirements of the Haber-Bosch Process

The Haber-Bosch process has been refined over the last century to make it as efficient as possible. There are several alternative hydrogen sources that can be used to fuel the Haber-Bosch process (natural gas, coal). However, most of the plants use natural gas as a hydrogen source as it leads to lower energy consumption and higher efficiencies.

Most of the energy required to synthesize ammonia through the Haber-Bosch process comes from natural gas. Hence, the largest energy expenditure is due to steam methane reforming (Fig. 2.5). Usually, a Haber-Bosch plant produces more steam that it consumes. However, the additional steam output can be used to feed other facilities nearby, such as

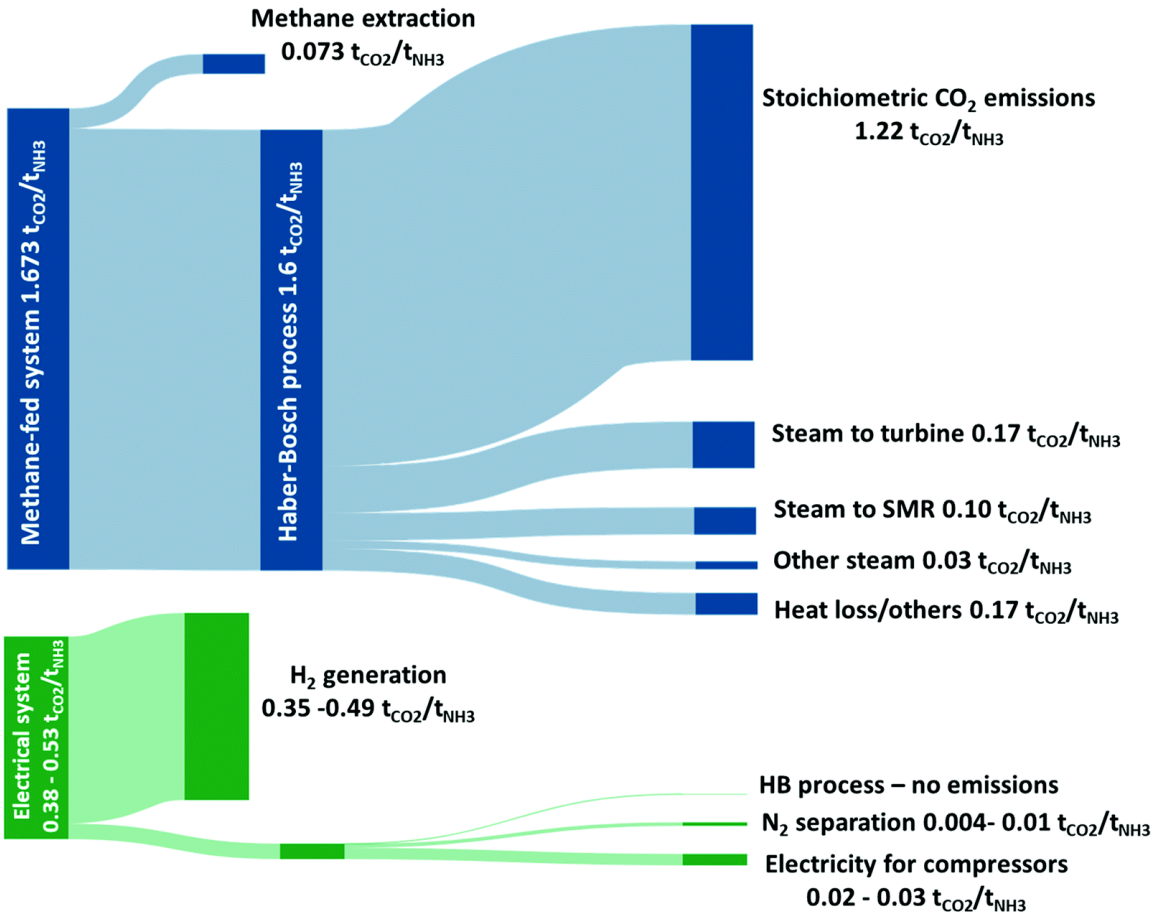

Figure 2.4: Direct CO_2 emissions from the methane-fed and the electrically driven Haber–Bosch processes. [22]

urea plants or other facilities. Hence, this output steam can be counted as work produced by the system.

A Haber-Bosch plant produces ammonia which has a chemical energy (LHV) of 318 kJ/mol. However, the total energy consumption of a Haber-Bosch plant is much higher 542 kJ/mol [27]. Most of the energy comes from burning natural gas and some electric energy is required to operate pumps and compressors (Table. 2.1)[27]. However, depending on the size and specific system requirements, the energy consumption values for a Haber-Bosch facility can vary between 540 kJ/mol to 800 kJ/mol [28, 29, 30]. Hence the Haber-Bosch process typically operates at energy efficiencies between 40% and 60%, with most methane-fed systems operating close to 60% (Fig. 2.5) .

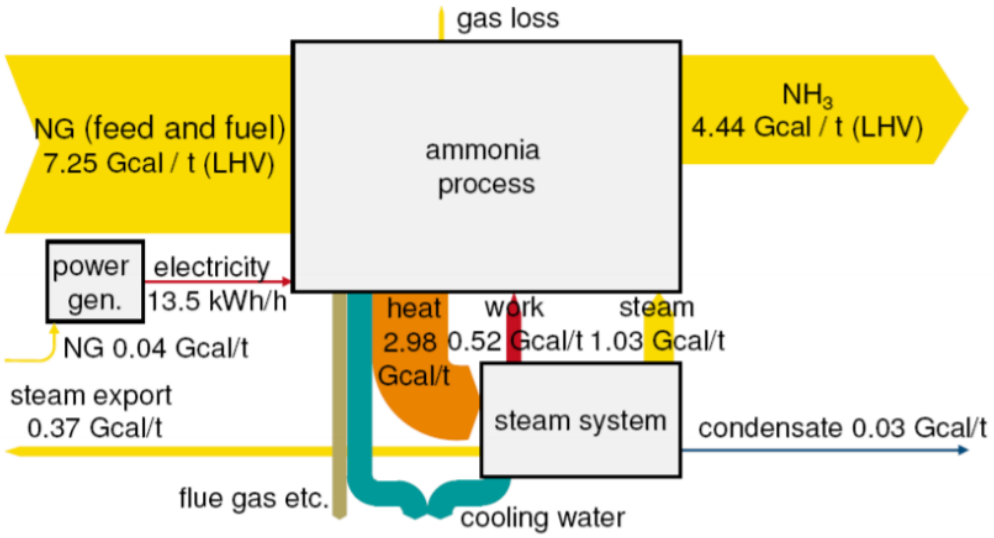

Figure 2.5: Net energy consumption of a Haber-Bosch ammonia plant based on natural gas reforming. [27]

Table 2.1: Net energy consumption of a Haber-Bosch ammonia plant based on natural gas reforming. [27]

Component	Energy (kJ/mol$_{NH3}$)
Natural Gas Feed	568.55
Electricity	3.06
Steam Export	-28.76
Total	542.84

Economics of the Haber-Bosch Process

As mentioned in the previous chapter, the fertilizer industry has taken advantage of the economies of scale by building massive Haber-Bosch facilities to minimize the price of the produced fertilizer. However, the cost of the Haber-Bosch process does not scale down, making the Haber-Bosch process not practical for small-scale fertilizer production. The levelized cost of ammonia produced by a Haber-Bosch plant with a capacity of 2000 tons per day is 170 dollars per ton of ammonia produced [4]. Fifty five percent of the cost is due to Natural Gas, 32% of the cost is attributed to capital expenditures, and 13% is attributed to plant operation and maintenance costs [4]. Additionally, the Haber-Bosch process has an

economy of scale sizing exponent (x) of 0.65[31]. Thus, the capital and operational costs of Haber-Bosch facilities as a function of production volume is:

$$C_B = C_A * (\frac{S_B}{S_A})^x \tag{2.1}$$

where C_A is the cost of the base case facility, C_B is the cost of a facility of arbitrary size, S_A is the size of a base case facility, S_B is the desired size of the facility of study, and x is the sizing exponent (0.65). In this case we used the values of C_A of \$170/ton and S_A of 2000 ton/day. Accordingly, we can calculate the levelized cost of ammonia produced by Haber-Bosch facilities at different production capacities (Fig. 2.6). We find that the price of the ammonia produced by the Haber-Bosch process increases significantly as the plant size decreases.

A facility with an output of 2,000 tons/day can produce fertilizer for up to 6 million hectares of arable land (which is equivalent to 77 times the size of New York City). This facility is able to produce fertilizers at a cost of \$170/ton due to the economies of scale. However, a plant which outputs 10 tons/day and produces fertilizer for 30,000 hectares (250 family farms) cost \$600/ton (which is the average selling price for ammonia for fertilizers). If the plant was further scaled down to 0.027 tons/day, producing fertilizers for a small 100 hectare farm, the production prices would see a significant increase due to the small scale of the plant, with ammonia prices nearing \$4,000/ton. This analysis shows how the Haber-Bosch process is only viable at very larger scales. Hence, alternative technologies should be developed in order to achieve truly decentralized fertilizer production.

2.3.2 Haber-Bosch Coupled with Electrochemical Hydrogen Production

Replacing steam reforming with water splitting reduces carbon emission by 1.2 t_{CO2}/t_{NH3} (Fig. 2.4). In this modified Haber-Bosch process, the initial reactant is air and water (Fig. 2.3). Water is supplied to the electrolysis cell and split into hydrogen and oxygen. The nitrogen is separated from air through cryogenic separations, adsorbers, or membranes.

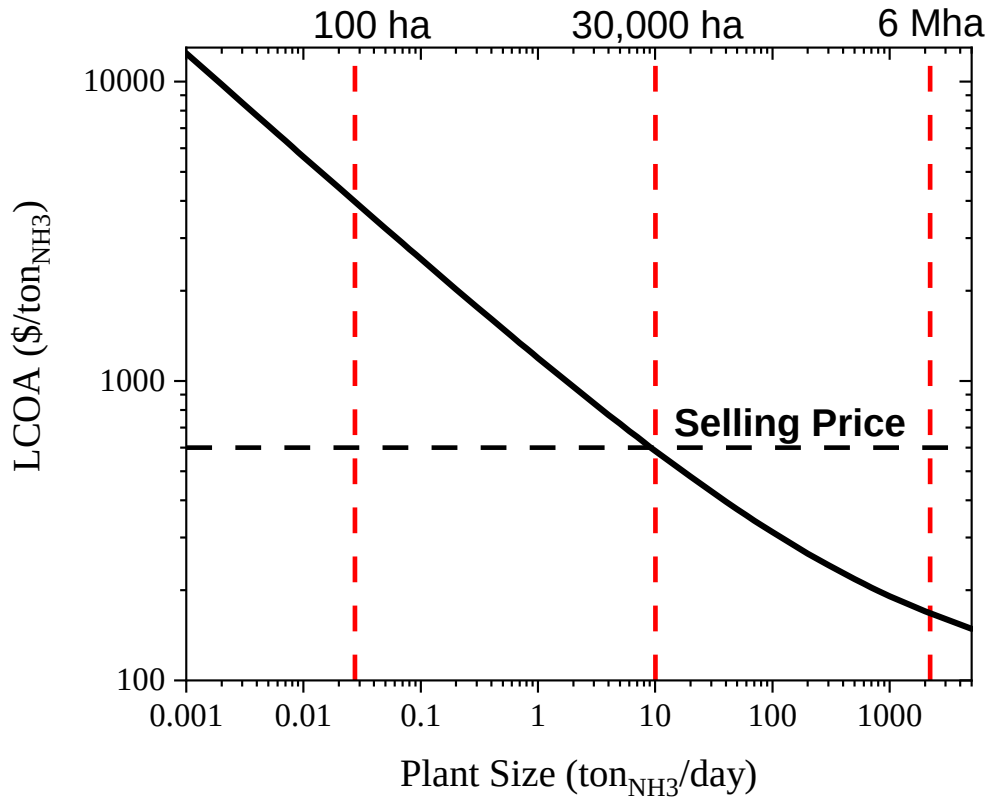

Figure 2.6: Levelized cost of ammonia produced by the Haber-Bosch process at different plant size (tons/day). The black dotted horizontal line indicates the standard LCOA of ammonia. The vertical red dotted lines indicate the plant size needed to meet demands at various farm size in hectares (ha).

The oxygen is often discarded, and the nitrogen and hydrogen are transferred into a closed reactor (Haber-Bosch process). The ammonia is then distilled from the outflow stream and the nitrogen and oxygen are recycled. The primary difference between this approach and the traditional Haber-Bosch process is the hydrogen source.

Energy Requirements of the Haber-Bosch Process Coupled with Electrochemical Hydrogen Production

A Haber-Bosch plant coupled with water electrolysis produces ammonia which has a chemical energy (LHV) of 318 kJ/mol. The energy efficiency of water electrolysis can approach 70% [32], whereas steam methane reforming has an energy efficiency of 65%. Thus, using

water electrolysis in place of steam reforming reduces the theoretical operational energy expenditure of hydrogen production by 4.36 kWh/kg$_H$2 (from 61.05 kWh/kg$_H$2 to 56.69 kWh/kg$_H$2). This energy savings corresponds to savings equivalent to 16 kJ/mol$_{NH3}$. Hence, the energy efficiency of the Haber-Bosch process coupled with electrochemical hydrogen production is 60.4%, which is marginally more efficient than the methane-fed Haber-Bosch process.

Economics of the Haber-Bosch Process Coupled with Electrochemical Hydrogen Production

The cost of the Haber-Bosch process coupled with electrochemical hydrogen production is highly dependent on the capital cost of the electrolysis cell and the cost of electricity. With the current electric prices (0.0612 $/kWh) the Haber-Bosch process coupled with electrochemical hydrogen production cannot produce ammonia under the market value of 600 $/ton [33]. Hence, with current electricity prices, this technology would not be economically feasible. However, if the electricity price decreases to the 2030 target (0.03 $/kWh [33]) the Haber-Bosch process coupled with water electrolysis achieves costs of ammonia under today's market price. The market price of $600/ton is achieved at production rates higher than 60 tons/day, which is equivalent to producing fertilizer for an arable area of approximately 180,000 hectares (Fig. 2.7). Thus, the benefit of coupling the Haber-Bosch process with a water electrolysis cell is primarily in the decarbonization of hydrogen production. Since the Haber-process for ammonia synthesis is still used, there will still be challenges with scaling this technology to lower production values. Hence, this could be a viable approach to attain large scale renewable ammonia but may not be feasible for small-scale or farm-scale ammonia production.

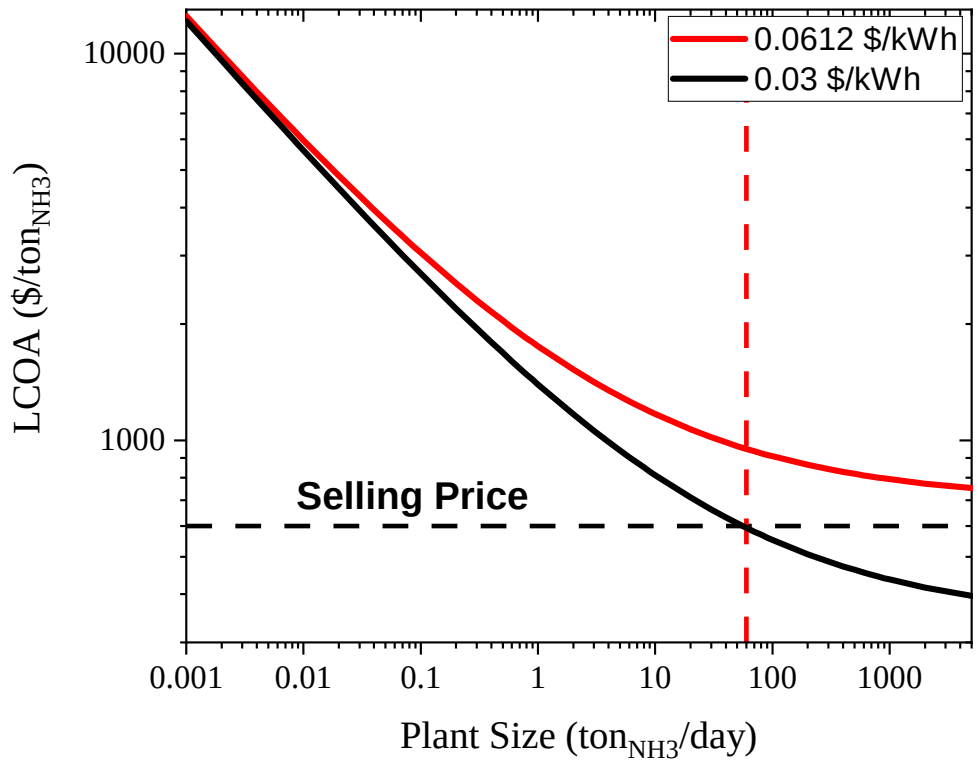

Figure 2.7: Levelized cost of ammonia produced by the Haber-Bosch process coupled with water electrolysis at different plant sizes. The red line represents the costs for an electricity price of $0.0612/kWh and the black line for an electricity price of $0.03/kWh.

2.3.3 Direct Electrochemical Ammonia Production

Direct electrochemical ammonia synthesis is third alternative to the traditional Haber-Bosch process. Direct electrochemical conversion methods transform electrical energy into chemical energy, using primarily voltage as the driving force for catalysis. Electrochemical ammonia synthesis can operate at small scales and can be operated at any temperature with renewable energy resources. The direct electrochemical conversion of nitrogen to ammonia consists of one electrolysis cell in which water enters the anode and is split into protons and oxygen. Then, the protons travel through the electrolyte and combine in the cathode to produce ammonia and hydrogen (as a biproduct). A system for the direct electrochemical conversion of nitrogen to ammonia would require additional components for air separation,

compression and heating of the reactants, and separation of the products. By coupling a system for the electrochemical conversion of nitrogen to ammonia with a renewable energy source, it is possible to nearly eliminate the carbon dioxide emissions. For example, if wind energy is used (which emits 11.2 gCO2-eq/kWh) to run an electrochemical system with an energy efficiency of 60%, the total carbon emission can theoretically be reduced to around 0.1 t_{CO2}/t_{NH3}.

Energy Requirements of Electrochemical Ammonia Production

The maximum energy efficiency reported for direct low-temperature electrochemical conversion of nitrogen to ammonia (LHV=318 kJ/mol) is ≈30% [8]. This value is high due to the low operating current density ($10^{-3} mA/cm^2$), which is 5 orders of magnitude smaller than the current density target of 300 mA/cm^2 This equates to an energy requirement of 1,060 kJ/mol_{NH3}. In reality, most systems have energy efficiencies around 1%. This excess energy required for low temperature electrochemical systems is one reason preventing the technology from being used. Further improvements in the energy efficiency are needed to make the electrochemical production of ammonia feasible. The low energy efficiency is primary due to the high electrochemical overpotential for nitrogen reduction. Therefore efforts aimed at reducing this system loss may enable more reasonable system energy efficiency.

Economics of Electrochemical Ammonia Production

The cost of electrochemical ammonia production is highly dependent on the capital cost of the electrolysis cell and the cost of electricity. With current electricity prices (0.0612 $/kWh [33]) and the best energy efficiency achieved in a lab scale system at low temperatures (30% [8]), the minimum levelized cost of ammonia (LCOA) would be close to 1000 $/ton. In order to decrease the price, the levelized cost of electricity needs to decrease or the energy efficiency of the system needs to increase. For example, at an energy efficiency of

30%, and electricity price around 0.037 $/kWh the LCOA would be 600 $/ton. If energy efficiency approaches 50%, and the electricity price is maintained at 0.0612 $/kWh the LCOA would be 600$/ton (approaching State of Art). Since electricity prices are projected to decrease over the next few decades, the electrochemical production of ammonia at low temperature may be a viable long-term option to produce renewable ammonia at small scales necessary for decentralized fertilizer production.

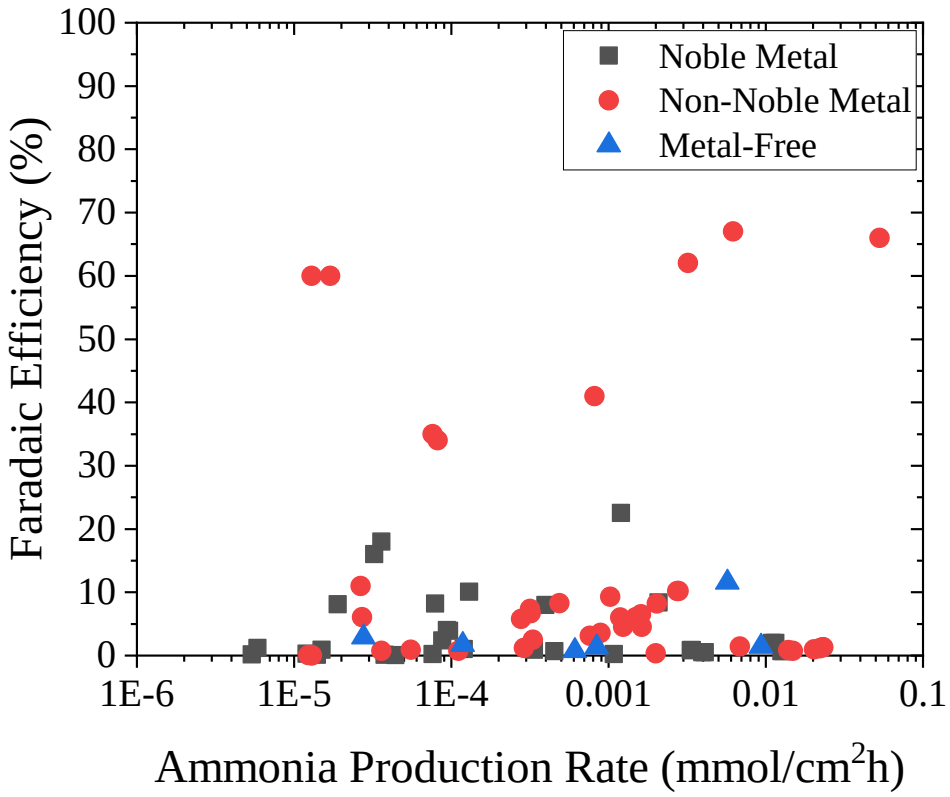

Figure 2.8: Performance Maps of the low-temperature electrochemical nitrogen reduction separated by the catalyst's chemical composition.

2.3.4 Electrocatalysts for Low-Temperature Nitrogen Reduction to Ammonia

The electrocatalysts that have been developed can be split into three categories: (a) noble metal, (b) non-noble metal, and (c) metal-free catalysts. Each catalyst has a variable activity and selectivity for nitrogen reduction depending on the catalyst binding strength associated

Table 2.2: Low temperature ammonia electrosynthesis performance using noble metal-based catalysts.

Catalyst	Electrolyte	Production Rate ($mmol*cm^{-2}h^{-1}$)	FE (%)	T (^oC)	Ref.
Ru/Ti	0.05M KOH	4.30E-04	-	30	[34]
Rh/Ti	0.05M KOH	5.40E-05	-	30	[34]
Ru	2M KOH	1.50E-05	0.92	90	[35]
Ru	2M KOH	7.60E-05	0.24	90	[35]
Ru	2M KOH	1.20E-05	0.28	25	[35]
AuNR/Cp	0.1M KOH	9.70E-05	3.9	25	[36]
Au/CeO_2-rGO/CP	0.1M HCl	1.30E-04	10.1	20	[37]
Au-TiO_2/Cp	0.1M HCl	1.90E-05	8.1	20	[38]
Au	0.1M KOH	1.40E-05	0.12	20	[39]
Ag-Au@ZIF	0.2M $LiCF_3SO_3$ + THF	3.60E-05	18	20	[40]
PtNC/CB/GC	K_2SO_4	1.20E-04	1	25	[41]
AuNC/CB/GC	K_2SO_4	1.20E-03	22.5	25	[41]
Ru	2M KOH	3.36E-04	0.92	20	[42]
Pt	Nafion	1.15E-02	2	25	[43]
Pt	Nafion	1.26E-02	0.7	25	[43]
Pt	Nafion	3.96E-03	0.52	25	[43]
Ag	0.2M $LiClO_4$ + EtOH + THF	2.09E-03	8.4	25	[44]
Pd/C	0.05M H_2SO_4	4.40E-05	0.042	25	[45]
Pd/C	0.1M PBS	8.76E-05	2.35	25	[45]
Pd/C	0.1M PBS	7.90E-05	8.2	20	[45]
Pd/C	0.1M NaOH	3.77E-05	0.087	25	[45]
Au/C	0.1M PBS	5.85E-06	1.178	25	[45]
Pt/C	0.1M PBS	5.39E-06	0.189	25	[45]
Rh	0.1M KOH	4.54E-04	0.7	25	[46]
Pt	Nafion	1.08E-03	0.2	40	[47]
Pt	Nafion	3.35E-03	0.85	80	[47]
Pt	Li_2SO_4	3.37E-03	0.83	80	[47]

GC = glassy carbon; CP = carbon paper; CB = carbon black; NR = Nanorod

with nitrogen, hydrogen and water. In addition, each catalyst varies in its environmental abundance and cost. Noble metals are efficient catalysts for a wide variety of reactions, including nitrogen reduction. Gold (Au), Ruthenium (Ru), Platinum (Pt), and Rhodium (Rh) have all been investigated. The current performance of noble metal catalysts is shows in Table 2.2.

In general, noble metal catalysts have high activity. This high activity extends to other competing side reactions such as hydrogen evolution reaction. Thus, high activity noble metal catalysts suffer from low faradaic efficiencies (low selectivity). This tradeoff be-

tween activity and selectivity is challenging, and it is desirable to produce a certain yield (production rate) of product, but ultimately, high selectivity is required to efficiently utilize renewable electrons. The best faradaic efficiency for noble metal catalysts was achieved by Gold nanocubes on carbon black on a K_2SO_4 electrolyte [41]. The K_2SO_4 ions enhance the nitrogen reduction reaction and suppress the hydrogen evolution reaction, allowing for higher faradaic efficiencies. The highest production rate, however, was achieved by platinum catalysts with a Nafion electrolyte or by Platinum in liquid electrolytes at 80^oC. The higher temperatures improve the kinetics of the reaction. The production rate and faradaic efficiencies for most noble metal catalysts are still too low for practical applications. Furthermore the cost of noble metals tends to be 30,000 $/Kg which is prohibitively expensive.

Non-noble metals are an attractive alternative to noble metals due to their low cost and relative abundance. Particularly, catalysts based on transition metals have been widely studied as electrocatalysts for the nitrogen reduction reaction (Table 2.3). In general, the performance of non-noble metal catalysts is similar to noble metal catalyst. The best selectivity however has been achieved with non-noble metal catalysts, largely due to the catalyst ability to suppress the hydrogen evolution reaction. The best faradaic efficiency was achieved by Bismuth nanoparticles in a K_2SO_4 electrolyte [41]. The Bismuth nanoparticles in a K_2SO_4 electrolyte achieve faradaic efficiencies of 67%. Bismuth exhibits high activity for electrochemical nitrogen reduction due to the strong interaction between the 6p band in Bismuth atoms and the 2p orbitals of nitrogen. Additionally, potassium ions in the electrolyte stabilize the reaction intermediates and increase the nitrogen selectivity. Optimizing both the catalyst and surface and the catalyst-electrolyte interface is necessary in order to improve the electrocatalytic reduction of nitrogen to ammonia. The cost of non-noble metal catalyst varies greatly but tends to be less cost prohibitive ranging from 0.1-500 $/Kg.

Most of the catalyst found in literature are either noble metal or non-noble metal-based catalyst. Recently, there has been an increased interest on developing metal-free catalysts with high selectivity towards nitrogen (Table 2.4). In general, the performance of a metal-

Table 2.3: Low temperature ammonia electrosynthesis performance using non-noble metal-based and non-metal catalysts.

Catalyst	Electrolyte	Production Rate ($mmol*cm^{-2}h^{-1}$)	FE (%)	T (^oC)	Ref.
Fe NPs on CNTs	0.1M $KHCO_3$	1.23E-05	0.03	20	[42]
ZnS	1M KOH	2.04E-02	0.964	25	[48]
NiS	1M KOH	1.39E-02	0.849	25	[48]
CdS	1M KOH	1.49E-02	0.741	25	[48]
ZnSe	1M KOH	2.32E-02	1.293	25	[48]
TiB_2	1M KOH	2.20E-02	1.11	25	[48]
Mo	0.2M $LiClO_4$ + EtOH + THF	7.63E-04	3.1	25	[44]
Ti	0.2M $LiClO_4$ + EtOH + THF	2.03E-03	8.2	25	[44]
Fe	0.2M $LiClO_4$ + EtOH + THF	1.48E-03	6	25	[44]
Ni	0.2M $LiClO_4$ + EtOH + THF	1.61E-03	6.5	25	[44]
Co	0.2M $LiClO_4$ + EtOH + THF	1.53E-03	6.1	25	[44]
Zn	0.2M $LiClO_4$ + MeOH + THF	1.24E-03	4.5	25	[44]
Fe/FTO	[P6,6,6,14][eFAP]	1.30E-05	60	25	[49]
Stainless Steel	SS-[C2-mpyr]	7.63E-05	35	25	[49]
Mo	0.01M H_2SO_4	3.60E-05	0.72	25	[50]
Fe-MOF	2M KOH	6.84E-03	1.4	80	[51]
$Bi_4V_2O_{11}/CeO_2$	HCL	2.80E-03	10.16	20	[52]
Fe-phtnalocyanine	1M KOH	2.00E-03	0.34	25	[53]
BiNPs/CB/GC	K_2SO_4	8.17E-04	41	25	[41]
BiNPs/CB/GC	K_2SO_4	3.20E-03	62	25	[41]
BiNPs/CB/GC	K_2SO_4	6.20E-03	67	25	[41]
BiNPs/CB/CP	K_2SO_4	5.30E-02	66	25	[41]
MoS_2/CC	0.1M Na_2SO_4	2.91E-04	1.17	25	[54]
Mo NF	0.5M H_2SO_4	1.11E-04	0.72	25	[55]
Mo_2N	0.1M HCl	1.63E-03	4.5	25	[56]
Fe_2O_3/CNTs	0.5M $LiClO_4$	1.29E-05	0.035	20	[42]
Fe/Fe_3O_4	0.1M PBS	4.88E-04	8.29	20	[57]
o-Fe_2O_3-Ar	0.1M KOH	2.71E-05	6.04	25	[58]
α-Fe@Fe_3O_4	1mM H_2SO_4	2.65E-05	11	20	[59]
VN/CC	0.1M HCl	8.93E-04	3.58	25	[60]
VN NPs	0.05M H_2SO_4	1.19E-03	6	25	[61]
$Bi_4V_2O_{11}/CeO_2$	HCl	2.73E-03	10.16	20	[52]
TiO_2/Ti	0.1M Na_2SO_4	3.30E-04	2.5	25	[62]
Ti_3C_2TxMxene	0.1M Na_2SO_4	2.78E-04	5.78	25	[63]
Nb_2O_5	0.1M HCl	1.03E-03	9.26	25	[64]
CoP HNC	0.1M KOH	3.17E-04	7.36	25	[65]
$CrO_{0.66}N_{0.56}$	1mM H_2SO_4	3.21E-04	6.7	20	[66]
Porous Ni	2-Propanol/H_2SO_4	5.54E-05	0.89	20	[67]

free catalyst is fairly poor. However, the best performance was achieved by using carbon nanospikes on a $LiClO_4$ electrolyte. The carbon nanospikes achieved a maximum faradaic efficiency of 11.56%. The electric field concentrates at the tip of the carbon nanospikes, promoting the electroreduction of nitrogen to ammonia near the electrode. Additionally, the choice of $LiClO_4$ as an electrolyte also helps in enhancing the nitrogen reduction reaction. However, more research is needed in developing metal-free catalysts with high activity and selectivity.

2.3.5 Electrolytes for Low-Temperature Nitrogen Reduction to Ammonia

The performance of a system for nitrogen reduction also depends on the electrolyte selection. An electrolyte can help improve the selectivity of the reaction by limiting proton transfer and improving nitrogen availability near the catalyst surface. Currently, electrolytes for low-temperature nitrogen fixation can be divided into aqueous electrolytes (Liquid electrolyte), non-aqueous (Liquid electrolyte), solid polymer electrolytes (Solid electrolyte), and ionic liquid electrolyte. When moving to higher temperatures, ceramic solid electrolytes are also used. A performance map of the current research separated by the electrolyte type is shown is Figure 2.9.

Table 2.4: Low temperature ammonia electrosynthesis performance using metal-free catalysts.

Catalyst	Electrolyte	Production Rate ($mmol*cm^{-2}h^{-1}$)	FE (%)	T (^oC)	Ref.
PEBCD	0.5M Li_2SO_4	1.18E-04	1.71	25	[68]
PEBCD	0.5M Li_2SO_4	2.76E-05	2.91	25	[68]
N-Carbon	0.05M H_2SO_4	8.40E-04	1.3	25	[69]
N-Carbon	0.05M H_2SO_4	6.10E-04	0.75	25	[69]
N-Carbon	0.05M H_2SO_4	9.36E-03	1.4	25	[69]
Carbon nanospikes	0.25M $LiClO_4$	5.7E-03	11.56	25	[70]

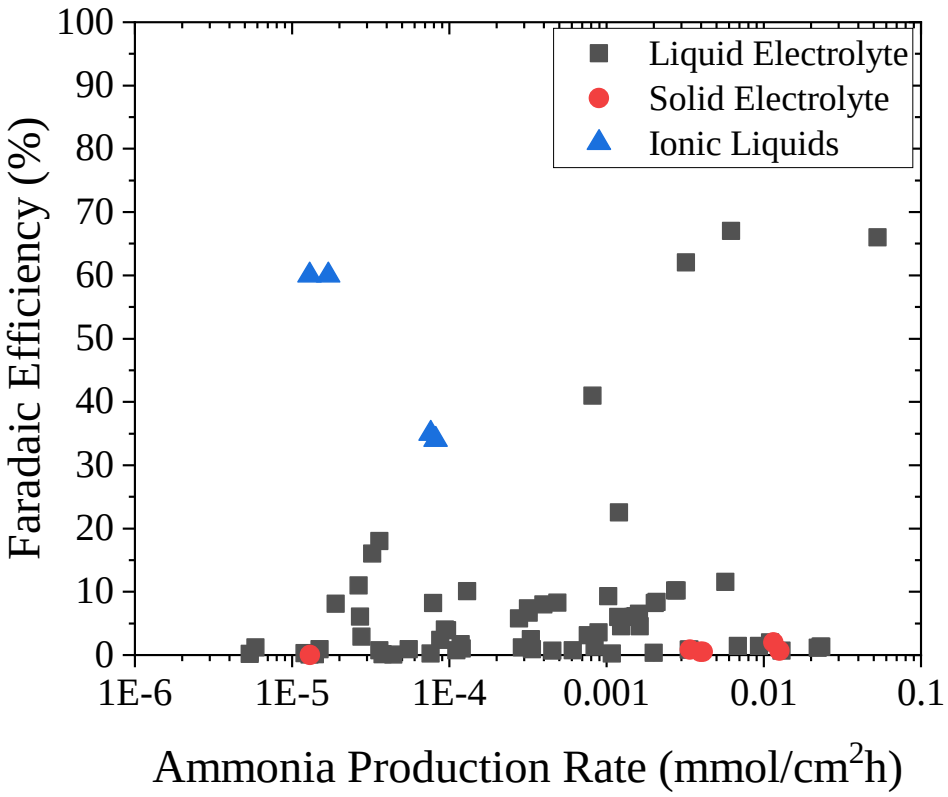

Figure 2.9: Performance Maps of the low-temperature electrochemical nitrogen reduction separated by the type of electrolyte used.

Aqueous Electrolytes

Aqueous electrolytes are heavily investigated due to ease of use, low cost, and often times sustainability (green electrolytes). Generally, aqueous-based liquid electrolytes are non-flammable and comprised of salt-based monotonic. Occasionally, organic solvents are added to the aqueous electrolytes to increase the solubility of nitrogen and to mitigate the concentration of water. Minimizing the water concentration aids in suppress the hydrogen evolution reaction. The best performance achieved by a reactor using a liquid electrolyte was achieved by a reactor using K_2SO_4, in which the potassium ions enhance the nitrogen reduction reaction and inhibit the hydrogen evolution reaction. In some cases, non-aqueous electrolytes have been investigated. This allows for a complete suppression of hydrogen

evolution. Yet non-aqueous electrolytes are often flammable creating safety concerns.

Solid Polymer Electrolytes

The most common solid electrolyte for the low-temperature electrochemical nitrogen reduction is Nafion. This is primarily due to Nafion having the highest reported proton conductivity. Nafion however was developed for hydrogen fuel cells, and thus there are several challenges with the use of Nafion in ammonia synthesis cells. For instance, ammonia can react with the Nafion membrane, affecting the membrane's proton conductivity and decreasing the cell's performance and stability. Additionally, the water content in solid polymer electrolytes cannot be easily controlled. By reducing the hydration sphere around the nitrogen molecules, the hydrogen reduction reaction can be inhibited, and the nitrogen reduction reaction can be enhanced. A final challenge is that ammonia easily can perform an ion exchange process with protons in the membrane. This ammonia storage within the membrane can result in contamination effects. There have been little investigations on what other polymer solid electrolytes may be more ideal for electrochemical nitrogen reduction, and may be an important area as systems develop.

Ionic Liquid Electrolytes

Ionic liquids exhibit considerably higher solubility for nitrogen than aqueous electrolytes. Additionally, ionic liquids have a hydrophobic nature, which inhibit the hydrogen evolution reaction in the electrode. Common ionic liquids used for the electrochemical nitrogen reduction reaction are [C4mpyr][eFAP] and [P6,6,6,14][eFAP]. Additionally, DFT calculations show that ionic liquids allow for nitrogen accumulation at the cathode and improve performance. While there has been significant promise in this area, the potential cost of ionic liquid remains on challenge. The cost of ionic liquid may be 2-100 times more than other electrolytes [71].

CHAPTER 3
THERMODYNAMIC AND KINETIC CONSIDERATIONS FOR AMMONIA ELECTROSYNTHESIS

In theory, if a large enough overpotential is applied to an electrochemical cell, thermodynamics predicts that an electrochemical reactor can achieve a similar reactant conversion to a thermocatalytic (Haber-Bosch) reactor driven at elevated temperatures and pressures (Fig. 3.1) [72]. In reality electrochemical systems have exibited significantly lower performance (production rate, product selectivity, energy efficiency), as thermodynamics alone cannot determine system performance. Here, we briefly outline some of the prospects and challenges associated with the thermodynamics and kinetics of electrochemical ammonia synthesis.

3.1 Thermodynamic Considerations for Ambient Temperature and Pressure Ammonia Synthesis

The equilibrium conversion (X) of a reaction corresponds to the fraction of the reactants (N_2 and H_2 or H_2O) that are transformed into desired products (NH_3). A conversion equal to one corresponds to an equilibrium composition where all reactants are converted to products (all products). A a conversion equal to zero corresponds to an equilibrium composition where no reactants are converted to products (all reactants). It is measured by

$$X = \frac{n_{N_2,initial} - n_{N_2,final}}{n_{N_2,initial}} \tag{3.1}$$

where $n_{N_2,initial}$ represents the initial molar concentration of nitrogen, and $n_{N_2,final}$ represents the final molar concentration of nitrogen. The initial molar concentration of nitrogen and hydrogen is defined by the stoichiometric ratios of the reaction (y_{H_2} = 3/4, y_{N_2} = 1/4).

For a thermochemical reaction, the equilibrium constant is calculated using the change in the Gibbs Free Energy ΔG, which is calculated using tabulated properties for the change in enthalpy ΔH and change in entropy entropy ΔS for the reaction at the operating conditions [73]. The equilibrium constant is

$$K_{eq} = e^{\frac{-\Delta G}{RT}} \tag{3.2}$$

where R is the universal gas constant and T is the operating temperature. The equilibrium constant can be correlated to the reactant and product partial pressure

$$K_{eq} = \frac{p_{products}^{v_p}}{p_{reactants}^{v_r}} \tag{3.3}$$

where P_i corresponds to the partial pressures of i (i=products or reactants), and v_p and v_r corresponds to the stoichiometric ratios for the products and reactants. The relation between temperature, pressure, and the equilibrium conversion (X) can be calculated combining equations 3.1 - 3.3.

$$e^{\frac{-\Delta G}{RT}} = \frac{2X * (4 - 2X)}{(1 - X)^{1/2} * (3 - 3X)^{3/2}} \frac{1}{P} \tag{3.4}$$

The highest conversion of nitrogen to ammonia in a thermochemical process is achieved at low temperatures and low pressures due to the Le Chatelier's principle (Fig. 3.1a - Region 1). However, in reality, systems are operated at elevated temperatures (400^{o}C) to increase the rate of production and maximize profit. As the cell moves to a higher temperature, the equilibrium is shifted, promoting lower conversion of reactant to products (Fig. 3.1a - Region 2). To overcome this negative shift in conversion equilibrium, the cell is pressurized (3.1a - Region 3). The use of elevated temperatures and pressures often require additional system level auxiliary (heat exchangers, compressors and/or pump), and safety measures be used. This can add to the system energy balance and cost.

For an electrochemical system the equilibrium conversion is determined as a function

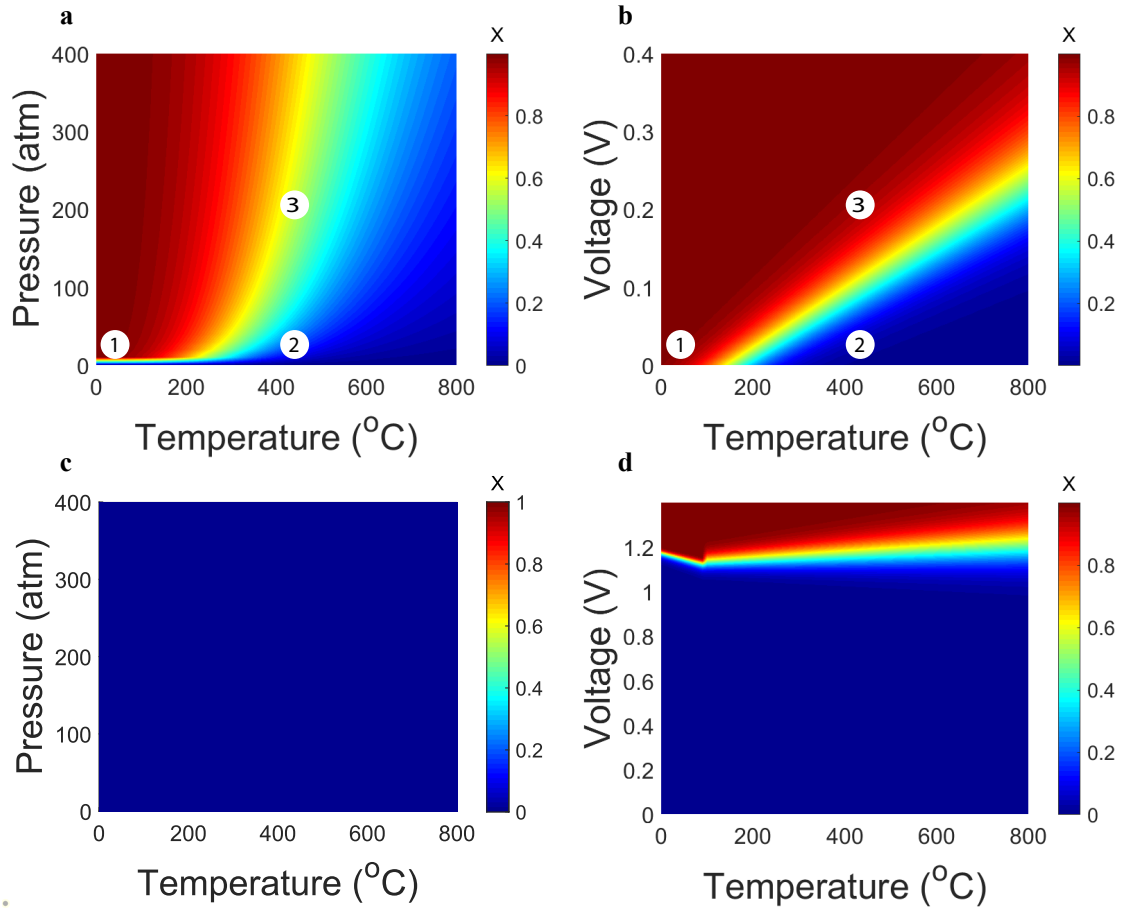

Figure 3.1: Thermodynamic equilibrium conversion of nitrogen to ammonia for (a) H_2 + N_2 thermochemical system, (b) H_2 + N_2 electrochemical system, (c) H_2O + N_2 thermochemical system, and (d) H_2O + N_2 electrochemical system.

of voltage through nernst equation.

$$V = \frac{\Delta G}{nF} + \frac{RT}{nF} ln(\frac{p^{v_p}_{products}}{p^{v_r}_{reactants}}) \tag{3.5}$$

The highest conversion of nitrogen and hydrogen to ammonia in an electrochemical process is achieved at low temperatures and high voltages (Fig. 3.1b). As the cell moves to a higher temperature, the equilibrium shifts, promoting lower conversion (Fig. 3.1b - Region 2). To overcome this negative shift in conversion equilibrium at elevated temperatures, higher cell voltages are required (3.1b - Region 3). The potential to achieve near similar conversion of reactants with products with voltage, is one of the primary motivators

for exploring direct electrochemical nitrogen reduction.

The advantage of electrochemical routes for nitrogen reduction is most visible when exploring pathways to conversion of nitrogen and water to ammonia. For a thermochemical process with nitrogen and water as reactants (Fig. 3.1c) the equilibrium conversion is zero at all temperatures and pressures. This means that this reaction is not possible through thermochemical methods. However, in an electrochemical process (Fig. 3.1d) if the voltage is increased above 1.2V the formation of ammonia is favored and the equilibrium conversion rapidly approaches one.

3.2 Kinetic considerations for high activity

Despite the potential outlined above (see sec. 3.1), thermodynamics are not the only considerations for determining whether a catalytic process is effective. The kinetics or rate of production must be determined to ultimately explore if the reaction pathways is viable. To date, there has been far less analyses which focus on comparing the kinetics of ammonia electrosynthesis.

The reaction rate of the thermochemical reduction of nitrogen to ammonia is calculated by a modified form of the Temkin equation [74], developed by Dyson and Simon in 1968 [75]. Due to the high temperatures and pressures, the activities of the gases are used instead of the partial pressures.

$$R_{NH_3} = 2 * k * [K_a^2 * a_{N_2} * (\frac{a_{H_2}^3}{a_{NH_3}^2})^{\alpha} - (\frac{a_{NH_3}^2}{a_{H_2}^3})^{1-\alpha}] \tag{3.6}$$

where a_{H_2}, a_{N_2}, a_{NH_3}, k, K_a, and α are the activity coefficients for nitrogen, hydrogen and ammonia (eqn. 3.8 - eqn. 3.11), rate constant for the reverse reaction (eqn. 3.13), reaction equilibrium constant (eqn. 3.12), and transfer coefficient.

The activity of a component (a_i) is defined as the ratio between the fugacity of the component at a particular chosen state (f_i) to the fugacity of the pure component at ambient

pressure and a temperature equal to the system (f_i^*).

$$a_i = \frac{f_i}{f_i^*} \tag{3.7}$$

Additionally, the activity of a component in a mixture can be calculated using the molar fraction of the component (y_i), the fugacity coefficient of the component (Φ), and the pressure at which the reaction takes place (P).

$$a_i = y_i * \Phi_i * P \tag{3.8}$$

The reaction rates are highly dependent on the molar fractions of the products and reactants. For our calculations, we chose to use a 10% molar concentration of ammonia ($y_{NH_3} = 0.1$, $y_{N_2} = 0.225$, $y_{H_2} = 0.675$) and a 1% molar concentration of ammonia ($y_{NH_3} = 0.01$, $y_{N_2} = 0.2475$, $y_{H_2} = 0.7425$). The fugacity coefficients for nitrogen [76, 77], hydrogen [76, 78], and ammonia [76, 77] can be calculated using the following equations:

$$\Phi_{N_2} = 0.93431737 + 0.3101804 * 10^{-3} * T + 0.295895 * 10^{-3} * P \\ - 0.270729 * 10^{-6} * T^2 + 0.4775207 * 10^{-6} * P^2 \tag{3.9}$$

$$\Phi_{H_2} = exp[e^{(-3.8402 * T^{0.125} + 0.541)} * P - e^{(-0.1263 * T^{0.5} - 15.980)} * P^2 \\ + 300 * [e^{(-0.011901 * T - 5.941)}] * (e^{(-P/300)} - 1)] \tag{3.10}$$

$$\Phi_{NH_3} = 0.1438996 + 0.2028538 * 10^{-2} * T - 0.4487672 * 10^{-3} * P - 0.1142945 * 10^{-5} * T^2 + 0.2761216 * 10^{-6} * P^2 \quad (3.11)$$

The reaction equilibrium constant (K_a) can be calculated using the following equation [79]:

$$log(K_a) = -2.691122 * log(T) - 5.519265 * 10^{-5} * T + 1.848863 * 10^{-7} * T^2 + \frac{2001.6}{T} + 2.67899 \quad (3.12)$$

Finally, the reaction rate constant (k) is calculated as a function of temperature using the Arrhenius equation:

$$k = A * e^{\frac{-Ea}{RT}} \quad (3.13)$$

where A is the frequency factor, Ea is the activation energy for the reaction, R is the universal gas constant, and T is the temperature of the reaction. The values for the catalyst properties used for ammonia synthesis are shown in the table below.

Table 3.1: Catalyst Kinetic Properties [75]

α	A (kmol*m^{-3})	Ea (kJ*kmol^{-1})
0.5	8.8490*10^{14}	1.7056*10^5

Using a symmetric transfer coefficient ($\alpha = 0.5$) is preferred as it simplifies the rate equation and fits the data as well as the more complicated rate expression using other values of α. In fact, Dyson and Simon state that the model using $\alpha = 0.75$ fits the data only slightly better than the model using $\alpha = 0.5$. However, they recommend the use of $\alpha = 0.5$ due to the simpler rate equations [75].

For the electrochemical synthesis of ammonia, the rate is calculated using the following

equation:

$$r_{NH_3} = k_b * e^{-\frac{\alpha*3*F*\eta}{R*T}} - k_f * e^{\frac{(1-\alpha)*3*F*\eta}{R*T}} \tag{3.14}$$

where k_b and k_f are rate constants for the reaction, F is Faraday's constant, α is the transfer coefficient, and η is the cell overpotential. In order to find a parallel between the performance of electrochemical and thermochemical reactions we calculated the values for k_b and k_f using equation 3.16. The resulting equations used to calculate k_b and k_f are shown below:

$$k_b = 2 * k * K_a^2 * a_{N_2} * (\frac{a_{H_2}^3}{a_{NH_3}^2})^{\alpha} \tag{3.15}$$

$$k_f = 2 * k(\frac{a_{NH_3}^2}{a_{H_2}^3})^{1-\alpha} \tag{3.16}$$

Finally, the rate equations presented above result is a rate with units of $kmol*m^{-3}*h^{-1}$. We transfed this rate to the preferred units of $mol * g^{-1} * s^{-1}$ by using the catalyst density (2.35 g/cm^3) [80].

Finding information about the transfer coefficient (α) was challenging, especially for electrocatalysis. Hence, based on the findings from Dyson and Simon we have decided to use a symmetric transfer coefficient for all the calculations unless otherwise specified. Here, we study the effect variations of the transfer coefficient have in the rate equation for thermochemical (Fig. 3.2) and electrochemical (Fig. 3.3) synthesis. We find that larger transfer coefficients lead to larger reaction rates. However, the comparison with the Haber-Bosch process (red line) falls in the same location regardless of the transfer coefficient and the trends between electrochemical and thermochemical reactions are the same regardless of the transfer coefficient. Hence, we find the use of a symmetric transfer coefficient appropriate as it simplifies the calculations.

A thermochemical reactor operating at low temperature results in low production rates

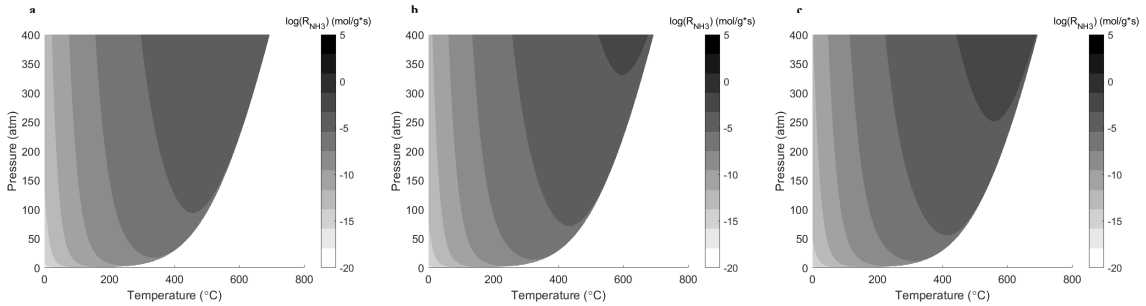

Figure 3.2: Rate of ammonia produced at various temperatures and pressures for thermochemical synthesis with a transfer coefficient (a) $\alpha = 0.5$, (b) $\alpha = 0.6$, and (c) $\alpha = 0.7$. The rate of the Haber-Bosch process is provided as a reference (red line)

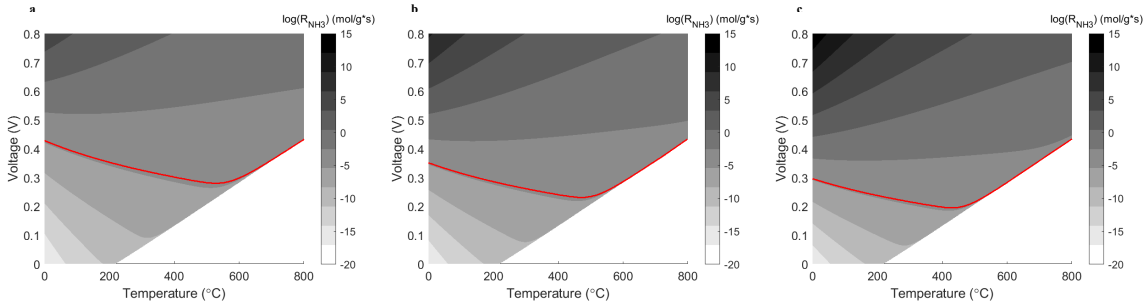

Figure 3.3: Rate of ammonia produced at various temperatures and voltage for electrochemical synthesis with a transfer coefficient (a) $\alpha = 0.5$, (b) $\alpha = 0.6$, and (c) $\alpha = 0.7$. The rate of the Haber-Bosch process is provided as a reference (red line)

at nearly all pressures (Fig. 3.4a,b – zone 1). Increasing the temperature only marginally increases production rates, as the shifting equilibrium point begins to favor ammonia decomposition. Thus, a reactor operating at high temperature ends up suffering from low conversion efficiency (Fig. 3.4a,b – zone 3). The use of elevated pressure is necessary to offset this equilibrium shift, and maximize product yield in the Haber-Bosch process. The optimal operating temperature and pressure for thermocatalytic conversion of nitrogen to ammonia also depends on the concentration of ammonia in the reactor. For instance increasing the concentration from 1% (Fig. 3.4a) to 10%(Fig. 3.4c) shifts the optimum temperature and pressure up. Overall, optimal operation occurs at intermediate temperature ($\sim$400 °C) and moderate pressure ($\sim$ 200 atm)(Fig. 3.4a,b – zone 2).

In a electrocatalytic reactor, an applied voltage drives the catalytic process instead of temperature (Fig. 3.4c and d). Theoretically, an electrochemical cell can achieve similar

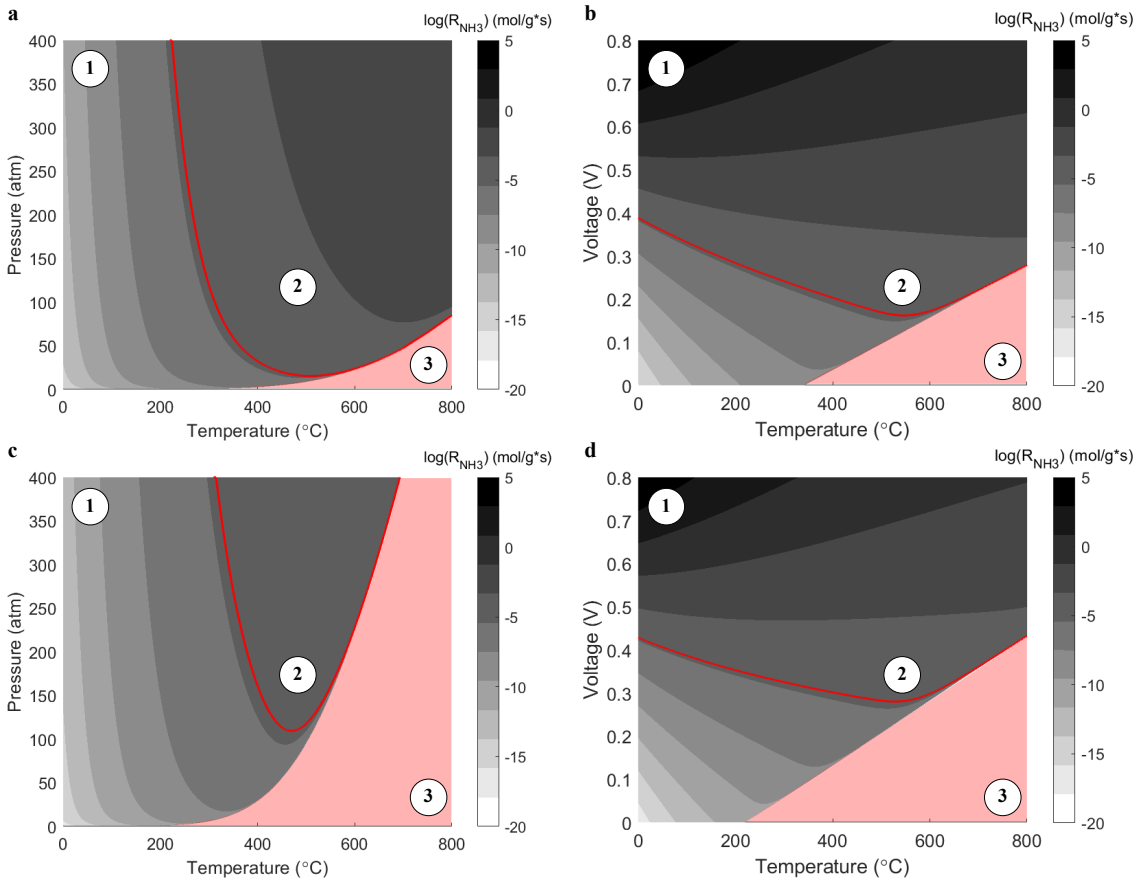

Figure 3.4: Rate of ammonia produced at various temperatures and pressures for thermochemical synthesis with an ammonia molar fraction of 1% (a) and 10% (c), and various temperatures and voltages for electrochemical synthesis at ambient pressures with an ammonia molar fraction of 1% (b) and 10% (d). The rate of the Haber-Bosch process is provided as a reference (red line). Additionally, the red area in the figures represents the operating conditions at which no ammonia will be produced. The figure has three regions (1,2, and 3) representing the three temperature regimes (low, intermediate, and high). Zone 1 represents operation at ambient temperatures. A thermochemical reactor operating at ambient temperatures cannot achieve high rates due to poor kinetics. However, an electrochemical reactor operating at ambient temperatures can achieve high rates by increasing the voltage. The main advantage of operating at near ambient temperatures is the possibility of operating at higher ammonia concentrations because to the equilibrium conversion of nitrogen to ammonia decreases with temperature. Zone 2 represents operation at intermediate temperatures (400-600 °C). This is the optimal operation regime as it results in enhanced kinetics due to the elevated temperatures and in good equilibrium conversions. Finally, zone 3 represents operation at high temperatures (800°C). At this temperature regime, the reaction kinetics are favorable due to the high temperatures. However, at these temperatures, the equilibrium conversion of nitrogen to ammonia is nearly zero (0). Hence, achieving high rates is only feasible at low concentrations of ammonia and at high pressures and voltages.

production rates as a thermocatalytic reactor. For instance, if the voltage is increased to 450 mV, an electrochemical reactor can achieve a production rate comparable to a thermocatalytic reactor at ambient temperature (red line represents a production rate of 6x10^{-6} mol/g*s). However, this voltage results in a 300 mV overpotential, which is considered sluggish. This high of an overpotential is often deemed prohibitively expensive, because the cost of electricity dominates the levelized cost of ammonia [81, 82]. To put this overpotential into perspective, hydrogen evolution reaction overpotentials are on the order of 10s-100 mV, whereas the oxygen evolution reaction occurs with a overpotential of $\sim$300-500 mV[83].

In order for electrochemical ammonia synthesis to become a viable option, this reaction overpotential needs to decrease. A possible way to minimize the required voltage is to operate at temperatures above ambient temperature (Fig. 3.4c,d). For instance, increasing the temperature of the cell to 600 °C, decreases the required potential to 200-300 mV and the overpotential to 60-160 mV (Fig.3.4c,d – zone 2). This is still energy intensive, but is a significantly better entry point for electrochemical ammonia synthesis than ambient temperature electrosynthesis. Increasing the temperature too high is not advisable, as the overpotential begins to increase. For instance at 800^{o}C the required overpotential to achieve desired performance increases to 200-300mV (Fig. 3.4c,d – zone 3). However, low-temperature approaches are more favorable for rural applications as the technology used for high-temperature electrosynthesis requires higher levels of sophistication and is more complicated to operate and maintain. There are also safety issues associated with operating at high temperatures. Hence, the improvement in reaction kinetics should come from catalyst development if low temperature approaches are to be used.

An additional advantage of electrochemical approaches over thermochemical systems is the ability to attain a desired production rate over a wider range of temperatures and concentrations (ammonia). Achieving high rates in a thermochemical reactor at low temperatures is not feasible. However, an electrochemical reactor can achieve high rates at low

temperatures by simply increasing the voltage. Even though increasing the temperature improves the reaction kinetics, operating at too high temperatures can hurt the reactor's performance. For instance, an electrochemical reactor operating at 800^{o}C would require an overpotential of 500mV to produce ammonia at 10% molar concentration. However, a thermochemical reactor operating at 800^{o}C and 10% molar concentration of ammonia would require pressures upwards of 400 atm to produce ammonia. In thermochemical approaches the required pressure to maintain the same production rate increases by 300% when the concentration of ammonia increases from 1% to 10% for a thermochemical reactor operating at 400^{o}C. A similar increase in ammonia concentration only requires a 70% increase in the required voltage for an electrochemical reactor operating at 600^{o}C. However, the energy increase associated with a 70% increase in the voltage (37.6 kJ/mol$_{NH3}$) is higher than the energy increase associated with a 300% pressure increase (27.5 kJ/mol$_{NH3}$).

3.3 Energy Efficiency Considerations

The Haber-Bosch process is highly efficient (60%) [84] when compared to electrochemical synthesis-based technologies (1%) [84]. Improving the Haber-Bosch energy efficiency is still possible (thermodynamic limit is $\sim$ 90%) [27], and efforts which succeed in increasing this efficiency will aid in minimizing the carbon emissions associated with the Haber-Bosch process. The energy efficiency for an electrochemical synthesis route most likely would not need to be as high as a thermocatalytic system if the electrons were provided by a renewable source. Yet, appreciable energy efficiency is still required to limit system size and capital costs. Thus, improving the energy efficiency of electrochemical routes is imperative in order for ammonia electrosynthesis to become viable. The energy efficiency for an electrochemical system is largely governed by faradays law.

Faradays law relates the rate of ammonia produced to the electrons supplied to the cell

$$R_{NH_3} = \frac{i * FE}{n * F * m_l} \tag{3.17}$$

where i is the current density, FE is the faradaic efficiency, n is the number of electrons involved in the reaction, F is Faraday's constant, m_l is the catalyst loading. A faradaic efficiency of 100% indicates that all the current is utilized to reduce nitrogen. However, most electrocatalysts achieve faradaic efficiencies between (10^{-2}-10%) [84]. Higher faradaic efficiencies have been reported, but typically are obtained at impractically low current[84]. The energy efficiency of the system can further be related to faradaic efficiency .

$$\eta_{EE} = \frac{LHV * FE}{n * F * V} \tag{3.18}$$

where LHV is the lower heating value of ammonia, FE is the faradaic efficiency, n is the number of electrons involved in the reaction, F is Faraday's constant, and V is the cell voltage. Which can be modeled using the activation overpotential (η_{act}),the ohmic overpotential (η_{ohm}), and the concentration overpotential (η_{conc}).

$$\eta_{total} = \eta_{act} + \eta_{ohm} + \eta_{conc} \tag{3.19}$$

The activation overpotential can be approximated using the Butler-Volmer equation. As discussed in the previous section, we have assumed that the reaction has symmetric electron transfer coefficient (α = 0.5). This assumption is done to simplify the calculations. However, this assumption is justified in the work done by Dyson and Simon, in which it is shown that a charge transfer coefficient of 0.5 has good agreement with experimental kinetic data [85].

$$\eta_{act} = \frac{RT}{n\alpha F} * sinh^{-1}(\frac{i}{2i_0}) \tag{3.20}$$

where R is the universal gas constant, F is the Faraday's constant, T is the reactor operating temperature, n is the number of electrons involved in the reaction (n = 3), α is the electron transfer coefficient, i is the operational current and i_0 is the exchange current density.

The exchange current density of a reaction improves with temperature. The relationship

between the exchange current density and temperature can be modeled using the following equation:

$$i_0 = i_0^{ref} * exp((-Ea/(R*T)) * (1 - (T/T_ref)) \tag{3.21}$$

where i_0^{ref} is the reference exchange current density at ambient temperature.

The ohmic overpotential can be described by the Ohm's law

$$\eta_{ohm} = i * R_{electrolyte} \tag{3.22}$$

where $R_{electrolyte}$ is the area specific resistance of the electrolyte. We neglected the resistance due to the gas diffusion layer and the electrical components because these losses are negligible when compared to the losses in the solid electrolyte (which has poor ionic conductivity). The area specific resistance of an electrolyte is

$$R_{electrolyte} = \frac{1}{\sigma} * L \tag{3.23}$$

where σ is the electrolyte conductivity and L is the electrolyte thickness. For low temperature electrosynthesis we used the conductivity of a Nafion membrane. For a fully humidified proton exchange membrane made of Nafion, the conductivity can be approximated by the following equation [86].

$$\sigma = 0.1098 * e^{1268*(\frac{1}{303} - \frac{1}{T})} \tag{3.24}$$

Moreover, for a liquid electrolyte, the conductivity is assumed to be 0.8 S/cm [87]. The concentration overpotential accounts for the losses due to mass transport.

$$\eta_{conc} = -\frac{RT}{nF} * log(1 - \frac{i_{density}}{i_{lim}}) \tag{3.25}$$

where the limiting current density (i_{lim}) is the maximum current achievable with the mass

transport properties of system. The limiting current density depends on the effective diffusion coefficient of the reactant and the concentration of the reactant.

$$i_{lim} = \frac{nFD_{eff}C}{\delta} \tag{3.26}$$

where D_{eff} is the effective diffusion coefficient of the reactant, C is the reactant concentration. For liquid electrolytes, the reactant concentration is limited by the solubility of nitrogen in water [88]. Finally, δ is the thickness of the layer in which the mass transport takes place. For mass transport through a porous gas diffusion layer, δ corresponds to the thickness of the gas diffusion layer. However, for mass transport through a liquid electrolyte, δ corresponds to the thickness of the electrical double layer. The effective diffusion coefficient depends on the species and the medium in which the mass transport takes place.

The effective diffusion coefficient on a liquid electrolyte depends on the liquid medium and the gaseous reactant [89]. On a porous gas diffusion layer, the effective diffusion coefficient can be approximated using (eqn. 3.27) [90].

$$D_{eff} = \epsilon^{1.5} D_{bulk} \tag{3.27}$$

where ϵ is the porosity of the gas diffusion layer (ϵ = 0.8) and D_{bulk} is the bulk diffusion coefficient of the species [91],[92].

In order for ambient-temperature electrochemical ammonia synthesis to approach the energy efficiency of the Haber-Bosch process, a system needs to attain 90% FE (Fig. 5.3a). This is not feasible with aqueous-based electrolytes, and is challenging in a non-aqueous environment at relevant current densities. Furthermore, even if energy efficiency requirements were relaxed, the minimum FE would be greater than 70%. This indicates that new approaches are needed to attain high efficiency with moderate FE. Some of these approaches might include operating at slightly higher temperatures and pressures or designing systems that couple with water electrolysis cells to operate with hydrogen and nitrogen in

order to increase the energy efficiency.

In order for intermediate-temperature electrochemical ammonia synthesis to approach the energy efficiency of the Haber-Bosch process, a system needs to attain 50-70% FE (Fig. 5.3b). While this is still ambitious, it is far more feasible than 90%. To put this into perspective, carbon dioxide based electrolysis systems, which struggle with many of the same selectivity challenges, have been able to obtain FE which approach 50-80% for the conversion of CO_2 to CO [93, 94]. This suggests that electrosynthesis cells with well-designed catalyst may be able to achieve these desired performance metrics for nitrogen fixation.

Increasing FE requires the design of catalyst with a high degree of selectivity for nitrogen reduction. This is a significant challenge as the redox potential for nitrogen reduction (E°=0.148 vs RHE) resides close to the more facile hydrogen evolution reaction (E°=0 vs RHE). Furthermore, most surfaces preferentially bind H* rather than N* which promotes the formation of few active sites for nitrogen activation. Catalyst design and system operations are therefore critical in order to overcome these challenges. However, low-temperature ammonia electrosynthesis can become viable through smart system design (see 5)

Increasing the energy efficiency of the system can also be accomplished through reducing system losses. While a complete electrochemical system will have many components (compressors, pumps, separation devices), most system losses are associated with the electrochemical cell. Losses within the electrochemical cells, termed overpotentials, must be reduced to maximize efficiency. The three primary overpotentials are ohmic, activation, and mass transport losses.

The largest ohmic loss in an electrochemical reactor is due to the ionic conductivity of the electrolyte. Within low temperature electrolysis systems, the electrolyte is largely polymer based, and the conductivity (inverse of resistance) increases moderately with temperature (Fig. S3) [86, 95]. The low temperature electrolytes have conductivity order of

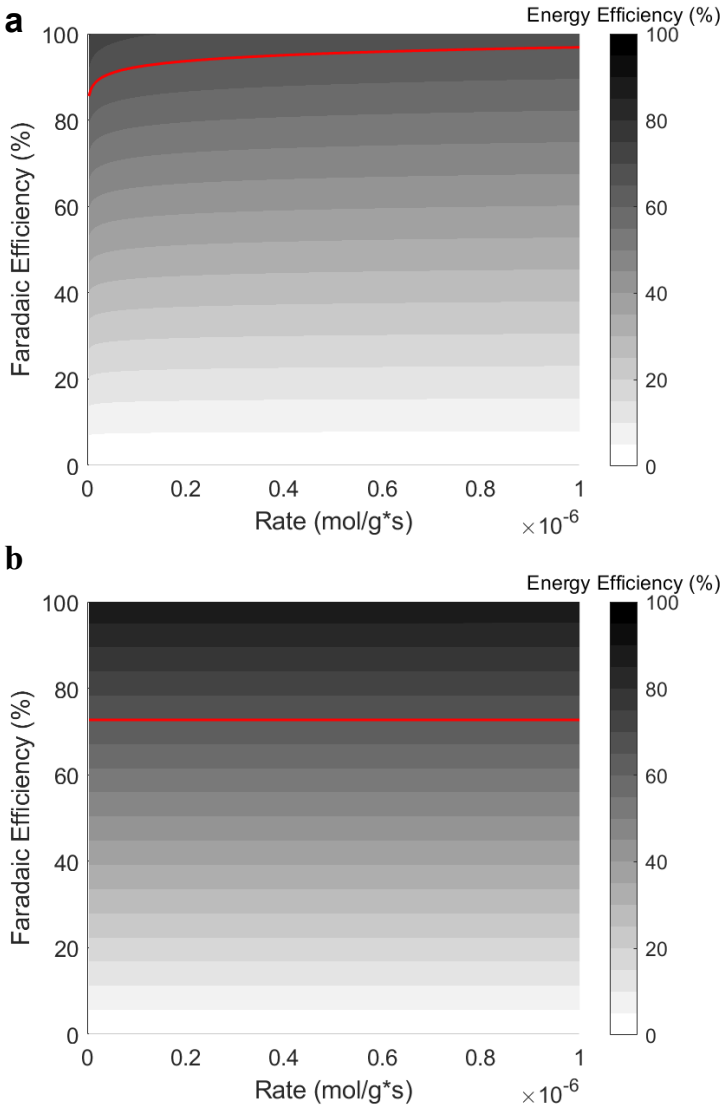

Figure 3.5: Energy efficiency of a low temperature electrochemical ammonia synthesis cell with an exchange current density of 10^{-10} A/cm^2, an electrolyte ionic conductivity of 0.8 S/cm, a electrolyte thickness of 60 μm, and catalyst loading is 1 mg/cm^2(a). Energy efficiency of a intermediate temperature electrochemical ammonia synthesis cell (600^{o}C), with an exchange current density of 10^{-10} A/cm^2, an electrolyte ionic conductivity of 0.014 S/cm, a electrolyte thickness of 50 μm, and catalyst loading is 1 mg/cm^2(b).

0.1 S/cm [86] (Fig. 3.6a). For intermediate temperature operation, the ionic conductivity of solid electrolytes is highly dependent on temperature. Solid electrolytes have poor ionic conductivity at low temperatures (0.002 S/cm) [95], but improve at intermediate and high temperatures (0.01-0.04 S/cm). Therefore, even when operating optimally the intermediate

temperature solid electrolytes are about an order of magnitude more resistive than the low temperature polymer based electrolytes (Fig. 3.6b). For this reason, the ohmic losses are generally negligible with respect to the other losses in a low temperature electrolysis cell, but dominant cell losses in an intermediate temperature electrolysis cell(Fig. 3.6).

The activation overpotential depends on the kinetics of the reaction and improves as temperature increases due to the Arrhenius relationship. A reactor operating at ambient temperature has an activation overpotential of 700 mV. As temperature increases to 600°C, the activation overpotential decreases to as low as 0.3 mV. For these reasons, highly active electrocatalyst (such as certain precious metals) are desirable for low temperature cells, whereas less active (such as earth abundant metals) electrocatalyst are generally acceptable for higher temperature cells. Temperature effects will have a marginal impact on transport related losses. Increasing the temperature increases the diffusivity of nitrogen in aqueous media, allowing for a slight decrease in mass transport losses. Higher temperatures will also promote the use of gas-diffusion layer based cells which have significantly less transport related losses than liquid aqueous phase systems [96].

As ammonia electrosynthesis continues to grow as a field, care must be placed on understanding kinetic limitations of various operation conditions. Low temperature ammonia electrosynthesis is possible. However, in order to achieve energy efficiencies similar to the Haber-Bosch process a system would require a faradaic efficiency close to 90%. Thus, these analyses suggest catalyst design is important in improving the selectivity of a desired reactants.

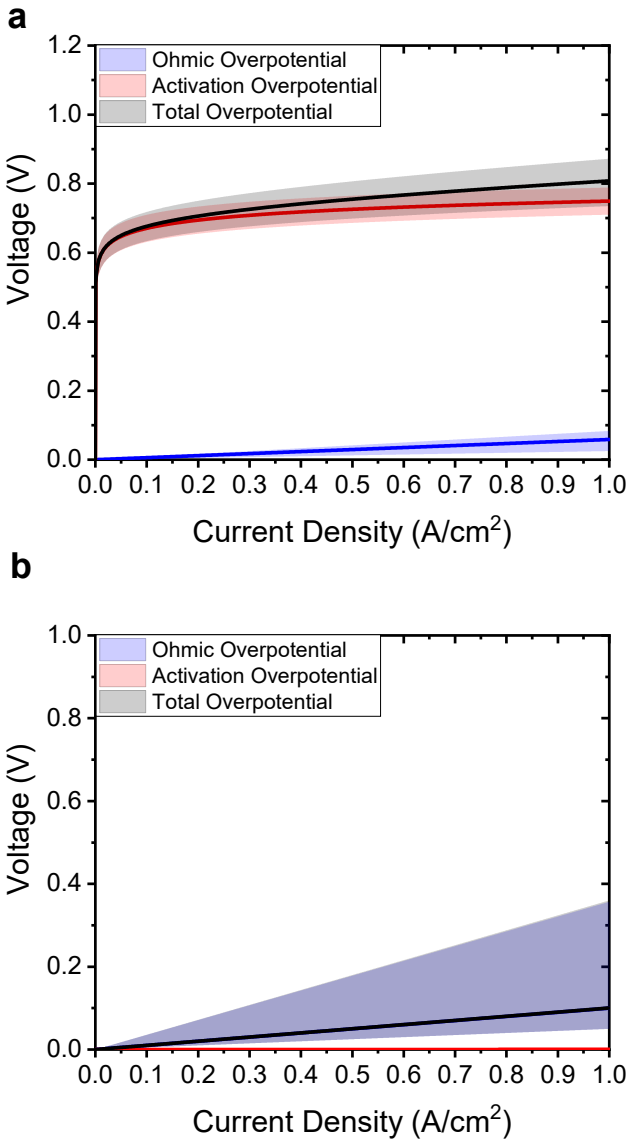

Figure 3.6: Cell over-potentials of a low temperature ammonia electrosynthesis reactor. Lower edge of shaded region assumes the exchange current density is 10^{-9} A/cm^2, the middle of the shaded region assumes the exchange current density is 10^{-10} A/cm^2, the upper edge of the shaded region assumes an exchange current density of 10^{-11} A/cm^2. In each chase the electrolyte ionic conductivity is 0.8 S/cm and the electrolyte thickness is 60 μm (a). Cell over-potentials of a intermediate temperature ammonia electrosynthesis reactor T=600^{o}C.Lower edge of shaded region assumes the exchange current density is 10^{-9} A/cm^2, the middle of the shaded region assumes the exchange current density is 10^{-10} A/cm^2, the upper edge of the shaded region assumes an exchange current density of 10^{-11} A/cm^2. In each chase the electrolyte ionic conductivity ranged from 0.014 S/m at the upper edge to 0.05 S/m lower edge, and the electrolyte thickness was 50 μm(b).

CHAPTER 4

SYSTEM MODEL

4.1 Electrochemical Modeling

The reversible energy demand for an electrochemical reaction corresponds to the change in enthalpy of the reaction (ΔH), which is a combination of the electrical energy demand or the change in the Gibbs free energy (ΔG) and the thermal energy demand which is the change in the product's temperature times the entropy of the system ($T\Delta S$).

$$\Delta H = \Delta G + T\Delta S \tag{4.1}$$

The thermal energy ($\Delta Q = T\Delta S$) and electrical energy demand (ΔG), are temperature dependent (Fig. 4.1). For a cell operated with $N_2 + H_2O$ reactants, the electrical energy demand decreases as temperature rises for temperatures below $100^{\circ}C$ (Fig. 4.1a). However, at temperatures above the evaporation temperature of water ($100^{\circ}C$), the electrical energy demand increases as temperature rises. The required heat for the reaction (ΔQ) increases as temperature rises for temperatures below the evaporation temperature of water. However, as the temperature reaches the evaporation temperature, the heat required for the reaction drops with a magnitude equal to the latent heat of vaporization of water. At temperatures higher than the evaporation temperature of water, the heat required for the reaction decreases as temperature rises. Even though the electrical energy required and the thermal energy required are dependent on temperature, the total energy required for the reaction remains unchanged as temperature rises. For a cell operated with $N_2 + H_2$ reactants, the electrical energy demand for the reaction (ΔG) increases as temperature rises and the thermal energy demand for the reaction (ΔQ) decreases as temperature rises (Fig. 4.1b).

In an electrochemical system, the open circuit voltage (OCV) of the reaction is defined

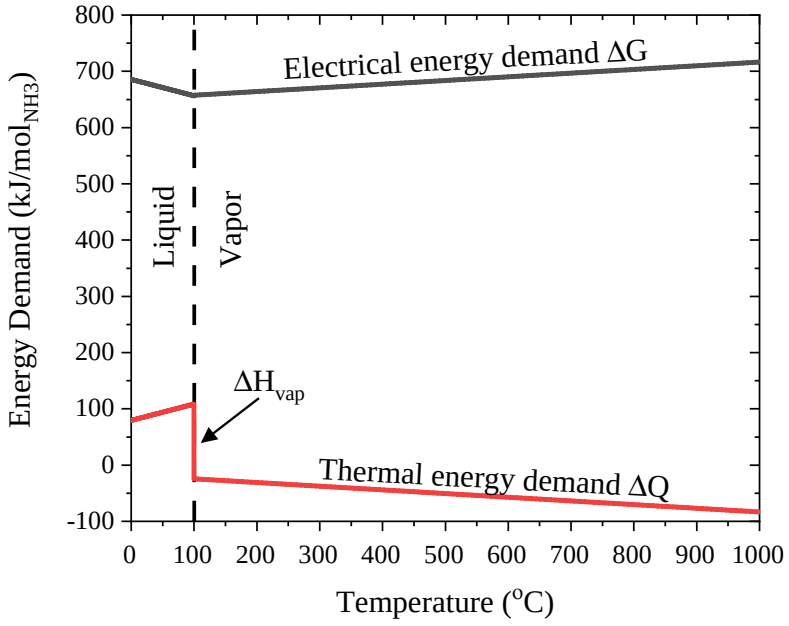

(a)

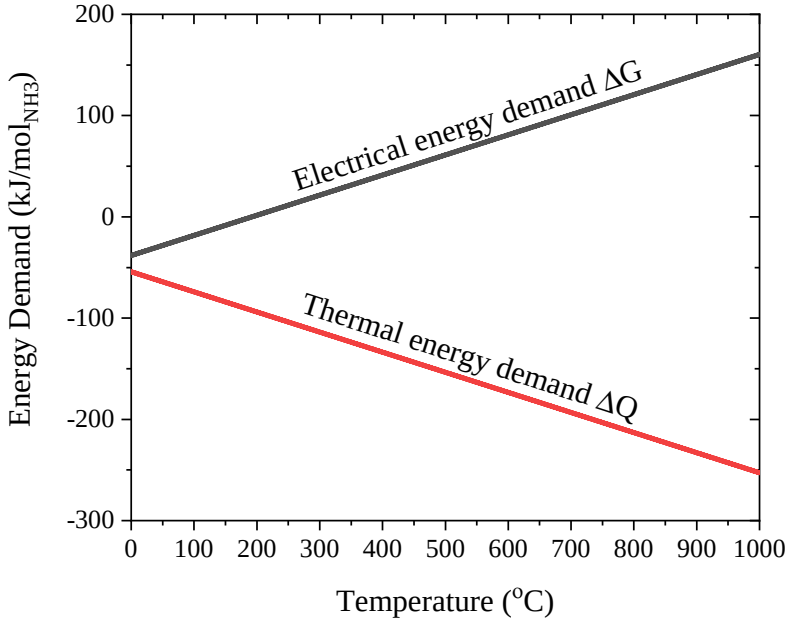

(b)

Figure 4.1: Thermal (ΔQ) and electrical(ΔG) energy demand of the nitrogen reduction reaction as function of temperature for (a) a reaction with nitrogen and water as reactants and (b) a reaction with nitrogen and hydrogen as reactants.

as the change in the Gibbs free energy (ΔG) divided by the number of electrodes involved in the reaction (n = 6) and the Faraday's constant (F = 96,485 C/mol).

$$V_{OCV} = \frac{\Delta G}{nF} \tag{4.2}$$

For a cell operated with $N_2 + H_2O$ reactants, the open circuit voltage of the reaction decreases as temperature increases for temperatures below the evaporation temperature of water (Fig. 4.2). The open circuit voltage goes from 1.17V at ambient temperature to 1.14V at $100°C$. At temperatures above $100°C$ the open circuit voltage of a cell operated with $N_2 + H_2O$ reactants increases from 1.14V at $100°C$ to 1.18V at $500°C$. For a cell operated with $N_2 + H_2$ reactants, the open circuit voltage of the reaction increases as temperature increases (Fig. 4.2). The open circuit voltage goes from -0.06V at ambient temperature to 0.11V at $500°C$. The negative open circuit voltage at low temperatures indicates that the reaction is spontaneous.

The open circuit voltage refers to the minimum voltage required for the reaction in an ideal system. However, in real systems, losses are inevitable, and the performance cannot be quantified solely by the open circuit voltage. The actual cell potential is determined by the reversible cell potential (V_0) and the cell overpotential (η_{total}).

$$V = V_0 + \eta_{total} \tag{4.3}$$

V_0 refers to the reversible cell potential determined by the Nernst equation.

$$V_0 = V_{OCV} + \frac{RT}{nF} ln(\frac{a_{reactants}}{a_{products}}) \tag{4.4}$$

where a_i corresponds to the activity of the reactants and products. Since the reactants and products are gases, their activity can be approximated using the partial the partial pressures. The activity of water is approximated to be one (a_{H_2O} = 1) because water is the predominant solvent in the solution.

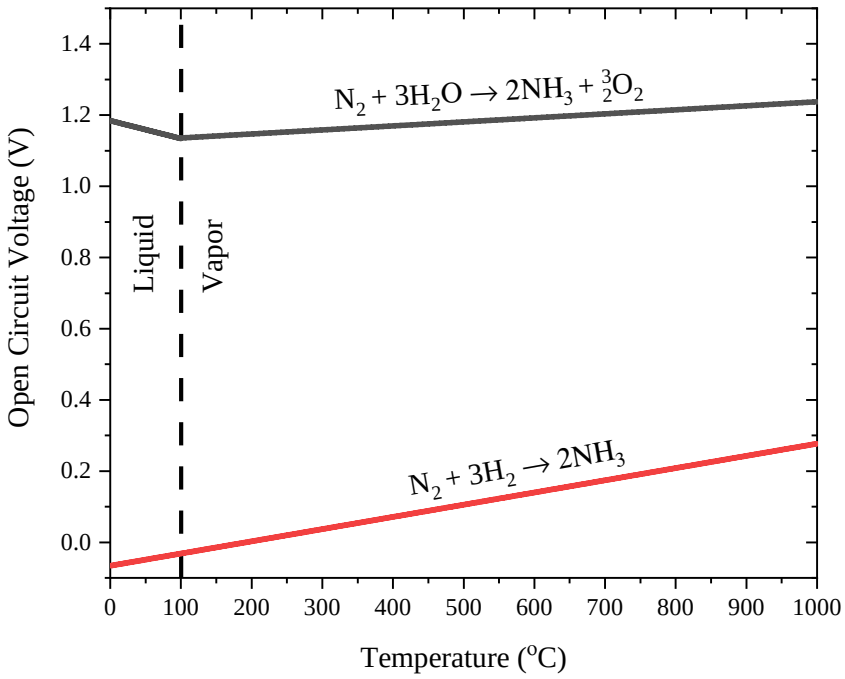

Figure 4.2: Open circuit voltage for the electrochemical nitrogen reduction reaction.

The total cell overpotential is the combination of the activation overpotential (η_{act}),the ohmic overpotential (η_{ohm}), and the concentration overpotential (η_{conc}) and is discussed in Section 3.3 and in equations 3.19 to 3.27.

4.1.1 Thermodynamic Modeling

The thermodynamic performance of an electrochemical system for ammonia synthesis is quantified using the energy efficiency of the whole system. The energy efficiency is calculated by dividing the chemical energy produced by the system ($LHV_{NH_3} * \dot{N}_{NH_3}$) by the total work required by the system ($\sum W_i$). The lower heating value of ammonia (LHV_{NH_3}) represents the chemical energy stored in each mole of ammonia and the molar flow rate ($\dot{N}_{NH_3}$) is the amount of ammonia produced. The total work required by the system is the

combination of the work required by all the components.

$$\eta_{en} = \frac{LHV_{NH_3} * \dot{N}_{NH_3}}{\sum W_i} \tag{4.5}$$

Electrolysis Cell Energy Input

The electric energy input to the electrolysis cell is

$$W_{electric} = I * V \tag{4.6}$$

where the current, in Amps, is calculated using Faraday's Law

$$I = \frac{\dot{N}_{NH_3} * F * 3}{FaradaicEfficiency} \tag{4.7}$$

where $\dot{N}_{NH_3}$ is the molar flow rate of ammonia produced and V is the cell voltage.

The thermal energy input to the electrolysis cell is

$$Q_{heat,PEM} = \dot{N}_{N_2} * T * \Delta S - I * (\eta_{total}) \tag{4.8}$$

In some instances, the irreversibilities within the electrolyzer produce enough heat to sustain the reaction, and no external heat source is needed.

Pump Energy Input

The pump is assumed to operate adiabatically and under incompressible flow. The work input into the pump is

$$W_{Pump} = \frac{\dot{m}_{H_2O} * v_{H_2O} * (P_2 - P_{ambient})}{\eta_{Pump}} \tag{4.9}$$

where $\dot{m}_{H_2O}$ is the mass flow rate of water flowing through the pump; v_{H_2O} is the specific volume of water; η_{Pump} is the pump's isentropic efficiency (assumed to be $85\ \%$); and P_2

is the electrolyzer operating pressure [97]. The pump outlet temperature is

$$T_2 = \frac{W_{Pump} - W_{Pump,Ideal}}{\dot{m}_{H_2O} * C_{H_2O}} + T_{ambient} \tag{4.10}$$

where $W_{Pump,Ideal}$ is the work input to a pump with isentropic efficiency (η_{Pump}) of 100 $\%$.

Compressor Energy Input

The compressor is assumed to operate adiabatically and under the assumptions of the ideal gas model. The work input into the compressor is

$$W_{Compressor} = \frac{\dot{m}_{air} * C_{p,air} * (T_{2,S} - T_{ambient})}{\eta_{Compressor}} \tag{4.11}$$

where $\dot{m}_{air}$ is the mass flow rate of air entering the compressor; $C_{p,air}$ is the average specific heat capacity of air; $\eta_{Compressor}$ is the compressor's isentropic efficiency (assumed to be 85 $\%$) ; and $T_{2,S}$ is the isentropic outlet temperature [97].

$$T_{2,S} = T_{ambient} * \frac{P_2}{P_{ambient}}^{(k-1)/k} \tag{4.12}$$

where P_2 is the electrolyzer operating temperature; and k is the specific heat ratio of air. The compressor outlet temperature is

$$T_2 = \frac{W_{Compressor}}{\dot{m}_{air} * C_{p,air}} + T_{ambient} \tag{4.13}$$

Heat Exchanger Energy Input

A heat exchanger is used in the system to heat the reactant streams to the same temperature as the electrolyis cell. The heat exchanger is assumed to operate isobarically.

$$Q_{HE} = \dot{m}_i * C_{p,i} * (T_{outlet} - T_{inlet}) \tag{4.14}$$

where $C_{p,i}$ represents the specific heat capacity of the reactant; $\dot{m}_i$ represents the mass flow rate of the reactant stream; T_{outlet} represents the operating temperature of the electrolysis cell; and T_{inlet} represents the heat exchanger inlet temperature.

4.1.2 Economic Modeling

The levelized cost of ammonia (LCOA) is a measure of the normalized cost per unit mass of produced ammonia.

$$LCOA = \frac{C_{Cap} * CRF + C_{O\ \&\ M} + C_{Energy}}{M_{NH3}} \tag{4.15}$$

where the capital cost of the system (C_{Cap}) is a function of sum of the cost of all the components in the electrolysis cell, including peripheral parts, and the balance of plant cost (Table 4.1).

Table 4.1: Component Cost per Area [98].

Component	**Price per Area**
Proton Exchange Membrane	\$50/m^2
Electrode	\$20/m^2
Bipolar Plate	\$35/m^2
Peripheral Parts	\$3.46/m^2

The capital recovery factor (CRF) transform the total cost into a constant annual payment accounting for inflation.

$$CRF = \frac{k_d * (1 + k_d)^j}{(1 + k_d)^j - 1} \tag{4.16}$$

where k_d corresponds to an inflation rate (6.5% [99]) and j corresponds to a system lifetime of 30 years [100]. The operational cost ($C_{O\ \&\ M}$) corresponds to 2% of the capital cost [99]. Finally, the electrical cost corresponds to the total power required by the system times the levelized cost of electricity [101].

CHAPTER 5
RESULTS AND DISCUSSION

5.1 System Description

There are two different electrochemical routes in which ammonia can be synthesized using renewable resources (Fig. 5.1 and Fig. 5.2). The first route involves the direct Nitrogen reduction with N_2 and H_2O as reactants (Fig. 5.1).

$$N_{2_{(g)}} + 3H_2O \longrightarrow 2NH_{3_{(g)}} + \frac{3}{2}O_{2_{(g)}} \tag{5.1}$$

Here, liquid water is used as the source of hydrogen and air is used as the source of nitrogen (Fig. 5.1). The oxygen in the air is removed to form pure nitrogen through cryogenic separations. This consists of the liquefaction and distillation of the Nitrogen, Oxygen, Argon, and other gases in the air [102]. Liquid water and gaseous nitrogen are compressed and heated to reach the desired operating conditions of the electrolysis cell. Nitrogen and water enter the electrolysis cell to produce ammonia and hydrogen. Finally, ammonia is separated from nitrogen and hydrogen. Ammonia has a significantly higher liquefaction temperature than hydrogen and nitrogen, so it can be separated by compressing the outlet flow to 0.8 MPa. At this pressure, ammonia condenses at 20 $^{\circ}C$ while hydrogen and nitrogen remain in a gaseous state [103]. Then, the liquid ammonia can be easily separated from the gaseous nitrogen and hydrogen using a distillation column. This process (Fig. 5.1) uses water as the source of hydrogen. Since this process uses a renewable source of hydrogen instead of methane or other hydrocarbons, it can be easily integrated with renewable energy sources to produce ammonia without carbon dioxide emissions.

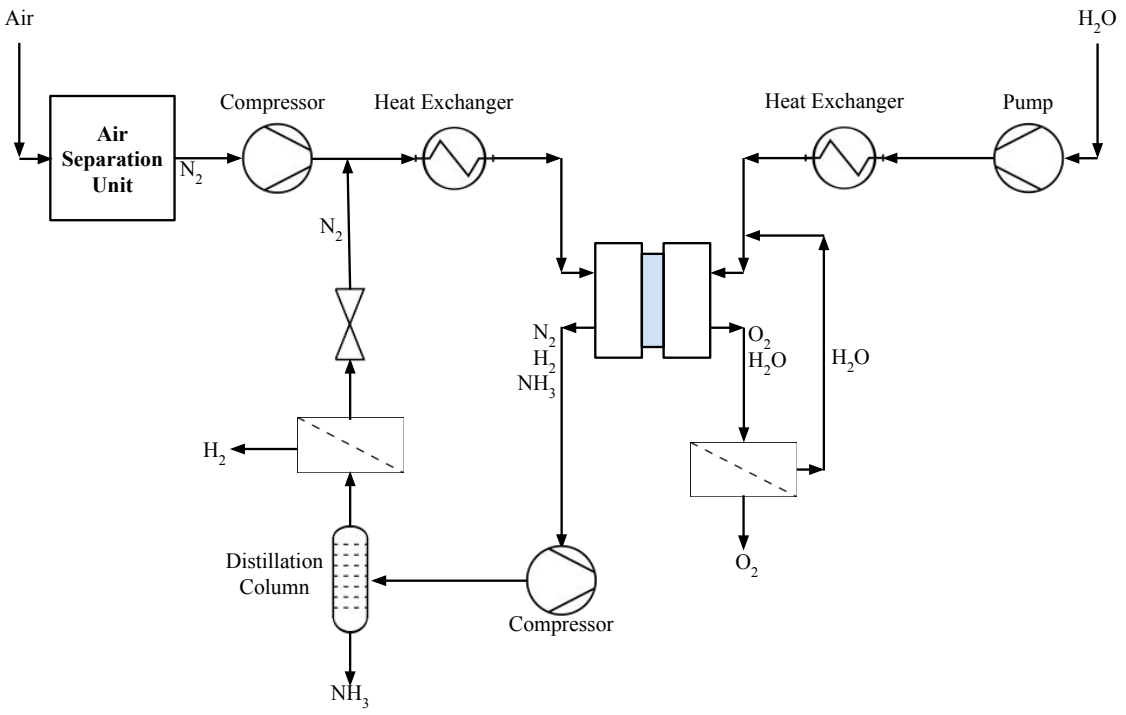

Figure 5.1: Direct Nitrogen reduction with N_2 and H_2O as reactants.

An alternative route is the Nitrogen reduction with N_2 and H_2 as reactants (Fig. 5.2).

$$N_{2_{(g)}} + 3H_{2_{(g)}} \longrightarrow 2NH_{3_{(g)}} \tag{5.2}$$

Similarly to the Haber-Bosch process, this reaction requires an external source of hydrogen. However, to achieve renewable ammonia, hydrogen is produced with a separate water electrolysis cell (Fig. 5.2). Similarly to the direct Nitrogen reduction with N_2 and H_2O as reactants (Fig. 5.1), the oxygen in the air is removed using cryogenic air separation and the gaseous hydrogen and nitrogen are compressed and heated to reach the desired operating conditions of the electrolysis cell. The main difference is that this process requires two separate electrolysis cells (one for water splitting and one for nitrogen reduction). The main byproduct of this reaction is hydrogen, which can be recycled and used as a reactant in the anode of the electrolysis cell. The third and final subprocess consists of the separation of the desired products (NH_3) from the outlet flow of the electrolysis cell. A

Nitrogen reduction system with N_2 and H_2 as reactant (Fig. 5.2) can use methane and other hydrocarbons as a hydrogen source. However, water is used for a carbon neutral process.

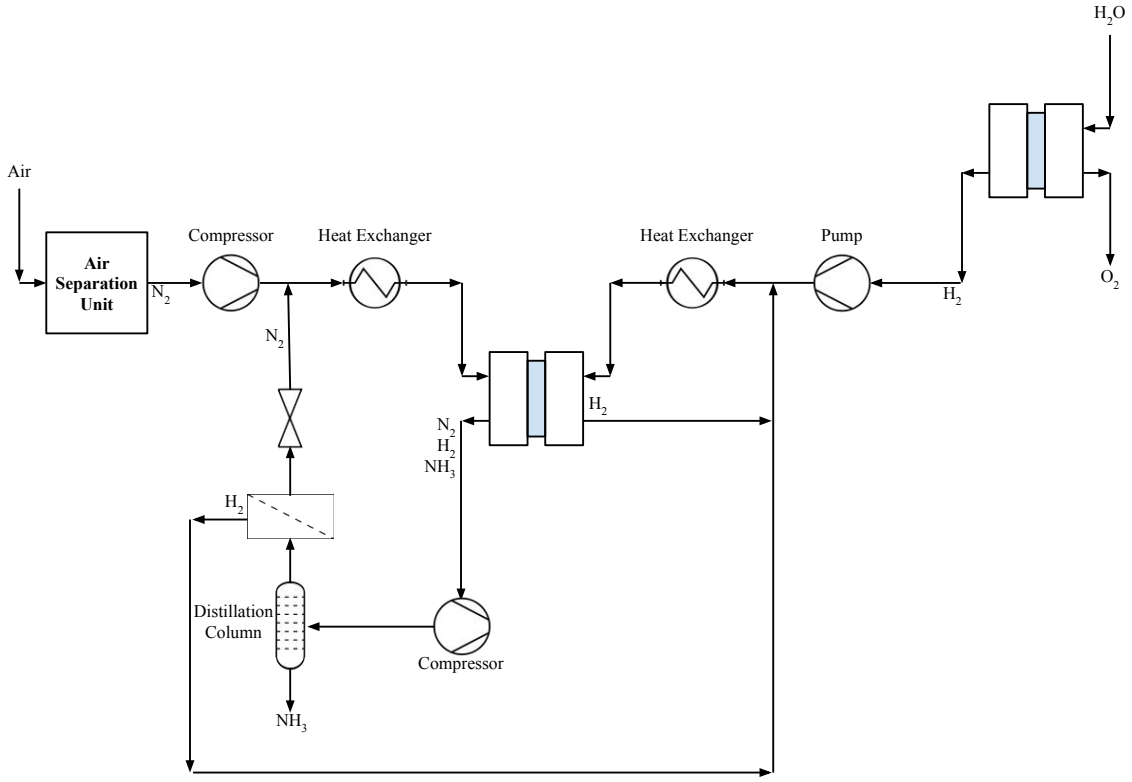

Figure 5.2: Nitrogen reduction with N_2 and H_2 as reactants.

The operating conditions are defined in Table 5.1 unless otherwise specified. These conditions are used as the base scenario.

Table 5.1: Base Case Parameters.

Parameter	**Base Case Value**
T	$25°C$
P	1atm
FE	10%
i_o	$10^{-9} A/m^2$
i	0.2 A/m^2

5.2 Reactor Design Considerations

There are three main reactor designs for the low-temperature electrochemical ammonia synthesis (Fig. 5.3

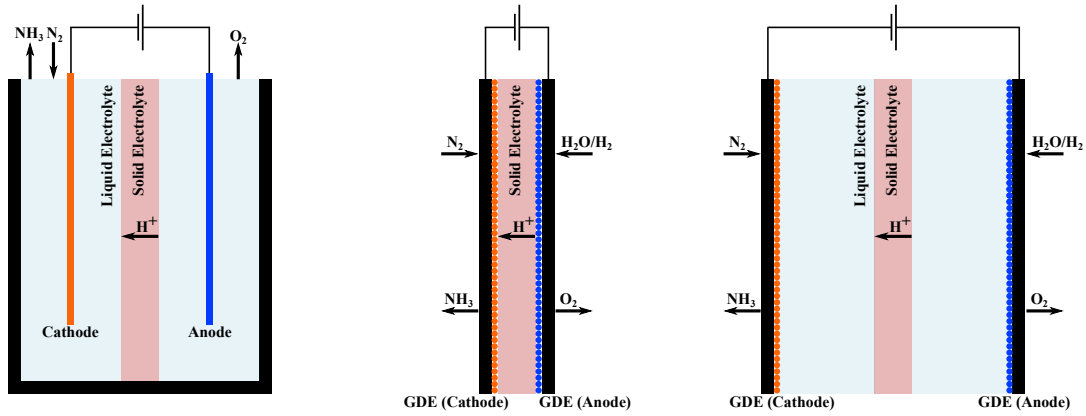

(a) (b) (c)

Figure 5.3: Different electrochemical ammonia production reactor schemes. (a) Alkaline reactor, (b) Proton exchange membrane reactor, or (c) Gas diffusion electrode reactor.

Most of the current research is performed in alkaline electrolysis reactors (Fig. 5.3a). This type of reactor consists of two electrodes immersed in an alkaline aqueous solution. The electrodes are separated by a membrane that allows for the transport of protons (H+) or hydroxide ions (OH-) but separates the products. An advantage of alkaline electrolyzers is that they can be manufactured using cheap and abundant materials [104].

In an alkaline reactor, the nitrogen gas is dissolved in the aqueous electrolyte in the cathode side of the reactor, which limits the maximum concentration of nitrogen in the cathode to 0.6 mol/m^3 [88]. Additionally, the nitrogen has to diffuse through the aqueous electrolyte in order to reach the electrode. The diffusion coefficient of nitrogen in water is 1.88e-9 m^2/s [89]. The biggest disadvantage of alkaline reactors is that the mass transport of nitrogen is limited by the concentration and poor diffusivity of nitrogen in water. Hence, an alkaline reactor experiences a limiting effective current density of around 7 mA/cm^2 (Fig. 5.4). Most of the voltage losses seen in an alkaline reactor for ammonia synthesis are activation losses due to the slow kinetics of both the nitrogen reduction reaction in

the cathode (NRR) and the oxygen evolution reaction in the anode (OER). However, the biggest drawback of this type of reactor is the mass transport limitations due to the poor solubility of nitrogen in water.

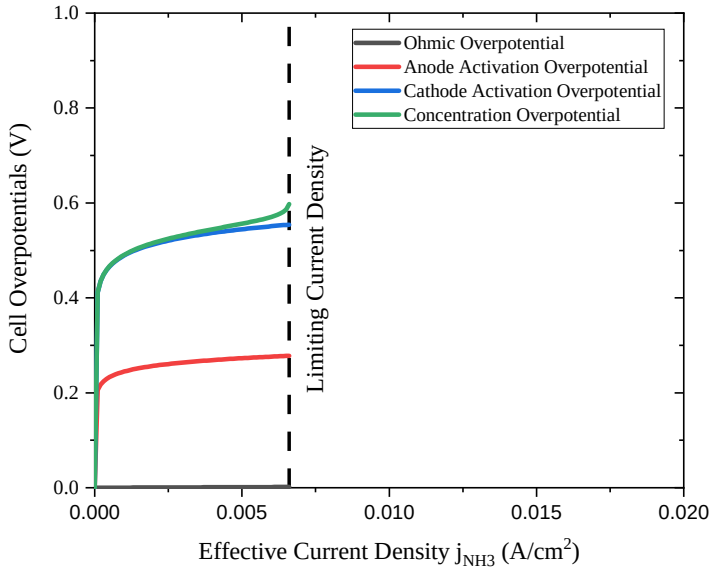

Figure 5.4: Overpotentials of an Alkaline reactor for nitrogen fixation for the direct Nitrogen reduction with N_2 and H_2O as reactants. T = 25 °, P = 1 atm, FE = 10%, i_o = $10^{-9} A/cm^2$, $L_{electrolyte}$ = 200 μm.

An alternative to alkaline reactors is the proton exchange membrane electrolysis cell (PEMEC). Proton exchange membrane electrolysis is mostly used for water electrolysis. However, there has been a number of studies that use proton exchange membrane reactors for the electrosynthesis of ammonia. These studies are just a proof of concept and lack the depth of the existing studies for alkaline reactors. These reactors consist of two electrodes which are placed in contact with a proton exchange membrane, usually made out of Nafion (Fig. 5.3b). The reactants are fed to the electrodes through a porous gas diffusion layer. The mass transport properties of the porous layer are vastly superior to those of a liquid electrolyte. Hence, proton exchange membrane electrolysis cells have an effective limiting current density of around 3 A/cm^2. Most of the losses in a PEM reactor for ammonia synthesis are activation losses. However, the anode activation overpotential of a direct

Nitrogen reduction reactor with N_2 and H_2O as reactants (Fig. 5.5a) is five times the anode activation overpotential of a Nitrogen reduction reactor with N_2 and H_2 as reactants. (Fig. 5.5b). This is due to the faster kinetics of the hydrogen evolution reaction than the oxygen evolution reaction. The PEM reactor also experience significant ohmic losses due to the poor conductivity of solid electrolytes.

Finally, the last reactor design that can be used for the low-temperature electrochemical synthesis of ammonia is the gas diffusion electrode (GDE) reactor. There has been no reported work done with this type of reactor for ammonia synthesis. However, they are gaining popularity for application on carbon dioxide conversion and some groups are starting to adapt the technology for nitrogen fixation. A gas diffusion electrode reactor consists of two electrodes formed by a catalyst supported on a porous carbon layer. The electrodes are separated by a liquid electrolyte and a membrane. The electrode creates a gas-solid-liquid interface in which the reaction takes place (Fig. 5.3c). Since the reactants are fed through a porous layer rather than through the liquid, a gas diffusion electrode reactor has similar mass transport characteristics as a PEM reactor. Accordingly, the limiting current density in a GDE reactor is 3 A/cm^2. The majority of the losses experienced in a GDE reactor can be attributed to activation losses, with the Nitrogen reduction reactor with N_2 and H_2 as reactants having a better performance than the direct Nitrogen reduction reactor with N_2 and H_2O as reactants due to the faster kinetics in the anode (Fig. 5.6).

This section highlights the key differences between alkaline, PEM, and GDE electrolysis cells. Alkaline electrolysis cells have the limitation of the solubility limit of nitrogen in aqueous electrolytes. At these low concentrations of nitrogen, mass transport limitation significantly hinders the reactor performance in effective current densities in the order of 7 mA/cm^2. Operating at low current densities increase the size and capital cost of the system. Hence, moving towards reactor designs that operate using gaseous nitrogen delivered to the cathode through porous gas diffusion layers can help overcome these performance and solubility challenges. We will focus on studying the thermodynamics and economics

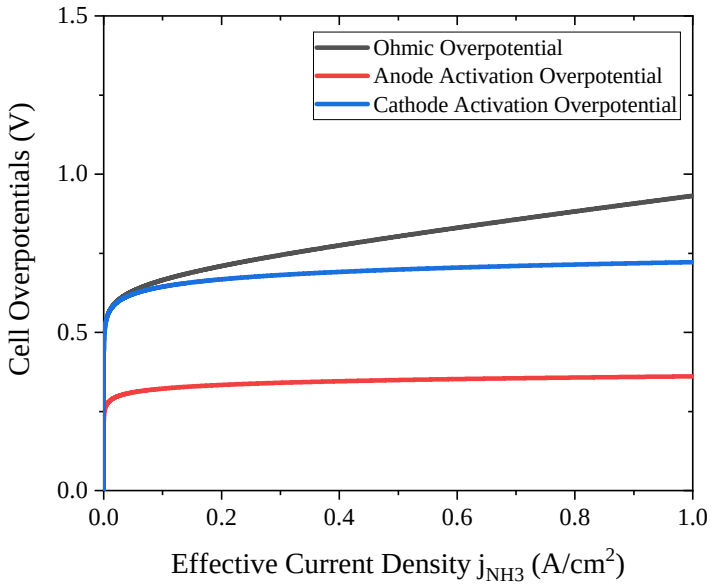

(a)

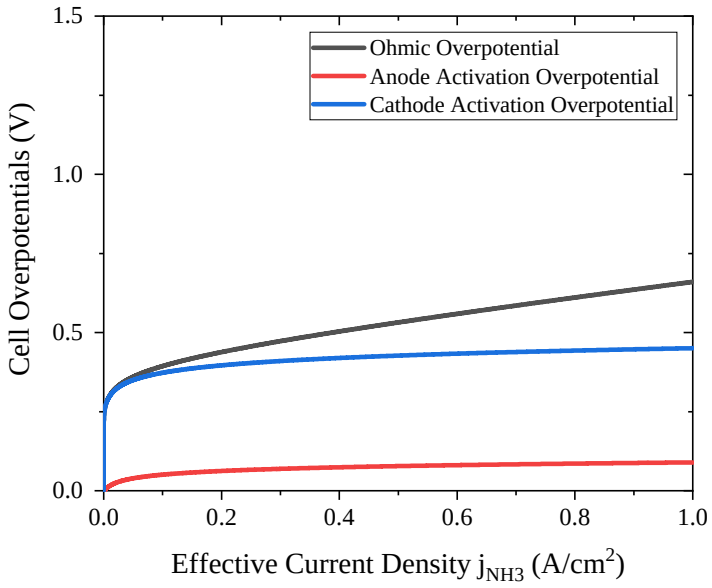

(b)

Figure 5.5: Overpotentials of a Proton Exchange Membrane reactor for nitrogen fixation for the direct Nitrogen reduction with N_2 and H_2O as reactants (a) and Nitrogen reduction with N_2 and H_2 as reactants (b). T = 25 °, P = 1 atm, FE = 10%, $i_o = 10^{-9} A/cm^2$, $L_{membrane}$ = 200 μm.

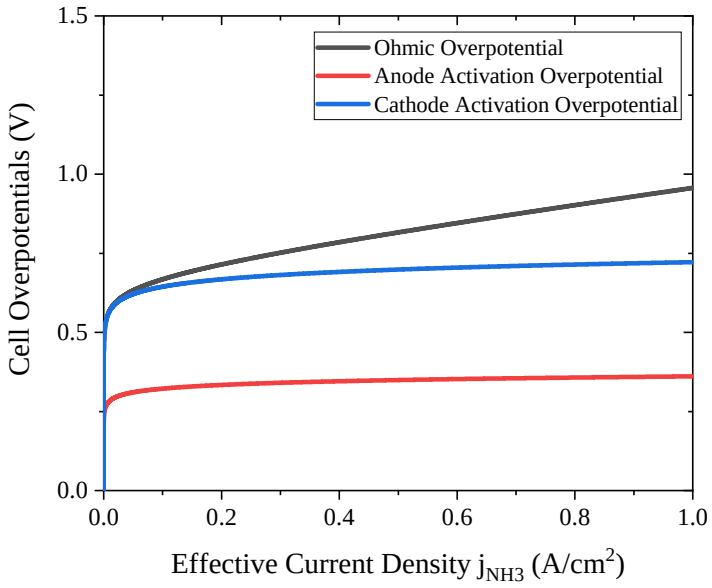

(a)

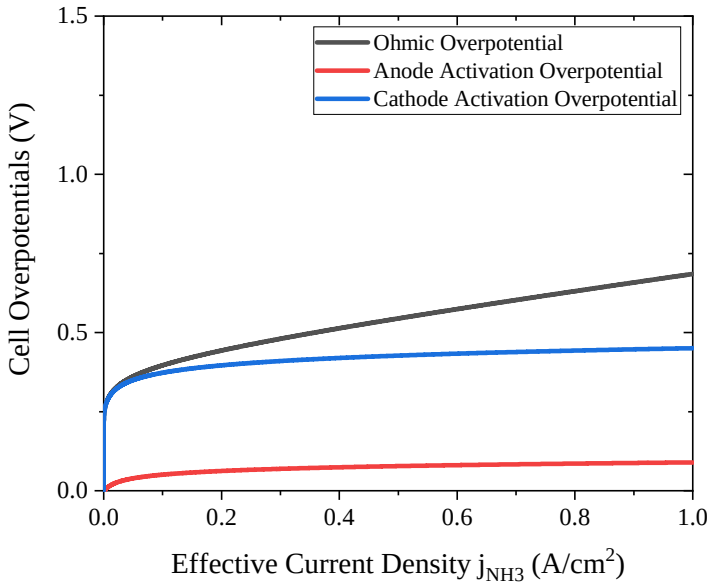

(b)

Figure 5.6: Overpotentials of a Gas Diffusion Electrode reactor for nitrogen fixation for nitrogen fixation for the direct Nitrogen reduction with N_2 and H_2O as reactants (a) and Nitrogen reduction with N_2 and H_2 as reactants (b). T = 25 °, P = 1 atm, FE = 10%, i_o = $10^{-9} A/cm^2$, $L_{membrane}$ = 200 μm, $L_{electrolyte}$ = 200 μm.

of reactors that implement porous gas diffusion layers to enhance mass transport in the next couple sections.

5.3 The Impact of Catalyst Performance and Operating Conditions on Electrochemical Ammonia Synthesis

The performance of an electrochemical system can be tuned by carefully selecting the operating conditions. It is important to understand the impact changing each one of the design parameters has on the performance of the system. Herein, we present a parametric study to determine the optimal operating conditions to maximize the energy efficiency of the system.

5.3.1 Impact of Temperature on Performance

Increasing the temperature have a positive effect on the reaction kinetics. Additionally, elevated temperatures lower the activation and ohmic overpotentials and improve the reactor efficiency. However, a downside of operating at elevated temperatures is that it entails additional heat input to increase the temperature of the reactants. A temperature range between $20\ ^{\circ}C$ and $100\ ^{\circ}C$ is chosen to ensure electrolyte stability.

For a direct Nitrogen reduction system with N_2 and H_2O as reactants, the energy efficiency increases as temperature increases. The total electric energy input required decreases as temperature increases due to a decrease in the open circuit voltage (Fig. 4.2) and a decrease in the activation and ohmic overpotentials due to an improvement on the reaction kinetics and the electrolyte conductivity. However, as temperature increases the heat input required to sustain the reaction increases as well (Fig. 4.1a). Additionally, the heat input required to heat the reactants increases linearly as temperature increases (eqn. 4.16). For a direct Nitrogen reduction system with N_2 and H_2O as reactants, the energy efficiency goes from 5.93$\%$ at $20\ ^{\circ}C$ to 6.73 $\%$ at $100\ ^{\circ}C$ (Fig. 5.7a).

Similarly, the energy efficiency of a Nitrogen reduction system with N_2 and H_2 as re-

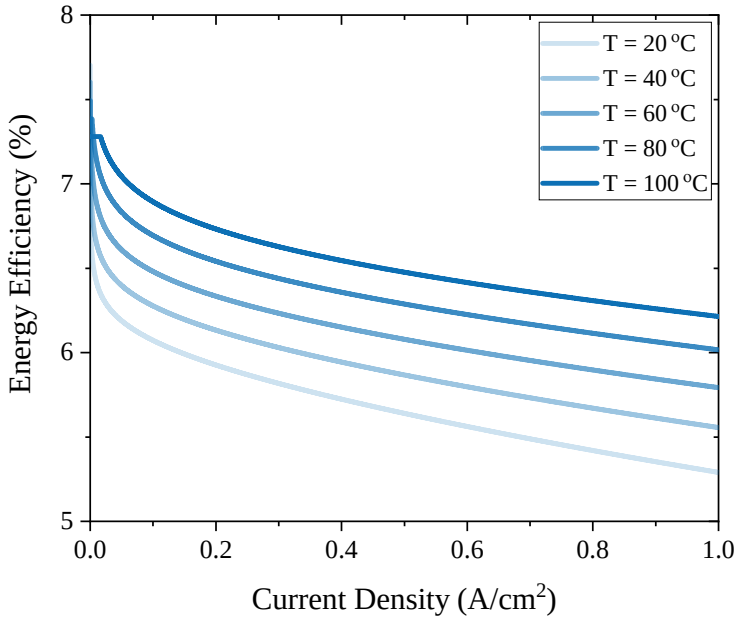

(a)

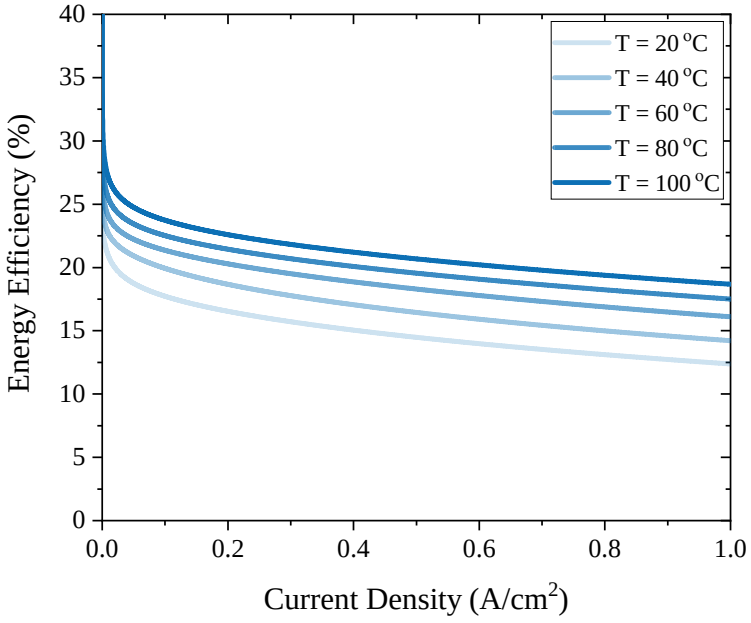

(b)

Figure 5.7: Impact of temperature on performance of a direct Nitrogen reduction system with N_2 and H_2O as reactants (a) and a Nitrogen reduction system with N_2 and H_2 as reactants (b).

actants increases as temperature increases. The total electric input required for the reaction decreases as temperature increases due to a decrease in the overpotentials. However, temperature has a negative effect in the open circuit voltage of this reaction and the open circuit voltage increases with an increase in temperature (Fig. 4.2). Finally, as temperature increases, the heat input required to sustain the reaction (Fig. 4.1b) decreases and the heat input required to heat the reactants increases. For a Nitrogen reduction system with N_2 and H_2 as reactants, the energy efficiency goes from 16.5% to 22.6% when the temperature increases from 20 $^{\circ}C$ to 100 $^{\circ}C$ (Fig. 5.7b).

Overall, increasing the temperature leads to improvements in efficiency in both a direct Nitrogen reduction system with N_2 and H_2O as reactants and a Nitrogen reduction system with N_2 and H_2 as reactants. However, the second system is more sensitive to changes in temperatures than the first system. In fact, a change in temperature from 20 $^{\circ}C$ to 100 $^{\circ}C$ leads to a 13.5% improvement for a direct Nitrogen reduction system with N_2 and H_2O as reactants and a 37% improvement for a Nitrogen reduction system with N_2 and H_2 as reactants. In order to maximize the energy efficiency of the system, we desire to increase the temperature as high as possible. However, the maximum temperatures are limited by the stability of the electrolyte. Hence, an operating temperature of 100 $^{\circ}C$ is ideal to achieve the best performance.

5.3.2 Impact of Pressure on Performance

Increasing the operating pressure has a positive effect on reaction rates and energy efficiency. Higher pressures improve the reaction kinetics, lowering the activation overpotential and favoring higher rates. However, a downside of operating at elevated pressures is the additional work input required for compression of the reactants during the pretreatment process and the increase in capital cost for the infrastructure required to operate at these pressures. A pressure range between 1 atm and 5 atm is chosen to minimize the infrastructure required and to minimize safety hazards due to the elevated pressures. However, there

is no physical limitations that would impede further increase in pressure.

For an electrochemical reaction, the overall energy efficiency improves with an increase in pressure. The total energy input decreases due to an enhancement of the reaction kinetics. However, for a direct Nitrogen reduction system with N_2 and H_2O as reactants, pressure has a negative impact on the reversible cell potential (eqn. 4.4). Higher pressures favor the backward reaction, increasing the voltage required for the reaction to take place. The opposite is true for a Nitrogen reduction system with N_2 and H_2 as reactants, higher pressure favors the forward reaction and decrease the reversible cell potential. Finally, the work required to compress the reactants increases as the operating pressure increases. However, the work required by the hydrogen compressor is significantly higher than the work required by the water pump.

The energy efficiency for a direct Nitrogen reduction system with N_2 and H_2O as reactants improves from 5.93% at 1 atm to 6.2% at 5 atm (Fig. 5.8a). For a Nitrogen reduction system with N_2 and H_2 as reactants, the energy efficiency goes from 16.5% to 19.8% when the pressure increases from 1 atm to 5 atm (Fig. 5.8b). This represents a 4.6% improvement for a direct Nitrogen reduction system with N_2 and H_2O as reactants and a 20% improvement for a Nitrogen reduction system with N_2 and H_2 as reactants. However, most of the performance improvement occurs at low pressures. For example, by increasing the pressure from 1 atm to 2 atm the performance of a Nitrogen reduction system with N_2 and H_2 as reactants improves 8%. Additionally, when the pressure increases from 4 atm to 5 atm the performance increases only 2.5%. Hence, increasing the pressure further will only result in marginal improvements in the system performance and are not worth the additional capital investments. Hence, increasing the pressure is attractive to increase the energy efficiency. However, the drawbacks of operating at high pressures (increased capital requirements) outweigh the benefits (increased energy efficiency). Hence, we have chosen to limit the operating pressures to 5 atm.

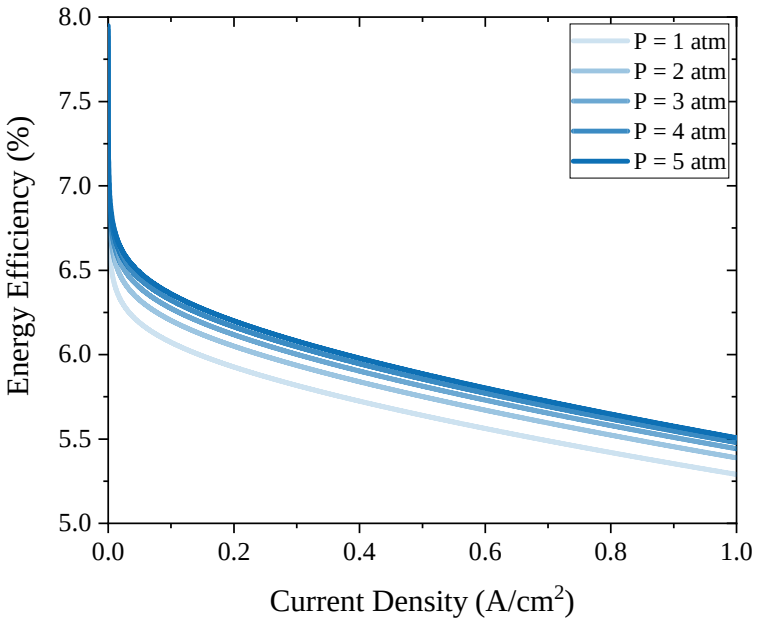

(a)

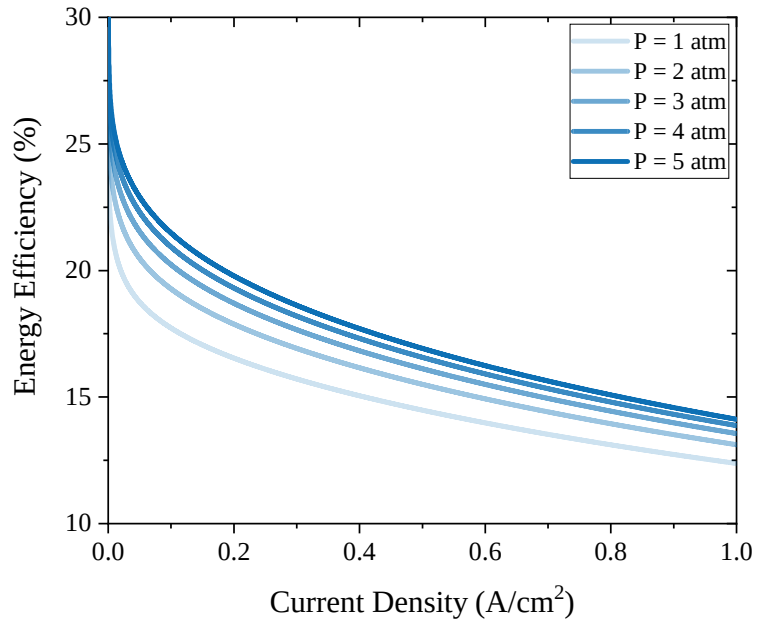

(b)

Figure 5.8: Impact of pressure on performance of a direct Nitrogen reduction system with N_2 and H_2O as reactants (a) and a Nitrogen reduction system with N_2 and H_2 as reactants (b).

5.3.3 Impact of Activity on Performance

A larger exchange current density signifies a faster reaction with lower activation overpotentials. A smaller exchange current density signifies a slower reaction with larger activation overpotentials. For both a direct Nitrogen reduction system with N_2 and H_2O as reactants and a Nitrogen reduction system with N_2 and H_2 as reactants, the performance improves with an increase in the exchange current density. For a direct Nitrogen reduction system with N_2 and H_2O as reactants, the energy efficiency improves from 5.93% at an exchange current density of 1e-9 A/cm^2 to 7.12% at an exchange current density of 1e-1 A/cm^2 (Fig. 5.9a). However, for Nitrogen reduction system with N_2 and H_2 as reactants, the energy efficiency goes from 16.5% to 31.1% when the exchange current density increases from 1e-9 A/cm^2 to 1e-1 A/cm^2 (Fig. 5.9b). This represents a 20% improvement for a direct Nitrogen reduction system with N_2 and H_2O as reactants and a 88% improvement Nitrogen reduction system with N_2 and H_2 as reactants. Hence, a direct Nitrogen reduction system with N_2 and H_2O as reactants is less sensitive to changes in the exchange current density than a Nitrogen reduction system with N_2 and H_2 as reactants. This is because a the first system has fast kinetics in the anode (HER) and slow kinetics in the cathode (NRR) and the second system suffers from poor kinetics in both the anode and the cathode (NRR and OER).

This section highlights the impact the catalyst activity has on the performance of an electrochemical system. For the electrochemical synthesis of ammonia, the theoretical energy efficiency improves with an increase in the exchange current density. Increasing the exchange current density decreases the activation overpotential. Hence, increasing the overall energy efficiency. In theory, the best performance is achieved at the highest possible exchange current density. However, the current available catalysts have poor exchange current densities. We envision that with further research the exchange current density can be improved to levels close to 1e-7 A/cm^2. Hence, when optimizing the system performance, we will limit the exchange current density to 1e-7 A/cm^2, as operating with higher exchange

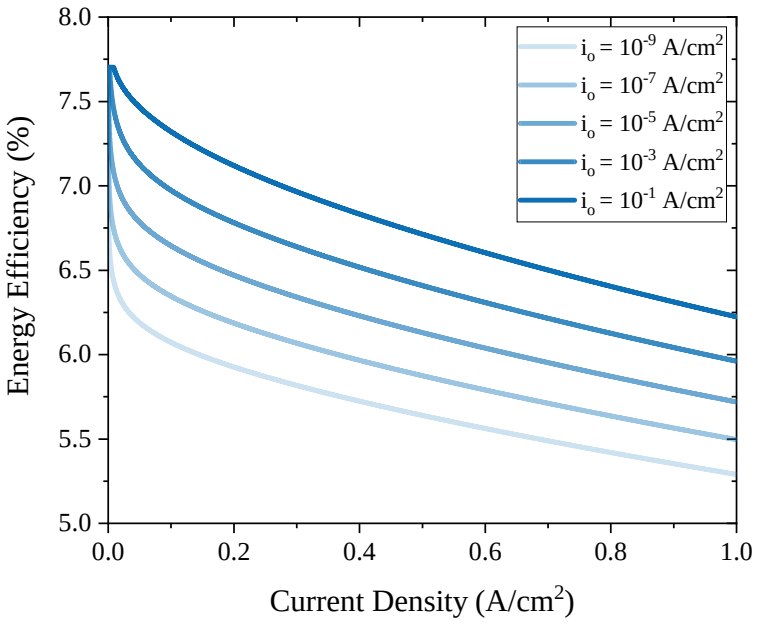

(a)

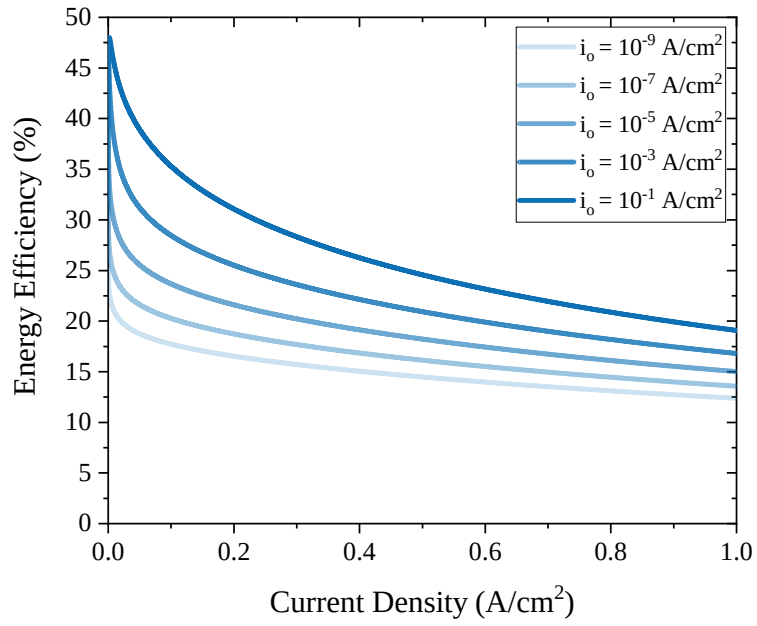

(b)

Figure 5.9: Impact of exchange current density on performance of a direct Nitrogen reduction system with N_2 and H_2O as reactants (a) and a Nitrogen reduction system with N_2 and H_2 as reactants (b).

current densities are unrealistic. Additionally, current research in developing catalysts for electrochemical nitrogen fixation do an excellent job on characterizing the selectivity of the catalyst. However, current research fails to characterize the activity of electrocatalysts for nitrogen fixation. In the future, research should include a complete characterization of the catalyst activity as well as its selectivity.

5.3.4 Impact of Selectivity on Performance

The biggest limitation of electrochemical nitrogen fixation is the poor selectivity at practical current densities. High faradaic efficiencies are usually achieved at low current densities. However, to reduce the cost of ammonia, the reactor should operate at current densities in the order of 0.1 A/cm^2. Hence, researchers need to study and improve the faradaic efficiency of catalysts at these current densities. This section investigates the dependency the system performance has on the faradaic efficiency for the different reactor types. The faradaic efficiency of a reaction describes the efficiency at which electrons are transferred to facilitate a reaction. Accordingly, higher faradaic efficiencies will reduce the total current needed to produce the same amount of ammonia. Lower currents lead to lower energy consumption. Hence, high faradaic efficiencies are preferred to maximize the energy efficiency of the system.

For both a direct Nitrogen reduction system with N_2 and H_2O as reactants and a Nitrogen reduction system with N_2 and H_2 as reactants, the performance improves with an increase in the faradaic efficiency. For a direct Nitrogen reduction system with N_2 and H_2O as reactants, the energy efficiency improves from 5.93$\%$ at a faradaic efficiency of 10% to 50% at a faradaic efficiency of 90% (Fig. 5.10a). However, for a Nitrogen reduction system with N_2 and H_2 as reactants, the energy efficiency goes from 16.5$\%$ to 44.35$\%$ when the faradaic efficiency increases from 10% to 90% (Fig. 5.10b). This represents a 743$\%$ improvement for a direct Nitrogen reduction system with N_2 and H_2O as reactants and a 170$\%$ improvement for a Nitrogen reduction system with N_2 and H_2 as reactants. Accord-

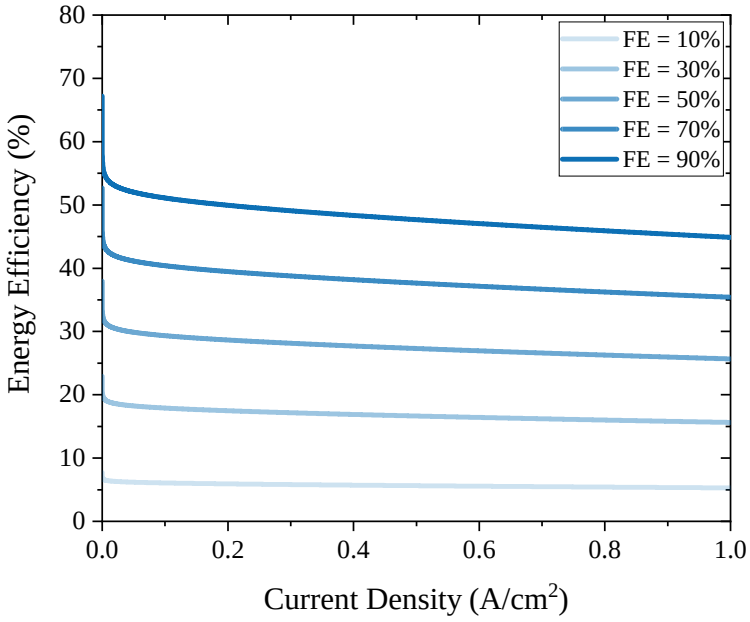

(a)

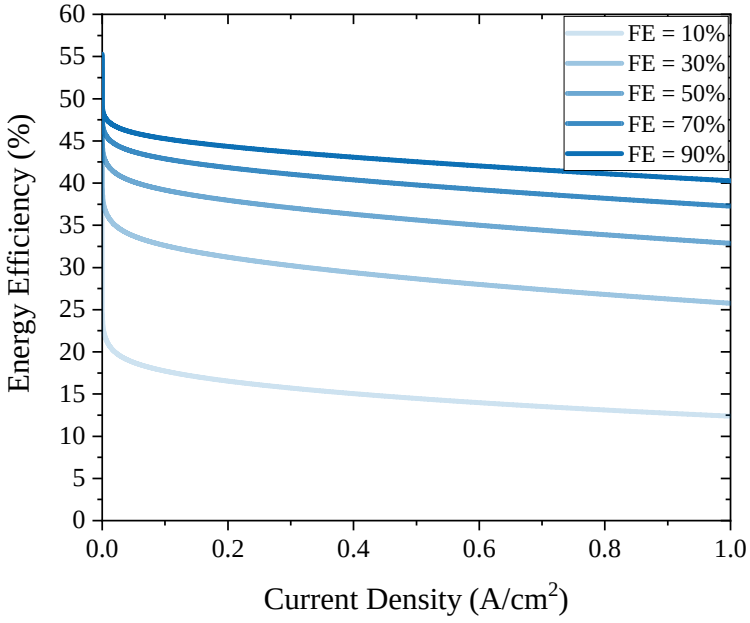

(b)

Figure 5.10: Impact of faradaic efficiency on performance of a direct Nitrogen reduction system with N_2 and H_2O as reactants (a) and a Nitrogen reduction system with N_2 and H_2 as reactants (b).

ingly, a direct Nitrogen reduction system with N_2 and H_2O as reactants is more efficient than a Nitrogen reduction system with N_2 and H_2 as reactants at high faradaic efficiencies (above 70%). However, a Nitrogen reduction system with N_2 and H_2 as reactants is more efficient at efficiencies below 70%.

This section highlights the impact the catalyst selectivity has on the performance of an electrochemical system. For the electrochemical synthesis of ammonia, the theoretical energy efficiency improves with an increase in the faradaic efficiency. The analysis shows that the best energy efficiency is achieved as the faradaic efficiency approaches 100%. However, in reality the best faradaic efficiencies found in research are in the order of 10%. However, these efficiencies are achieved at small current densities and the faradaic efficiencies at practical current densities are expected to be significantly lower. Realistically, we expect than in the next decades the faradaic efficiencies can be improved to around 30%. Hence, the optimal faradaic efficiencies for the practical optimization will be limited at 30%. Additionally, we recommend researchers to study the selectivity of catalyst at practical current densities, as this will give a better understanding of the catalyst's selectivity and durability at conditions that are realistic and practical for commercial applications.

5.4 Economic Considerations

The levelized cost of ammonia depends on the electrical cost and the capital cost of the system. We use a sensitivity analysis to understand the response of the system to varying the parameters. This can inform the correct direction to minimize the levelized cost of ammonia. We increased and decreased by 50% all the parameters that contribute to the levelized cost of ammonia and studied the variation from the base.

For a direct nitrogen reduction system with nitrogen and water as reactants, the biggest contributor to the levelized cost of ammonia is the electrical cost (Fig. 5.11). High electricity costs and poor catalyst selectivity drive the levelized cost of ammonia up. The capital cost of the system also contributes to a portion of the levelized cost of ammonia. However,

decreasing the cost of electricity and the catalyst selectivity are far more important than decreasing the capital cost as they have a bigger effect in the levelized cost of ammonia.

For a direct nitrogen reduction system with nitrogen and water as reactants, decreasing the cost of the components reduces the price linearly. For example, a 50% change in the cost of Nafion, leads to a 50% change in the contribution of Nafion to the levelized cost of ammonia. However, since most of the cost comes from the electrical cost, changing the cost of Nafion (or any other component) by 50% only results in a change in the levelized cost of ammonia of around 0.1%. The biggest contributor into the capital cost is the cost of Nafion and the cost of the bipolar plate.

Decreasing the electrical costs is primordial to decrease the levelized cost on ammonia. Increasing the energy efficiency of the system and reducing the cost of electricity will reduce the levelized cost of ammonia. The electrical costs account for most of the levelized cost of ammonia. A 50% change in the cost of electricity results in a 49% change in the levelized cost of ammonia. Increasing the energy efficiency also decreases the levelized cost of ammonia since producing ammonia will require less energy. In Section 5.3 we studied the relationship between the system parameters and the energy efficiency of the system. We found that increasing the temperature, pressure, faradaic efficiency, and exchange current density lead to an increase in efficiency. However, the biggest improvement in energy efficiency occurs when the faradaic efficiency is increased. Te relationship between the levelized cost of ammonia and faradaic efficiency is not linear or symmetric. In fact, a 50% increase in the faradaic efficiency will not lead to a change of the same magnitude as a 50% decrease in the faradaic efficiency. A 50% decrease in the faradaic efficiency results in a 99% increase in the levelized cost of ammonia. However, a 50% increase in the faradiac efficiency results in a 33% increase in the levelized cost of ammonia. Changing the other parameters, results in a 1-3% change in the levelized cost of ammonia.

For a nitrogen reduction system with nitrogen and hydrogen as reactants, the biggest contributor to the levelized cost of ammonia is the electrical cost (Fig. 5.12). However,

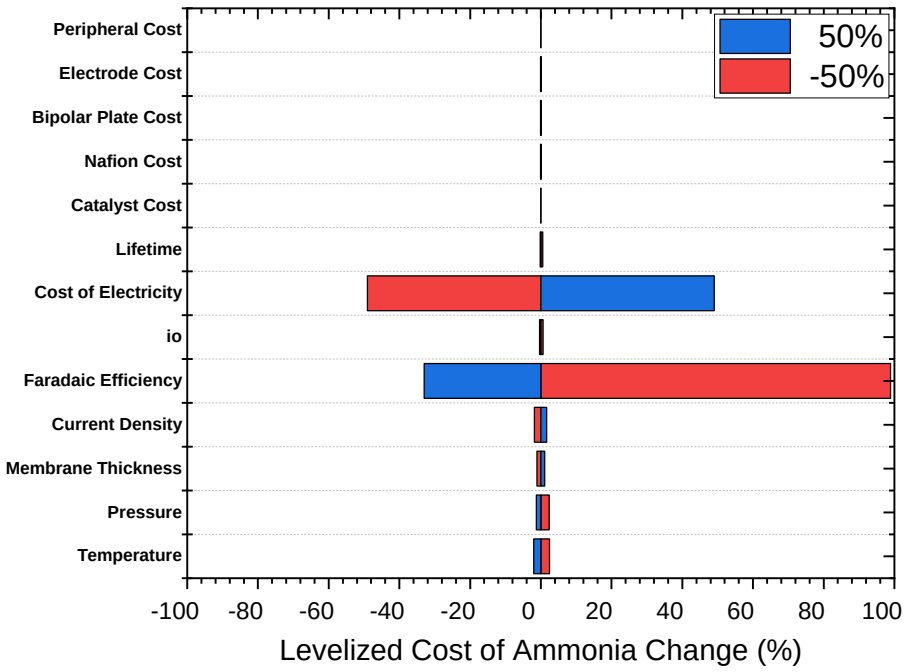

Figure 5.11: Sensitivity analysis of a direct Nitrogen reduction cell with N_2 and H_2O as reactants.

this system has a higher efficiency than a direct nitrogen reduction system with nitrogen and water as reactants because of the faster kinetics of the hydrogen reduction reaction. For this reason, the capital represents a higher percentage of the overall cost of the system. However, the poor performance of the system means that most of the cost comes from energetic losses.

For a nitrogen reduction system with nitrogen and hydrogen as reactants, changing the cost of the components changes the price linearly. However, most of the cost comes from the electrical cost, so changing the cost of Nafion (or any other component) by 50% only results in a change in the levelized cost of ammonia of around 0.3%. The biggest contributor into the capital cost is the cost of Nafion and the cost of the bipolar plate.

Increasing the energy efficiency of the system and reducing the cost of electricity will reduce the levelized cost of ammonia. The electrical costs account for most of the levelized

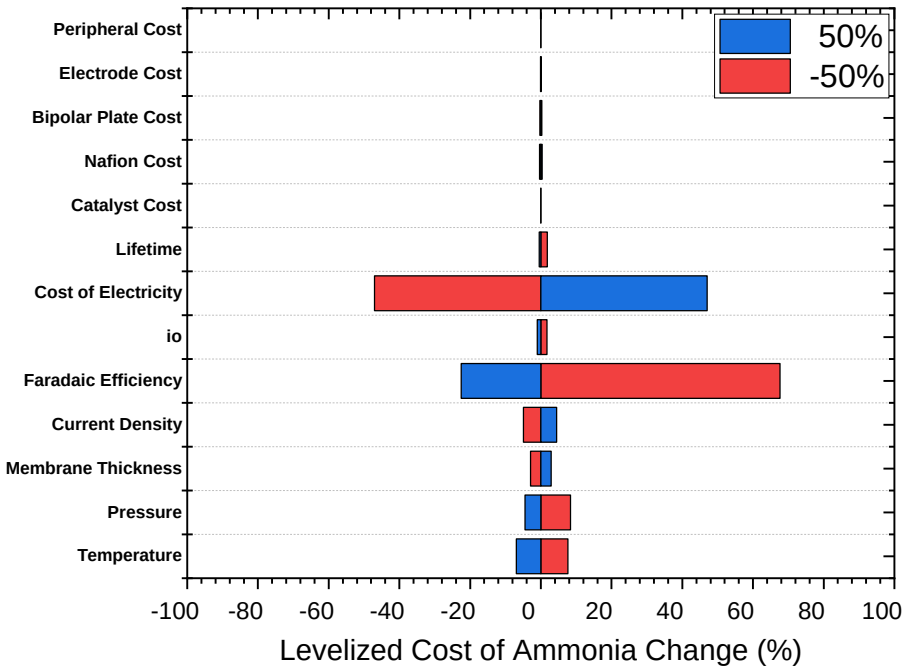

Figure 5.12: Sensitivity analysis of a Nitrogen reduction cell with N_2 and H_2 as reactants.

cost of ammonia. So, a 50% change in the cost of electricity results in a 47% change in the levelized cost of ammonia. Increasing the energy efficiency also decreases the levelized cost of ammonia since producing ammonia will require less energy. The biggest improvement in energy efficiency occurs when the faradaic efficiency is increased. The relationship between the levelized cost of ammonia and faradaic efficiency is not linear or symmetric. A 50% decrease in the faradaic efficiency results in a 68% increase in the levelized cost of ammonia. However, a 50% increase in the faradaic efficiency results in a 23% increase in the levelized cost of ammonia. Changing the other parameters, results in a 3-8% change in the levelized cost of ammonia.

A sensitivity analysis provides insight into which direction to take to minimize the levelized cost of ammonia. We found that decreasing the cost of electricity and increasing the faradaic efficiency have the biggest effect in decreasing the levelized cost of ammonia. We found that increasing temperature, pressure, exchange current density, faradaic efficiency,

and system lifetime; and that decreasing the cost of electricity, current density, membrane thickness, and component costs all have a positive impact in the levelized cost of ammonia.

Although a sensitivity analysis provided valuable insight into the relationships between the levelized cost of ammonia and different performance parameters and material properties, it is difficult to outline a sequential pathway to economic feasibility. Instead, we employ waterfall analysis (Fig. 5.13 - 5.14) to highlight a pathway of cumulative improvements informed from the sensitivity analysis. The values for the base case were calculated using ambient operating conditions, 10% faradaic efficiency, 10^{-9} A/cm^2, and a current density of 50 mA/cm^2 as most reported research occurs at similar conditions. We chose to use the cost of electricity target for 2030 (0.03 $/kWh). With these parameters we generate the base case which is shown on the far left of Figure 5.13 and 5.14. Additionally, we chose some limits in the faradaic efficiency and exchange current density to values that we think will be attainable over the next decades. We chose a maximum faradaic efficiency of 30% and a maximum exchange current density of 10^{-7} A/cm^2.

For a direct nitrogen reduction system operating with N_2 and H_2O, the system does not reach the target levelized cost of ammonia of 600$/ton. However, through sequential improvements, it is possible to reduce the levelized cost of ammonia for this system from 2,670 $/ton to 723 $/ton (Fig. 5.13).

Initially, we optimized the operating conditions. We increased the current density to 293 mA/cm^2, the operating temperature to 100 $^\circ C$, and the operating pressure to 1 atm. Increasing the current density to 293 mA/cm^2 will result in a 57$/ton increase to the levelized cost of ammonia. However, after all the other parameters are optimized, a current density of 293 mA/cm^2 will result in the lowest possible cost. Increasing the temperature from 25 $^\circ C$ to 100 $^\circ C$ results in a cost decrease of 305 $/ton. Increasing the pressure from 1 atm to 5 atm results in a cost decrease of 170 $/ton. Next, we assume enhancements in catalyst properties such as the catalyst selectivity and activity. Increasing the faradaic efficiency from 10% to 30% leads to a cost decrease of 1,478 $/ton. Finally, increasing the exchange

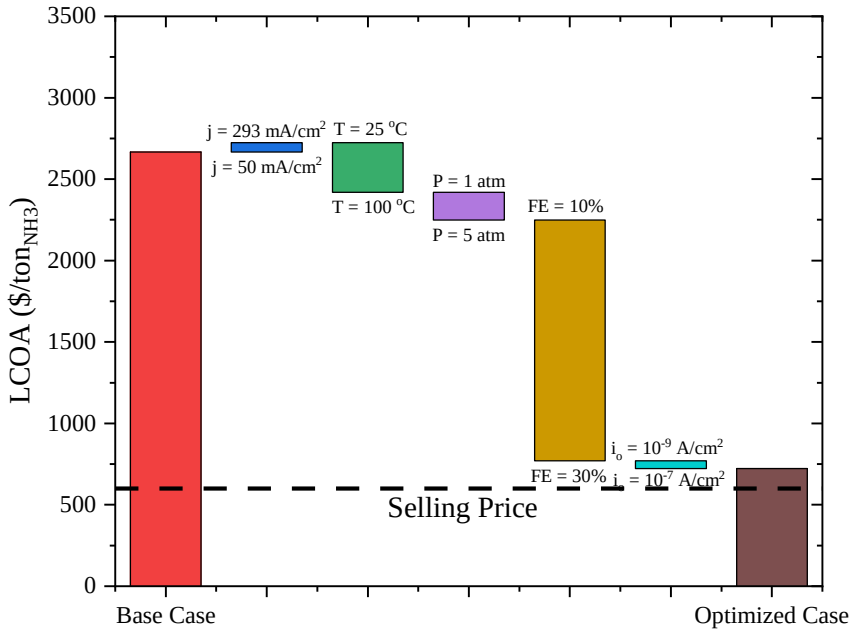

Figure 5.13: Waterfall analysis detailing the possible engineering improvements that could be made to the direct electrochemical production of ammonia using a proton exchange membrane reactor operating from nitrogen and water.

current density from 10^{-9} A/cm^2 to 10^{-7} A/cm^2 leads to a cost decrease of 48 \$/ton. Even though these improvements are not enough to react the target cost of 600 \$/ton, the improvements are able to reduce the levelized cost of ammonia by 73%. The improvement of the catalyst selectivity leads to the highest reduction of cost (65%). However, further improvements are needed to meet the target cost of 600 \$/ton.

For a nitrogen reduction system operating with N_2 and H_2, the system reaches the target levelized cost of ammonia of 600\$/ton. Through sequential improvements, it is possible to reduce the levelized cost of ammonia for this system from 1,005 \$/ton to 405 \$/ton (Fig. 5.14).

Initially, we optimized the operating conditions. We increased the current density to 129 mA/cm^2, the operating temperature to 100 $^\circ C$, and the operating pressure to 1 atm. Increasing the current density to 129 mA/cm^2 will result in a 4.7\$/ton decrease to the

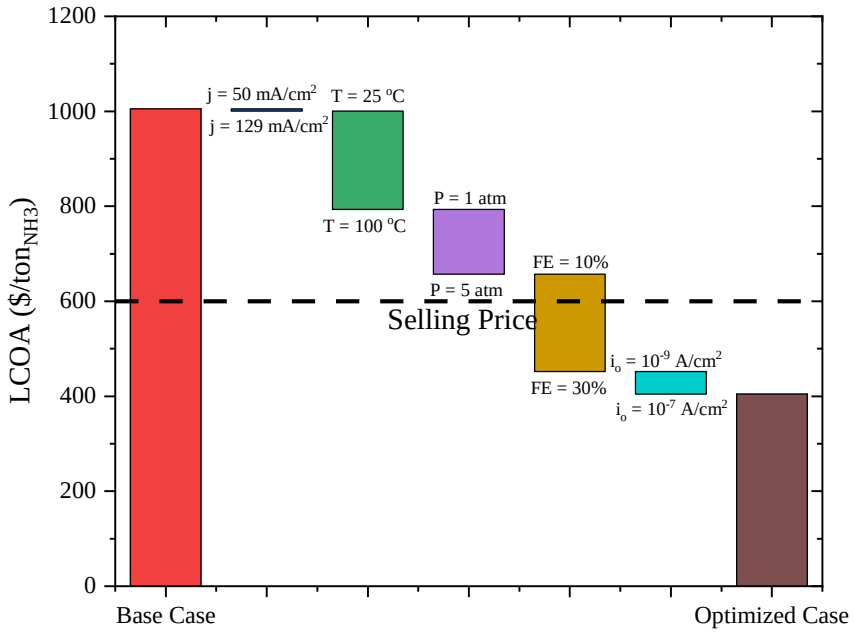

Figure 5.14: Waterfall analysis detailing the possible engineering improvements that could be made to the electrochemical production of ammonia using a proton exchange membrane reactor operating from nitrogen and hydrogen.

levelized cost of ammonia. However, after all the other parameters are optimized, a current density of 129 mA/cm^2 will result in the lowest possible cost. Increasing the temperature from 25 $^\circ C$ to 100 $^\circ C$ results in a cost decrease of 207 \$/ton. Increasing the pressure from 1 atm to 5 atm results in a cost decrease of 136 \$/ton. Next, we assume enhancements in catalyst properties such as the catalyst selectivity and activity. Increasing the faradaic efficiency from 10% to 30% leads to a cost decrease of 205 \$/ton. Finally, increasing the exchange current density from 10^{-9} A/cm^2 to 10^{-7} A/cm^2 leads to a cost decrease of 48 \$/ton. The sequential improvements are enough to reach the target cost of 600 \$/ton. In fact, the improvements are able to exceed the target cost and reach a minimum cost of 405 \$/ton. The improvements lead to an overall reduction of the levelized cost of ammonia of 60%.

Waterfall analyses help illustrate pathways to low-cost renewable electrochemical am-

monia synthesis. Even though the waterfall analyses provide a possible pathway for economic viability, there are other possible pathways that can be adopted with similar results. According to the sensitivity and waterfall analysis, the biggest contributors to the levelized cost of ammonia are the faradaic efficiency and the price of electricity. To identify the operating space for electronically ammonia synthesis, we examine constant cost curves (Fig. 5.15 - 5.16). Each line represents a fixed electricity cost. Here, we study the required faradaic efficiency and current densities to meet the target cost of 600 $/ton. The different lines represent lines with constant costs (600 $/ton) at varying electricity costs between 0.06 $/kWh and 0.02 $/kWh. We consider the optimized case discussed in the waterfall analyses. However, we vary the faradaic efficiency and current density.

For a direct nitrogen reduction system with N_2 and H_2O as reactants, achieving the target cost (600 $/ton) is possible even at the current electricity cost (0.06 $/kWh). However, the required faradaic efficiency to meet the cost targets is high (Fig. 5.15). The first thing we notice is that the optimal current density for a direct nitrogen reduction system with N_2 and H_2O as reactants is between 0.1 A/cm^2 and 0.3 A/cm^2. At higher electricity prices, lower current densities (0.1 A/cm^2) lead to the lowest cost; and at lower electricity prices, higher current densities (0.3 A/cm^2) lead to the lowest cost.

For a direct nitrogen reduction system with N_2 and H_2O as reactants, it is possible to produce ammonia at current electricity prices at under 600 $/ton. However, in order to produce ammonia at that cost, a faradaic efficiency of over 70% is required. Reaching a faradaic efficiency of 70% at a current density in the order of 0.1 A/cm^2 is improbable. However, another alternative to reduce the levelized cost of ammonia is by decreasing the cost of electricity. As the cost of electricity decreases, the required faradaic efficiency decreases as well. For example, if the electricity price is decreased to the next decade target (0.03 $/kWh) the required faradaic efficiency will decrease to 40%. If we decrease the electricity price further to 0.02 $/kWh, the system requires a minimum faradaic efficiency of 25% at a current density of 0.3 A/cm^2. A faradaic efficiency of 25% at a current density

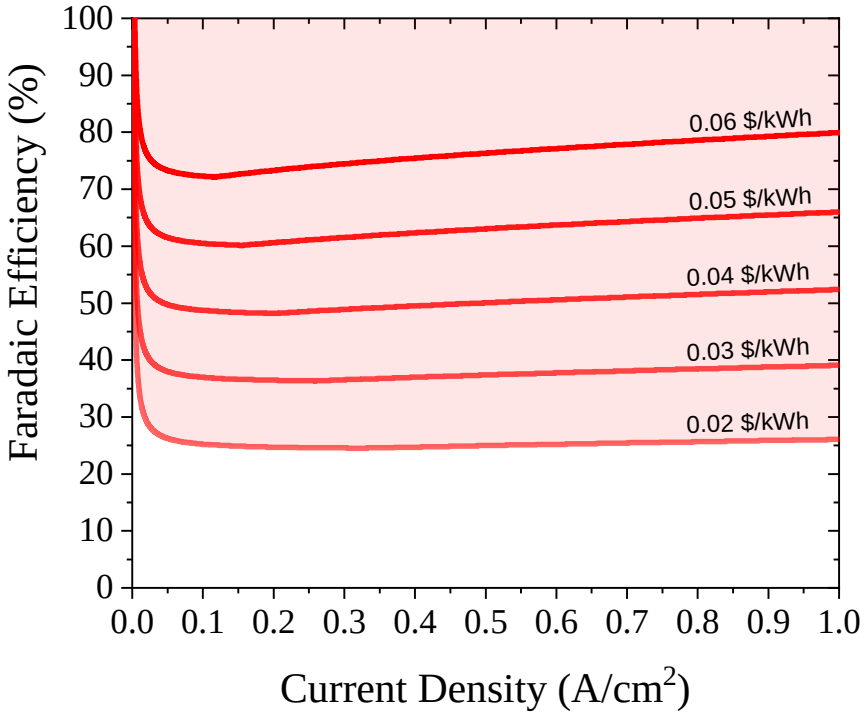

Figure 5.15: Design space for a direct Nitrogen reduction cell with N_2 and H_2O as reactant.

of 0.3 A/cm^2 is attainable. However, it will require significant improvements in the catalyst and activity in order to meet those targets.

For a nitrogen reduction system with N_2 and H_2 as reactants, achieving the target cost (600 $/ton) is impossible at the current electricity cost (0.06 $/kWh). However, this system is more sensitive to a decrease in the price of electricity. As the electricity price is decreased, the required faradaic efficiency can even reach values below 10% (Fig. 5.16). The first thing we notice is that the optimal current density for a nitrogen reduction system with N_2 and H_2 as reactants is around 0.1 A/cm^2. At higher electricity prices, the levelized cost of ammonia increases rapidly with an increase in current density. Lower electricity prices lead to a flatter curve and less increase in the levelized cost of ammonia with an increase in the current density.

For a nitrogen reduction system with N_2 and H_2 as reactants, it is impossible to produce ammonia at current electricity prices at under 600 $/ton. An electricity price of at least

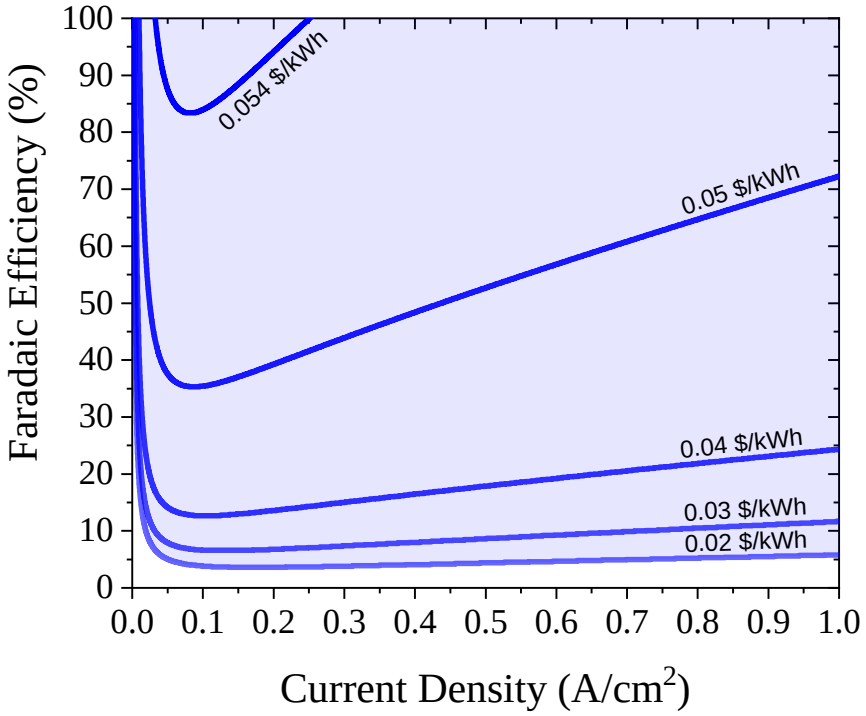

Figure 5.16: Design space for a Nitrogen reduction cell with N_2 and H_2 as reactants.

0.054 $/kWh is necessary to produce ammonia at 600 $/ton. To produce ammonia with that electricity price, the minimum faradaic efficiency is 85%. A faradaic efficiency of 85% at a current density of 0.1 A/cm^2 is nearly impossible. However, if the electricity price is decreased, the required faradaic efficiency decreases sharply. For example, if the electricity price is decreased to the next decade target (0.03 $/kWh) the required faradaic efficiency will decrease to 8%. Reaching a target of 8% faradaic efficiency will be less challenging than reaching a target of 40% faradaic efficiency (which is the target of the other system at and electricity cost of 0.03 $/kWh). If the electricity price is decreased even further to 0.02 $/kWh, the required faradaic efficiency to achieve a levelized cost of ammonia of 600 $/ton is 5%. Existing catalysts exhibit faradaic efficiencies around this range. However, it will be challenging to maintain these faradaic efficiencies while operating at high current densities ($>$ 0.1 A/cm^2).

Studying the design space of electrochemical ammonia synthesis helps illustrate the im-

portance of improving the different parameters and setting realistic targets for technology viability. For example, we can set targets in the current density and the faradaic efficiency. Combining these with the electricity cost targets set by the DOE we can estimate the future targets for this technology. We conclude that by 2030, with an expected electricity cost of 0.03 \$/kWh, the performance targets set for low temperature ammonia electrosynthesis are 40% for a direct nitrogen reduction system with N_2 and H_2O as reactants and 8% for a nitrogen reduction system with N_2 and H_2 as reactants. Hence, it is important to develop systems that operate with N_2 and H_2 as reactants and use a separate water electrolysis cell to provide hydrogen to the ammonia electrochemical reactor. Additionally, these analyses help us prioritize our efforts on technology development. For a direct nitrogen reduction system with N_2 and H_2O as reactants it is equally important to reduce the electricity cost and to increase the faradaic efficiency at high current densities because even at low electricity price, the required faradaic efficiency is still high. However, for a nitrogen reduction system with N_2 and H_2 as reactants it is more important to reduce the electricity price because the required faradaic efficiency with low electric prices approaches the faradaic efficiency of existing systems. Even though nitrogen reduction with N_2 and H_2 as reactants is not viable with the current electricity prices, as the electricity price decreases over the next decade it will be easier to develop and meet the target ammonia production costs.

These analyses help illustrate pathways to renewable electrochemical ammonia production. These analyses indicate that low-cost electrochemical ammonia is feasible. However, a significant amount of work is needed before these systems can be implemented. Based on the analysis presented, developing selective catalysts that can operate at current densities above 100 mA/cm^2 remains of paramount importance. However, advancements in renewable energy production that might help reduce the cost of electricity are equally important.

The levelized cost of ammonia of electrochemical ammonia based on the model suggest economic feasibility of nitrogen reduction with N_2 and H_2 as reactants (Fig. 5.18). However, for direct nitrogen reduction with N_2 and H_2O as reactants, the system fails to

produce ammonia at the target cost (Fig. 5.17). If the faradaic efficiency is increased further, this system would be economically feasible. For each of the reactions, we assumed a temperature of 100 °C, pressure of 5 atm, faradaic efficiency of 30%, and exchange current density of 10^{-7} A/cm^2. The system is operating at the optimal current density that leads to the lowest levelized cost of ammonia for these conditions. From these cost breakdowns (Fig. 5.17 - 5.18), the poor selectivity and activity of the nitrogen reduction reaction leads to significant electrical costs. Consequently, electrochemical ammonia production is not feasible at these conditions with a cost of electricity of 0.0612 $/ton. If the cost of electricity decreases to 0.03 $/ton, the electrical cost for both systems is more than halved. The reduction in the electrical cost results in the economic feasibility of nitrogen reduction with N_2 and H_2 as reactants, but it is not enough to result in the economic feasibility of direct nitrogen reduction with N_2 and H_2O as reactants.

The capital costs for an alkaline reactor are significantly higher than those of a PEM and GDE reactors. This is because the mass transport limitations lead to low current densities in alkaline reactors. Consequently, and alkaline reactor for direct nitrogen reduction with N_2 and H_2O as reactants has a capital cost of has a capital cost of 81 $/ton. For PEM and GDE reactors for direct nitrogen reduction with N_2 and H_2O as reactants, the capital cost is reduced to 27 $/ton due to a decrease in the system size that stems from an increase in the current density.

When comparing both systems, the electrical costs are higher for direct nitrogen reduction with N_2 and H_2O as reactants than for nitrogen reduction with N_2 and H_2 as reactants. This is because the energy efficiency of a nitrogen reduction system with N_2 and H_2 as reactants is higher than the energy efficiency of a direct nitrogen reduction system with N_2 and H_2O as reactants. Hence, the first system has an electrical cost of 690 $/ton and the second system has an electrical cost of 310 $/ton when the cost of electricity is 0.03 $/kWh. The opposite happens with the capital cost. The capital cost for direct nitrogen reduction with N_2 and H_2O as reactants is lower than the capital cost for nitrogen reduction with N_2

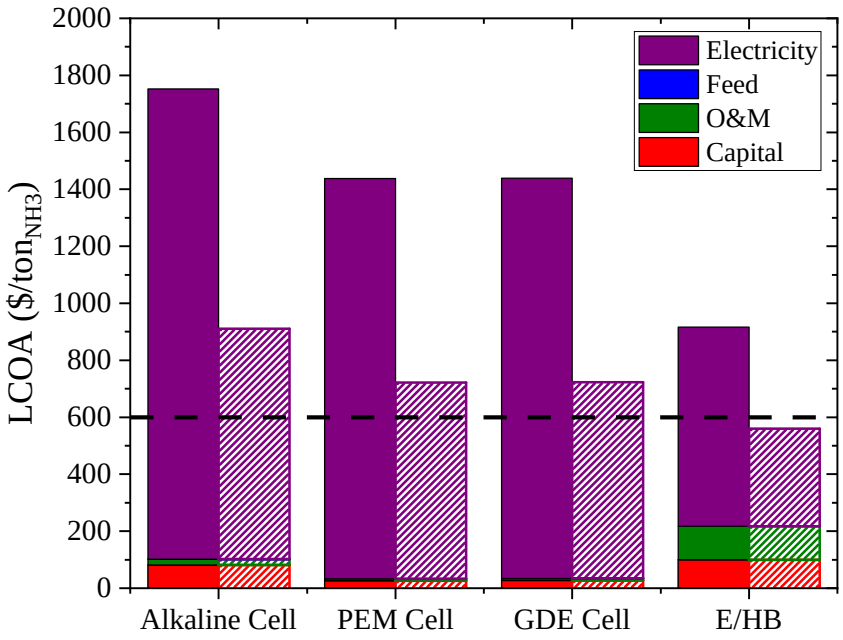

Figure 5.17: Cost comparison of electrochemical technologies operating with nitrogen and water.

and H_2 as reactants. This is because the second system requires two separate reactors. Consequently, the capital cost of direct nitrogen reduction system with N_2 and H_2O as reactants is 27 \$/ton and the capital cost of nitrogen reduction system with N_2 and H_2 as reactants is 27 \$/ton.

These analyses show the trade-offs in terms of capital and electrical costs for both systems. At first glance, it seems like a direct nitrogen reduction system with N_2 and H_2O as reactants has a higher levelized cost of ammonia than a nitrogen reduction with N_2 and H_2 as reactants due to the higher energy efficiency of the second system. However, if the energy efficiency of a direct nitrogen reduction system with N_2 and H_2O as reactants increases enough to match that of the energy efficiency of a nitrogen reduction system with N_2 and H_2 as reactants, the first system will have a lower levelized cost of ammonia. However, the first system is only favorable at current densities above 70%. Hence, developing and im-

plementing a cost competitive electrochemical ammonia system will be easier if hydrogen (from a water electrolyzer) is used as a reactant instead of water.

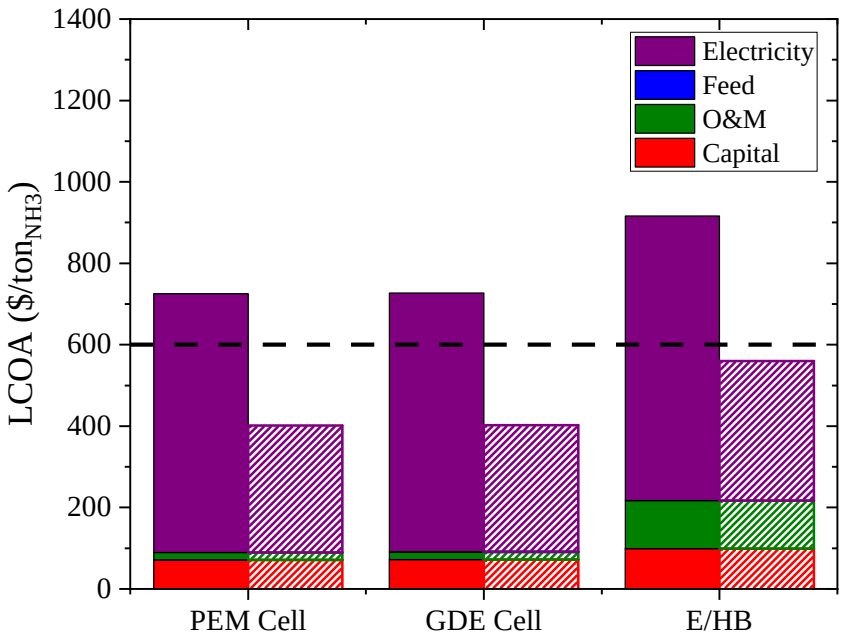

Figure 5.18: Cost comparison of electrochemical technologies operating with nitrogen and hydrogen.

Finally, we compared electrochemical systems with a modified Haber-Bosch process coupled with a water electrolyzer. This modified Haber-Bosch process uses water instead of methane as a hydrogen source to produce renewable ammonia. The modeled modified Haber-Bosch plant has an output of 91 mt/day. The modified Haber-Bosch coupled with water electrolysis has a capital cost of 99 \$/ton and an operational cost of 118 \$/ton. In contrast, the capital cost of electrochemical systems is 27 \$/ton for the direct nitrogen reduction system with N_2 and H_2O as reactants and 72 \$/ton for the nitrogen reduction system with N_2 and H_2 as reactants. However, the electrical cost of the modified Haber-Bosch coupled with water electrolysis is comparable to the electrical cost of the nitrogen reduction system with N_2 and H_2 as reactants. Both of these systems have a lower electrical

cost that the direct nitrogen reduction system with N_2 and H_2O as reactants. Accordingly, the modified Haber-Bosch process coupled with water electrolysis has a higher levelized cost of ammonia than the nitrogen reduction system with N_2 and H_2 as reactants but has a lower levelized cost of ammonia than the direct nitrogen reduction system with N_2 and H_2O as reactants.

CHAPTER 6

CONCLUSIONS AND RECOMMENDATIONS FOR FUTURE WORK

Here we examined the thermodynamic, kinetic, and economic consideration of low-temperature electrochemical ammonia synthesis. We have confirmed that while the thermodynamics of low temperature ammonia electrosynthesis are ideal for high conversion efficiency, there are several kinetic challenges which these systems will need to overcome to achieve high energy efficiency and rates of production. We show that a low-temperature electrochemical reactor needs to achieve a 90% faradaic efficiency to achieve a comparable energy efficiency to the Haber-Bosch process. Most of the losses in the electrochemical reactor come from the activation overpotential associated with nitrogen reduction, and therefore enhancing the catalyst selectivity and activity is also critical for enabling Haber-Bosch parity ammonia production.

We also developed a techno-economic model to evaluate the economic viability of low-temperature electrochemical ammonia synthesis technologies. Two electrochemical approaches were investigated. The first is through direct nitrogen reduction with N_2 and H_2O as reactants. The second is through nitrogen reduction with N_2 and H_2 as reactants. We also examined the impact of different reactor designs (alkaline electrolysis cells, proton exchange membrane electrolysis cells, and gas diffusion electrolysis cells). Alkaline electrolysis cells have mass transport limitations due to the solubility of nitrogen in aqueous streams and can only achieve effective current densities around $7 * 10^{-3} A/cm^2$. However, mass transport can be enhanced with gas diffusion layers. Reactors that use gas diffusion layer can achieve effective current densities around 7 A/cm^2. The levelized cost of ammonia is found to be most sensitive to variations in the cost of electricity and the faradaic efficiency, and least sensitive to variations in the capital cost of the system. Furthermore, we showed how to achieve economic feasibility through sequential improvements using

waterfall analyses. We found that for a direct nitrogen reduction system with N_2 and H_2O as reactants, it is possible to approach economic viability through sequential improvements. The sequential improvements consist of first optimizing the operating conditions and then improving the catalyst selectivity and activity. It is possible to approach economic viability by optimizing the operating conditions. However, this system requires faradaic efficiencies higher than 30% in order to produce ammonia at the target costs. For a nitrogen reduction system with N_2 and H_2 as reactants, it was possible to achieve economic viability through sequential improvements. In fact, it was possible to achieve ammonia costs as low at 400 \$/ton by optimizing the operating conditions and improving the faradaic efficiency to 30% and the exchange current density to $10^{-7} A/cm^2$. We found that a direct nitrogen reduction system with N_2 and H_2O as reactants can achieve costs bellow 600 \$/ton at the current electricity prices at faradaic efficiencies above 70% and current densities between 100 to 300 mA/cm^2. If the electricity prices are decreased to 0.03 \$/kWh, the required faradaic efficiency would be 40%. Hence, this system requires significant improvements in the catalyst selectivity. Another possible path is to use a nitrogen reduction system with N_2 and H_2 as reactants. This system requires electricity prices below 0.05 \$/kWh. However, if the electricity prices are decreased to 0.03 \$/kWh, this system only required faradaic efficiencies around 8%.

Potential future work should expand on the number of system configurations.Emphasis should also be placed on understanding the role of separation technologies (prior to and after the reactors). This includes analyses which target our understanding of the energy associated with separations conducted through membranes, absorbents, and cryogenic separations. Furthermore, analyses are needed which look at the impact of scaling on LCOA and energy efficiency. Finally, long term system level experimental and pilot scale testing is necessary to corroborate these findings.

Appendices

```
%% Model Parameters
Production_Rate = 100; %mol/s
T_Operation_C = 100; %Operation Temperature in Celsius (0-90)
P_Operation_atm = 5; %OPeration Pressure in Atmospheres (1-5)
Membrane_Thick = 200; %Membrane Thickness in Microns
i_density = 0.129; %Operation Current Density in A/cm^2
Faradaic_Efficiency = 30; %Faradaic Efficiency
Cathode_Exchange_Current_Density = 1e-7; %Cathode Exchange Current Density in A/cm^2
X = 0.1; %Nitrogen Conversion
Anode_Reactant = 1; %1 for Hydrogen and 2 for Water
Electricity_Cost = 0.03; %$/kWh
Product_Lifetime = 30;
Cathode_Catalyst_Loading = 0.0001; %kg/m^2
Cathode_Catalyst_Price = 32000; %$/kg
Anode_Catalyst_Loading = 0.0001; %kg/m^2
Anode_Catalyst_Price  = 32000; %$/kg 3.2 $/m2
Price_Per_Area_Nafion = 50; % 50 $/m^2
Price_Per_Area_Bipolar_Plate = 35; %$/m^2
Price_Per_Area_Electrode = 20; % 50 $/m^2
Price_Per_Area_Peripheral = 3.46; %$/m^2
SaltPrice = 0; % (0.1) $/kg
SaltMW = 0; % (174) kg/mol
Electrolyte_Conductivity = 0.8; %S cm (0.8)
Electrolyte_Gap = 0; %cm (0.02)
%% Model Input
[W_Air_Separation,W_H2,W_N2,Q_H2,Q_N2,W_Electric_PEM,Q_Heat_PEM,W_NH3_Separation,↙
LHV_NH3, Efficiency_Energy,W_Electric_H2,TP, Ammonia_Output,i_lim_N2,i_lim_H2,LCOA,↙
Cap_Cost,Op_Cost,Liquid_Electrolyte_Cost,Energy_Cost,Yearly_Production_Ammonia_ton] =↙
PEM_COST_MODEL(Production_Rate,T_Operation_C,P_Operation_atm,Membrane_Thick,i_density,↙
Faradaic_Efficiency,Cathode_Exchange_Current_Density,X,Anode_Reactant,Electricity_Cost,↙
Product_Lifetime,Cathode_Catalyst_Loading,Cathode_Catalyst_Price,↙
Anode_Catalyst_Loading,Anode_Catalyst_Price,Price_Per_Area_Nafion,↙
Price_Per_Area_Bipolar_Plate,Price_Per_Area_Peripheral,SaltMW,SaltPrice,↙
Electrolyte_Conductivity,Electrolyte_Gap,Price_Per_Area_Electrode);
Cost = [Cap_Cost,Op_Cost,Liquid_Electrolyte_Cost,Energy_Cost].↙
/Yearly_Production_Ammonia_ton;
```

```
function [W_Air_Separation,W_H2,W_N2,Q_H2,Q_N2,W_Electric_PEM,Q_Heat_PEM,↙
W_NH3_Separation, LHV_NH3, Efficiency_Energy,W_Electric_H2,TP, Ammonia_Output,i_lim_N2,↙
i_lim_H2,LCOA,Cap_Cost,Op_Cost,Liquid_Electrolyte_Cost,Energy_Cost,↙
Yearly_Production_Ammonia_ton] = PEM_COST_MODEL(Production_Rate,T_Operation_C,↙
P_Operation_atm,Membrane_Thick,i_density,Faradaic_Efficiency,↙
Cathode_Exchange_Current_Density,X,Anode_Reactant,Electricity_Cost,Product_Lifetime,↙
Cathode_Catalyst_Loading,Cathode_Catalyst_Price,Anode_Catalyst_Loading,↙
Anode_Catalyst_Price,Price_Per_Area_Nafion,Price_Per_Area_Bipolar_Plate,↙
Price_Per_Area_Peripheral,SaltMW,SaltPrice,Electrolyte_Conductivity,Electrolyte_Gap,↙
Price_Per_Area_Electrode)
%% Constants
    R = 8.314; %Ideal Gas Constant (KJ/KmolK)
    F = 96485; %Faraday's Constant
    P_ambient = 101325; %Ambient Pressure (Pa)
    T_ambient = 298.15; %Ambient Temperature (K)
%% Variables and Conversions
    T_PEM = T_Operation_C+273.15; %Reactor Temperature (K)
    p = P_Operation_atm*101325; %Reactor Pressure (Pa)
%% Current Output and Effective Currents
    [Current_Need,Current_NH3,Current_H2] = CurrentCalculation(Production_Rate,↙
Faradaic_Efficiency);
%% Reactor Area
    Reactor_Area = (Current_Need./i_density).*1e-4; %m^2
%% Molar Flowrate of Reactants and Products
    [N2_mole,H2O_mole,NH3_mole,~,H2_mole_OUT,~,H2_mole] = MolarFlowCalculation↙
(Current_Need,Current_NH3,Current_H2);
%% Lower Heating Value of Ammonia and Hydrogen
%4NH3(g) + 3O2(g) = 2N2(g) + 6H2O(g)
    [LHV_NH3,LHV_H2] = LHV_Calc;
%% Cell Reversible Potential
    %N2(g)+3H2O(l) = 2NH3(g) + 3/2O2(g)
    %Calculate Reversible Voltage
    [E,delS] = OCV_Calc(T_PEM,Faradaic_Efficiency,Anode_Reactant);
%% Cell Overpotentials
    [V,V_drop,i_lim_N2,i_lim_H2] = Cell_Overpotentials(Membrane_Thick,i_density,p,↙
P_ambient,T_PEM,E,Anode_Reactant,Cathode_Exchange_Current_Density,X,↙
Electrolyte_Conductivity,Electrolyte_Gap,Faradaic_Efficiency);
%% Mass Flowrates
    M_N2 = (N2_mole)*(28.0134/1000); %kg/s
    M_H2 = (H2_mole).*(2/1000); %kg/s
    M_H2_Recycle = (H2_mole_OUT).*(2/1000); %kg/s
    if Anode_Reactant == 1
        M_water = (H2_mole)*(18/1000); %kg/s
    elseif Anode_Reactant == 2
        M_water = (H2O_mole)*(18/1000); %kg/s
    end
%% Product Separation
    [W_NH3_Separation,M_N2_RECYCLE] = NH3_Separation(H2_mole_OUT,X,Anode_Reactant,↙
NH3_mole,p,T_ambient);
%% Air Separation
```

```
    [W_Air_Separation] = Air_Separation_Unit(M_N2);
%% Nitrogen Compressor
    [~,W_Compressor,T_Compressor_Exit,~,~] = N2_Compressor(p,T_ambient,P_ambient,M_N2);
    W_N2 = W_Compressor;
%% Nitrogen Heat Exchanger
    [~,~,Q_HeatExchanger_N2_In] = N2_HE(T_Compressor_Exit,M_N2,T_PEM,T_ambient,p,↙
P_ambient);
    [~,~,Q_HeatExchanger_N2_In_Recycle] = N2_HE(T_ambient,M_N2_RECYCLE,T_PEM,T_ambient,↙
p,P_ambient);
    Q_HeatExchanger_N2_In = Q_HeatExchanger_N2_In+Q_HeatExchanger_N2_In_Recycle;
    Q_N2 = Q_HeatExchanger_N2_In;
    Q_N2(Q_N2<0)=0;
%% Hydrogen Compressor/Water Pump
if Anode_Reactant == 1
    [~,W_Compressor_H2,T_Compressor_H2_Exit,~,~] = H2_Compressor(p,T_ambient,P_ambient,↙
M_H2);
     W_H2 = W_Compressor_H2;
else
    [~,~,W_Pump,T_Pump_Exit,~] = Water_Pump(p,M_water,P_ambient,T_ambient);
    W_H2 = W_Pump;
end
%% Hydrogen Heat Exchanger/ Water Heat Exchanger
if Anode_Reactant == 1
    [~,~,Q_HeatExchanger_H2_In] = H2_HE(T_Compressor_H2_Exit,M_H2,T_PEM,T_ambient,p,↙
P_ambient);
    [~,~,Q_HeatExchanger_H2_In_Recycle] = H2_HE(T_ambient,M_H2_Recycle,T_PEM,T_ambient,↙
p,P_ambient);
    Q_HeatExchanger_H2_In = Q_HeatExchanger_H2_In + Q_HeatExchanger_H2_In_Recycle;
    Q_H2 = Q_HeatExchanger_H2_In;
else
    [~,Q_HeatExchanger_Water_In,~] = Water_HE(T_Pump_Exit,M_water,T_PEM,T_ambient);
    Q_H2 = Q_HeatExchanger_Water_In;
end
    Q_H2(Q_H2<0)=0;
%% Work Hydrogen Production
    if Anode_Reactant == 1
    W_Electric_H2 = LHV_H2.*H2_mole/0.7;
    else
    W_Electric_H2 = 0;
    end
%% Electric Work PEM
    W_Electric_PEM = V.*Current_Need./1000; %Electric work required by the electrolyzer
    W_Elect = W_Electric_PEM;
%% Heat Input PEM
    [Q_heat_PEM] = HEAT_PEM( T_PEM,N2_mole,delS,Current_Need,V_drop);
    Q_Heat_PEM = Q_heat_PEM;
    Q_Heat_PEM(Q_Heat_PEM<0)=0;
%% Energy Efficiency and Normalized Energy Expenditure
    Efficiency_Energy = 100*(LHV_NH3*NH3_mole)./↙
(W_Air_Separation+W_H2+W_N2+Q_H2+Q_N2+W_Electric_PEM+Q_Heat_PEM+W_Electric_H2+W_NH3_Sep↙
```

```
aration);
    Total_Power =↙
W_H2+W_N2+Q_H2+Q_N2+W_Electric_PEM+Q_Heat_PEM+W_Electric_H2+W_Air_Separation+W_NH3_Sepa↙
ration;
    Nitrogen_Output = Production_Rate;
    Ammonia_Output = Nitrogen_Output;
    TP = Total_Power/Nitrogen_Output;
    W_H2 = W_H2./Nitrogen_Output;
    W_N2 = W_N2./Nitrogen_Output;
    Q_H2 = Q_H2./Nitrogen_Output;
    Q_N2 = Q_N2./Nitrogen_Output;
    W_Air_Separation = W_Air_Separation./Nitrogen_Output;
    W_NH3_Separation = W_NH3_Separation./Nitrogen_Output;
    W_Electric_PEM = W_Electric_PEM./Nitrogen_Output;
    Q_Heat_PEM = Q_Heat_PEM./Nitrogen_Output;
    W_Electric_H2 = W_Electric_H2./Nitrogen_Output;
 %% Yearly Production of Ammonia
    Yearly_Production_Ammonia_mol = Production_Rate.*3600.*24.*365; %molNH3/yr
    Yearly_Production_Ammonia_kg = Yearly_Production_Ammonia_mol.*17.031.*1e-3; %↙
kgNH3/yr
    Yearly_Production_Ammonia_ton = Yearly_Production_Ammonia_mol.*17.031.*1e-6; %↙
tonNH3/yr
  %% Energy Cost
    %Electricity_Cost = 0.0612 $/kWh
    Operation_Hours = 365.*24; %hours
    Energy_Cost = Electricity_Cost.*Operation_Hours.*Total_Power;
 %% Yearly Production of Ammonia
    Yearly_Production_Ammonia_mol = Production_Rate.*3600.*24.*365; %molNH3/yr
    Yearly_Production_Ammonia_kg = Yearly_Production_Ammonia_mol.*17.031.*1e-3; %↙
kgNH3/yr
    Yearly_Production_Ammonia_ton = Yearly_Production_Ammonia_mol.*17.031.*1e-6; %↙
tonNH3/yr
 %% Capital Recovery Factor
    k = 6.5/100;
    n = Product_Lifetime;
    CRF = (k*(1+k).^n)/(((1+k).^n)-1);
 %% Capital Cost Hydrogen
    Capital_Cost_H2 = Nitrogen_Output.*W_Electric_H2.*600; %Hydrogen Electrolyzer Proce↙
600 $/kW
    Cap_Cost_H2 = CRF.*Capital_Cost_H2;
 %% Catalyst Cost
    Cathode_Catalyst_Cost = Reactor_Area .*Cathode_Catalyst_Loading .↙
*Cathode_Catalyst_Price;
    Cap_Cost_Cathode_Catalyst = CRF.*Cathode_Catalyst_Cost;
    Anode_Catalyst_Cost = Reactor_Area .*Anode_Catalyst_Loading .*Anode_Catalyst_Price;
    Cap_Cost_Anode_Catalyst = CRF.*Anode_Catalyst_Cost;
 %% Electrolyte Cost
    RecycleElectrolyte = 0.99;
    Liquid_Electrolyte_Cost = (Current_Need./F).*SaltMW.*SaltPrice.* ( 1 -↙
RecycleElectrolyte );
```

```
    Nafion_Cost = CRF.*Price_Per_Area_Nafion.*Reactor_Area;
 %% Bipolar Plate Cost
    Bipolar_Plate_Cost = CRF.*Price_Per_Area_Bipolar_Plate.*Reactor_Area;
 %% Electrode Cost
    Electrode_Cost = CRF.*Price_Per_Area_Electrode.*Reactor_Area;
 %% Peripheral Parts Cost
    Peripheral_Cost = CRF.*Price_Per_Area_Peripheral.*Reactor_Area;
 %% BOP Cost
    Daily_Ammonia_Production = Yearly_Production_Ammonia_kg./365; %kg/day
    BopCosts = 47.*Daily_Ammonia_Production; %$
    BOPCost = CRF.*BopCosts;
 %% Electronics Cost
    ElectronicsCost = CRF.*Total_Power.*60; %$
 %% Capital Cost N2
    Cap_Cost =↙
(Cap_Cost_Cathode_Catalyst+Cap_Cost_Anode_Catalyst+Nafion_Cost+Bipolar_Plate_Cost+Perip↙
heral_Cost+BOPCost+Cap_Cost_H2+ElectronicsCost + Electrode_Cost); %$/yr
 %% O&M Cost
    Op_Cost = Cap_Cost.*2/(100.*CRF); %$/yr
 %% Total Yearly Cost
    Total_Cost = (Cap_Cost + Op_Cost + Liquid_Electrolyte_Cost + Energy_Cost); % $/yr
 %% Levelized Cost of Ammonia
    LCOA = Total_Cost./Yearly_Production_Ammonia_ton; % $/tonNH3
end
```

```
function [Current_Need,Current_NH3,Current_H2] = CurrentCalculation(Production_Rate,↙
Faradaic_Efficiency)
 %% Constants
    F = 96485; %Faraday's Constant
 %% Calculation
    %Production Rate in mol/*s
    Current_Need = Production_Rate.*3.*F; %Amps of current needed to produce the↙
nitrogen required
    Current_Need = Current_Need./(Faradaic_Efficiency./100);
    Current_NH3 = Current_Need.*(Faradaic_Efficiency./100);
    Current_H2 = Current_Need.*((100-Faradaic_Efficiency)./100);
end
```

```
function [N2_mole,H2O_mole,NH3_mole,O2_mole,H2_mole_OUT,H2_mole_IN,H2_mole] =↙
MolarFlowCalculation(Current_Need,Current_NH3,Current_H2)
%% Constants
    F = 96485; %Faraday's Constant
%% Calculations
    N2_mole = Current_NH3/(F*(6/1)); %Molar Flow of Nitrogen (mol/s)
    H2O_mole = Current_Need/(F*(6/3)); %Molar Flow of Water (mol/s)
    NH3_mole = Current_NH3/(F*(6/2)); %Molar Flow of Ammonia (mol/s)
    O2_mole = Current_Need/(F*(6/(3/2))); %Molar Flow of Oxygen (mol/s) )
    H2_mole_OUT = Current_H2/(F*(6/3));
    H2_mole_IN = Current_Need/(F*(6/3));
    H2_mole = H2_mole_IN-H2_mole_OUT;
end
```

```
function [LHV_NH3,LHV_H2] = LHV_Calc(T)
    [hf_NH3] = FindProperty('Enthalpy Of Formation','NH3(g)');
    [hf_O2] = FindProperty('Enthalpy Of Formation','O2(g)');
    [hf_N2] = FindProperty('Enthalpy Of Formation','N2(g)');
    [hf_H2Og] = FindProperty('Enthalpy Of Formation','H2O(g)');
    [hf_H2] = FindProperty('Enthalpy Of Formation','H2(g)');
    LHV_NH3 = -1*((2*hf_N2)+(6*hf_H2Og)-(4*hf_NH3)-(3*hf_O2))/4000; %KJ/molNH34
    LHV_H2 = -1*((2*hf_H2Og)-(2*hf_H2)-(hf_O2))/2000; %KJ/molNH34
end
```

```
function [E,delS] = OCV_Calc(T,Faradaic_Efficiency,Anode_Reactant)
%%%%%%%%%%%%%%%%%%%%%%%%%%%%%%%%%%%%%%%%%%%%%%%%%%%%%%%%%%%%%%%%%%%%%%%%%%%%
%SECTION 1: SYSTEM%
%SYSTEM REQUIREMENTS%
    %CONSTANTS%
    T_PEM = T+273.15; %K
    F = 96485; %Faraday's Constant
    FE = Faradaic_Efficiency./100;
%CALCULATING CELL REVERSIBLE POTENTIAL%
%SI UNITS%
%N2(g)+3H2(g) = 2NH3(g)
%N2(g)+3H2O(l) = 2NH3(g) + 3/2O2(g)
%H2O(l) = H2(g) + 1/2O2(g)
    T_ref = 298.15; %K
%FIND OCV OF NRR_H2
    n = 6; %mole- per mol of N2
    [hf_NH3] = FindProperty('Enthalpy Of Formation','NH3(g)');
    [hf_N2] = FindProperty('Enthalpy Of Formation','N2(g)');
    [hf_H2] = FindProperty('Enthalpy Of Formation','H2(g)');
    [sf_NH3] = FindProperty('Absolute Entropy','NH3(g)');
    [sf_N2] = FindProperty('Absolute Entropy','N2(g)');
    [sf_H2] = FindProperty('Absolute Entropy','H2(g)');
    %Calculate Gibbs Free Energy
    delH = (2.*FE.*hf_NH3)+(3.*(1-FE).*hf_H2)-(FE.*hf_N2)-(3*hf_H2);
    delS = (2.*FE.*sf_NH3)+(3.*(1-FE).*sf_H2)-(FE.*sf_N2)-(3*sf_H2);
    delG = delH-(T_ref*delS);
    %Calculate Reversible Voltage
    Er = delG/(n*F);
    Sr = delS/(n*F);
    delS_H2 = delS;
    OCV_H2 = -(Er - Sr*(T_PEM-T_ref)); %REVERSIBLE VOLTAGE
%FIND OCV OF NRR_H2O
    n = 6; %mole- per mol of N2
    [hf_NH3] = FindProperty('Enthalpy Of Formation','NH3(g)');
    [hf_O2] = FindProperty('Enthalpy Of Formation','O2(g)');
    [hf_N2] = FindProperty('Enthalpy Of Formation','N2(g)');
    [hf_H2O] = FindProperty('Enthalpy Of Formation','H2O(l)');
    [hf_H2O_g] = FindProperty('Enthalpy Of Formation','H2O(g)');
    [sf_NH3] = FindProperty('Absolute Entropy','NH3(g)');
    [sf_O2] = FindProperty('Absolute Entropy','O2(g)');
    [sf_N2] = FindProperty('Absolute Entropy','N2(g)');
    [sf_H2O] = FindProperty('Absolute Entropy','H2O(l)');
    [sf_H2O_g] = FindProperty('Absolute Entropy','H2O(g)');
    %Calculate Gibbs Free Energy
    delH = (2.*FE.*hf_NH3)+((3/2)*hf_O2)+(3.*(1-FE).*hf_H2)-(FE.*hf_N2)-(3*hf_H2O);
    delS = (2.*FE.*sf_NH3)+((3/2)*sf_O2)+(3.*(1-FE).*sf_H2)-(FE.*sf_N2)-(3*sf_H2O);
    delG = delH-(T_ref*delS);
    %Calculate Reversible Voltage
    Er = delG/(n*F);
    Sr = delS/(n*F);
```

```
    OCV_H2O_l = Er - Sr*(T_PEM-T_ref); %REVERSIBLE VOLTAGE
    delS_H2O_l = delS;
    delH = (2.*FE.*hf_NH3)+((3/2)*hf_O2)+(3.*(1-FE).*hf_H2)-(FE.*hf_N2)-(3*hf_H2O_g);
    delS = (2.*FE.*sf_NH3)+((3/2)*sf_O2)+(3.*(1-FE).*sf_H2)-(FE.*sf_N2)-(3*sf_H2O_g);
    delG = delH-(T_ref*delS);
    Er = delG/(n*F);
    Sr = delS/(n*F);
    OCV_H2O_g = Er - Sr*(T_PEM-T_ref); %REVERSIBLE VOLTAGE
    OCV_H2O = -max(OCV_H2O_g,OCV_H2O_l);
    delS_H2O_g = delS;
 %% Choose OCV depending on Cell Configuration
    if Anode_Reactant == 1
        E = -OCV_H2;
        delS = delS_H2;
    else
        E = -OCV_H2O;
        delS = delS_H2O_l;
    end



end
```

```
function [Value] = FindProperty(property,substance)
    if isequal(property,'Enthalpy Of Formation')
        Table = ["H2(g)",0;"N2(g)",0;"O2(g)",0;"H2O(g)",-241820;"H2O(l)",-285830;"NH3↙
(g)",-46190];
        [rows,~] = find(Table == substance);
        Value = str2double(Table(rows,2));
    elseif isequal(property,'Absolute Entropy')
        Table = ["H2(g)",130.57;"N2(g)",191.5;"O2(g)",205.03;"H2O(g)",188.72;"H2O(l)",↙
69.95;"NH3(g)",192.33];
        [rows,~] = find(Table == substance);
        Value = str2double(Table(rows,2));
    end
end
```

```
function [V,V_drop,i_lim_N2,i_lim_H2] = Cell_Overpotentials(Membrane_Thick,i_density,p,↙
P_ambient,T_PEM,E,Substance,Cathode_Exchange_Current_Density,X,↙
Electrolyte_Conductivity,Electrolyte_Gap,FE)
%% Ohmic Overpotential
   [V_ohm] = OHMIC_OVERPOTENTIAL(Membrane_Thick,T_PEM,i_density,↙
Electrolyte_Conductivity,Electrolyte_Gap);
%% Activation Overpotential
   [V_act] = ACTIVATION_OVERPOTENTIAL(p,P_ambient,T_PEM,i_density,Substance,↙
Cathode_Exchange_Current_Density);
%% Mass Transfer Overpotential
    [V_conc,i_lim_N2,i_lim_H2] = MassTransferOverpotential(p,T_PEM,i_density,FE,↙
Substance);
%% Nernst Overpotential
    [V_nernst] = CONCENTRATION_OVERPOTENTIAL(T_PEM,p,X,Substance);
    %CALCULATING THE IRREVERSIBLE CELL VOLTAGE%
    V = (E + V_act + V_ohm + V_conc + V_nernst); %Remove V_nerst for the paper figures.
    V_drop = (V_act + V_ohm + V_nernst + V_conc);
end
```

```
function [V_ohm] = OHMIC_OVERPOTENTIAL(Membrane_Thick,T_PEM,i_density,↙
Electrolyte_Conductivity,Electrolyte_Gap)
%% Constants/Assumptions/Variables
    Nafion_Water_Constent = 22; %Membrane assumed to be fully hydrated
    L = Membrane_Thick/10000;  %Electrolyte Thickness (cm)--(505microns)
%% Calculations
    sigma = ((0.005139.*Nafion_Water_Constent)-0.00326).*exp(1268.*((1/303)-(1.↙
/T_PEM))); %Conductivity (1/ohms*cm) PAGE 90 (REFERENCE)
    Are_Specific_R_Ohmic = (1./sigma).*L; %Area specific ohmic resistance (ohm*cm^2)
    V_ohm_LE = (1./Electrolyte_Conductivity).*Electrolyte_Gap.*i_density;
    V_ohm_PEM = Are_Specific_R_Ohmic.*i_density; %Ohmic Loss (V)
    V_ohm = V_ohm_PEM + V_ohm_LE;
end
```

```
function [Overpotential] = ACTIVATION_OVERPOTENTIAL(P,P_ref,T,i_density,Substance,↙
Cathode_Exchange_Current_Density)
%% Constants
    R = 8.314; %Ideal Gas Constant (KJ/KmolK)
    F = 96485; %Faraday's Constant
    alpha = 0.5; %Transfer Coefficient
%% Cathode Effective Exchange Current Density
    i_0_ref_Cathode = Cathode_Exchange_Current_Density; %A/cm^2
    [i_0_Cathode] = EXCHANGE_CURRENT_CALC(i_0_ref_Cathode,P,P_ref,T);
%% Cathode Activation Overpotential
    Overpotential_Cathode = ((R.*T)./(3.*alpha.*F)).*asinh(i_density./(2.↙
*i_0_Cathode));
%% Anode Effective Exchange Current Density
    if Substance == 1
    i_0_ref_Anode = 10^-2; %A/cm^2
    else
    i_0_ref_Anode = 10^-9; %A/cm^2
    end
    [i_0_Anode] = EXCHANGE_CURRENT_CALC(i_0_ref_Anode,P,P_ref,T);
%% Anode Activation Overpotential
    Overpotential_Anode = ((R.*T)./(3.*alpha.*F)).*asinh(i_density./(2.*i_0_Anode));
%% Cell Activation Overpotential
    Overpotential = Overpotential_Cathode+Overpotential_Anode;
end
```

```
function [i_0] = EXCHANGE_CURRENT_CALC(i_0_ref,P,P_ref,T)
    R = 8.314;
    n=6;
    F = 96485;
    gamma = 1;
    T_ref = 25+273.15;
    i_0 = i_0_ref.*((P./P_ref).^gamma).*exp((-103000./(R.*T)).*(1-(T./T_ref)));
end
```

```
function [V_conc,i_lim_N2,i_lim_H2] = MassTransferOverpotential(P,T,i_density,FE,↙
Substance)
%% Constants
    R = 8.314; %Ideal Gas Constant (KJ/KmolK)
    F = 96485; %Faraday's Constant
%% Diffusion Coefficient
    D_bulk = 1.55e-5; %m^2/s
    porosity = 0.8; %fraction 0-1
   [D_eff] = DiffusionCoefficientGDL(D_bulk,porosity)
%% Limiting Current Density
    GDL_thickness = 280e-5; %m
    MolarityN2 = P./(R.*T); %molNH3/m^3
    i_lim_N2 = (6.*F.*D_eff.*MolarityN2./GDL_thickness).*1e-4;
    i_lim_H2 = (2.*F.*D_eff.*MolarityN2./GDL_thickness).*1e-4;
%% Mass Transfer Overpotential
    V_conc_N2 = -((R.*T)./(3.*F)).*log(1-(i_density.*(FE./100)./i_lim_N2));
    V_conc_H2 = -((R.*T)./(3.*F)).*log(1-(i_density.*(FE./100)./i_lim_H2));
    if Substance == 2
        V_conc_H2 = 0;
        i_lim_H2 = inf;
    end
    V_conc = V_conc_N2 + V_conc_H2;
    i_lim = min(i_lim_N2,i_lim_H2);
    V_conc(i_density.*(FE./100)>i_lim) = inf;
end
```

```
function [D_eff] = DiffusionCoefficientGDL(D_bulk,porosity)
D_eff = D_bulk.*porosity.^1.5;
end
```

```
function [V_conc] = CONCENTRATION_OVERPOTENTIAL(T_PEM,P,X,Substance)
 R = 8.314; %Ideal Gas Constant (KJ/KmolK)
 F = 96485; %Faraday's Constant
 n=6; %Number of Electrons Involved in the Reaction
 T = T_PEM - 273.15;
 x = 0.001:0.001:X;
 if T < 100
 A = 8.07131;
 B = 1730.63;
 C = 233.426;
 else
 A = 8.14019;
 B = 1810.94;
 C = 244.485;
 end
 P_Sat = 133.322.*10^(A-(B./(C+T))); %Pa
 P_ambient = 101325; %Ambient Pressure (Pa)
 n_N2 = 1-x;
 n_H2 = 3-3.*x;
 n_H2O = 3-3.*x;
 n_NH3 = 2.*X;
 n_O2 = (3./2).*x;
 if Substance == 1
 n_T = n_N2 + n_H2 + n_NH3;
 y_H2 = n_H2./n_T;
 y_N2 = n_N2./n_T;
 y_NH3 = n_NH3./n_T;
 else
 n_T = n_N2 + n_H2O + n_NH3 + n_O2;
 y_H2O = n_H2O./n_T;
 y_N2 = n_N2./n_T;
 y_NH3 = n_NH3./n_T;
 y_O2 = n_O2./n_T;
 end
 if T < 100
     if Substance == 1
     A = ((y_H2.*P./P_ambient).^3).*(y_N2.*P./P_ambient)./((y_NH3.*P./P_ambient).^2);
     else
     A = ((1)^3).*(y_N2.*P./P_ambient)./(((y_NH3.*P./P_ambient).^2).*((y_O2.*P.↙
/P_ambient).^(3/2)));
     end
 else
     if Substance == 1
     A = ((y_H2.*P./P_ambient).^3).*(y_N2.*P./P_ambient)./((y_NH3.*P./P_ambient).^2);
     else
     A = ((y_H2O.*P./P_Sat).^3).*(y_N2.*P./P_ambient)./(((y_NH3.*P./P_ambient).^2).*↙
((y_O2.*P./P_ambient).^(3/2)));
     end
 end
 V_conc = (-(R.*T_PEM/(n.*F)).*log(A));
```

```
 V_conc = mean(V_conc);
end
```

```
function [W,M_N2] = NH3_Separation(H2_mole_OUT,X,Substance,NH3_mole,P,T_PEM) %Molar↙
Flow of Ammonia (mol/s))
 n_N2 = 1-X;
 n_H2 = 3-3.*X;
 n_H2O = 3-3.*X;
 n_NH3 = 2.*X;
 n_O2 = (3./2).*X;
 if Substance == 1
 n_T = n_N2 + n_H2 + n_NH3;
 y_H2 = n_H2./n_T;
 y_N2 = n_N2./n_T;
 y_NH3 = n_NH3./n_T;
 else
 n_T = n_N2 + n_H2O + n_NH3 + n_O2;
 y_H2O = n_H2O./n_T;
 y_N2 = n_N2./n_T;
 y_NH3 = n_NH3./n_T;
 y_O2 = n_O2./n_T;
 end
 mole_rate = NH3_mole./y_NH3;
 N2_mole = mole_rate.*y_N2;

 M_NH3 = (NH3_mole).*(17.031./1000); %kg/s
 M_N2 = (N2_mole).*(28.0134/1000); %kg/s
 M_H2 = (H2_mole_OUT).*(2.016./1000); %kg/s
 P_Exit = 800000; %Pa
 [~,W_Compressor_N2,~,~,~] = N2_Compressor(P_Exit,T_PEM,P,M_N2);
 [~,W_Compressor_H2,~,~,~] = H2_Compressor(P_Exit,T_PEM,P,M_H2);
 [~,W_Compressor_NH3,~,~,~] = NH3_Compressor(P_Exit,T_PEM,P,M_NH3);
 W = W_Compressor_N2+W_Compressor_H2+W_Compressor_NH3;
end
```

```
function [P_Compressor_Exit_atm,W_Compressor,T_Compressor_Exit,Sigma_Dot_Air_Comp,↙
Exergy_Destruction_Air_Comp] = NH3_Compressor(p,T_ambient,P_ambient,M_air)
    R = 8.314; %Ideal Gas Constant (KJ/KmolK)
    Cp_Air = 2.19; %kJ/kg*K
    k_Air = 1.31;
    Compressor_Efficiency = 0.85;   %Isentropic efficiency
    %Analysis
    P_Compressor_Exit = p;
    T_Exit_s = T_ambient*(P_Compressor_Exit/P_ambient).^((k_Air-1)/k_Air); %Ideal↙
temperature, K
    P_Compressor_Exit_atm = P_Compressor_Exit./(1.01325.*10^5); %atm
    W_Compressor_s = M_air.*Cp_Air.*(T_Exit_s-T_ambient); %Isentropic work input, kW
    W_Compressor = W_Compressor_s/Compressor_Efficiency;         %Actual work
    T_Compressor_Exit = ((T_Exit_s-T_ambient)/Compressor_Efficiency) + T_ambient; %↙
Actual temperature, K
    Sigma_Dot_Air_Comp = M_air.*((Cp_Air.*log(T_Compressor_Exit./T_ambient))-((R./29)↙
*log(p./P_ambient))); %Entropy Generation in Air Comp (kW/kgK)
    efi_Air_Compressor = (Cp_Air.*(T_ambient-T_ambient))-(T_ambient.*(((Cp_Air.*log↙
(T_ambient./T_ambient))-((R./29)*log(P_ambient./P_ambient)))));
    efe_Air_Compressor = (Cp_Air.*(T_Compressor_Exit-T_ambient))-(T_ambient.*(((Cp_Air.↙
*log(T_Compressor_Exit./T_ambient))-((R./29)*log(p./P_ambient)))));
    Exergy_Destruction_Air_Comp = W_Compressor + M_air.*(efi_Air_Compressor-↙
efe_Air_Compressor);
end
```

```
function [P_Compressor_Exit_atm,W_Compressor,T_Compressor_Exit,Sigma_Dot_Air_Comp,↙
Exergy_Destruction_Air_Comp] = N2_Compressor(p,T_ambient,P_ambient,M_air)
    R = 8.314; %Ideal Gas Constant (KJ/KmolK)
    Cp_Air = 1.04; %kJ/kg*K
    k_Air = 1.4;
    Compressor_Efficiency = 0.85;   %Isentropic efficiency
    %Analysis
    P_Compressor_Exit = p;
    T_Exit_s = T_ambient*(P_Compressor_Exit/P_ambient).^((k_Air-1)/k_Air); %Ideal↙
temperature, K
    P_Compressor_Exit_atm = P_Compressor_Exit./(1.01325.*10^5); %atm
    W_Compressor_s = M_air.*Cp_Air.*(T_Exit_s-T_ambient); %Isentropic work input, kW
    W_Compressor = W_Compressor_s/Compressor_Efficiency;         %Actual work
    T_Compressor_Exit = ((T_Exit_s-T_ambient)/Compressor_Efficiency) + T_ambient; %↙
Actual temperature, K
    Sigma_Dot_Air_Comp = M_air.*((Cp_Air.*log(T_Compressor_Exit./T_ambient))-((R./29)↙
*log(p./P_ambient))); %Entropy Generation in Air Comp (kW/kgK)
    efi_Air_Compressor = (Cp_Air.*(T_ambient-T_ambient))-(T_ambient.*(((Cp_Air.*log↙
(T_ambient./T_ambient))-((R./29)*log(P_ambient./P_ambient)))));
    efe_Air_Compressor = (Cp_Air.*(T_Compressor_Exit-T_ambient))-(T_ambient.*(((Cp_Air.↙
*log(T_Compressor_Exit./T_ambient))-((R./29)*log(p./P_ambient)))));
    Exergy_Destruction_Air_Comp = W_Compressor + M_air.*(efi_Air_Compressor-↙
efe_Air_Compressor);
end
```

```
function [P_Compressor_Exit_atm,W_Compressor,T_Compressor_Exit,Sigma_Dot_Air_Comp,↙
Exergy_Destruction_Air_Comp] = H2_Compressor(p,T_ambient,P_ambient,M_air)
    R = 8.314; %Ideal Gas Constant (KJ/KmolK)
    Cp_Air = 14.32; %kJ/kg*K
    k_Air = 1.41;
    Compressor_Efficiency = 0.85;   %Isentropic efficiency
    %Analysis
    P_Compressor_Exit = p;
    T_Exit_s = T_ambient*(P_Compressor_Exit/P_ambient).^((k_Air-1)/k_Air); %Ideal↙
temperature, K
    P_Compressor_Exit_atm = P_Compressor_Exit./(1.01325.*10^5); %atm
    W_Compressor_s = M_air.*Cp_Air.*(T_Exit_s-T_ambient); %Isentropic work input, kW
    W_Compressor = W_Compressor_s/Compressor_Efficiency;         %Actual work
    T_Compressor_Exit = ((T_Exit_s-T_ambient)/Compressor_Efficiency) + T_ambient; %↙
Actual temperature, K
    Sigma_Dot_Air_Comp = M_air.*((Cp_Air.*log(T_Compressor_Exit./T_ambient))-((R./29)↙
*log(p./P_ambient))); %Entropy Generation in Air Comp (kW/kgK)
    efi_Air_Compressor = (Cp_Air.*(T_ambient-T_ambient))-(T_ambient.*(((Cp_Air.*log↙
(T_ambient./T_ambient))-((R./29)*log(P_ambient./P_ambient)))));
    efe_Air_Compressor = (Cp_Air.*(T_Compressor_Exit-T_ambient))-(T_ambient.*(((Cp_Air.↙
*log(T_Compressor_Exit./T_ambient))-((R./29)*log(p./P_ambient)))));
    Exergy_Destruction_Air_Comp = W_Compressor + M_air.*(efi_Air_Compressor-↙
efe_Air_Compressor);
end
```

```
function [Power_Air_Separation] = Air_Separation_Unit(M_N2)
R = 8.314; %J/molK
Pressure =  1*101325; %Pa
Temperature = 273.15; %K
FlowRate = 36000; %m^3/h
n = (Pressure.*FlowRate)./(R.*Temperature); %mol/h
MM = 28.0134; %g/mol
M_out = (n.*MM./1000)./3600; %kg/s
Power = 2270; %kW
E = Power./M_out; %kJ/kg
Power_Air_Separation = E.*M_N2; %kW
end
```

```
function [Sigma_Dot_Air_HE,Exergy_Destruction_Air_HE,Q_HeatExchanger_Air_In] = N2_HE
(T_Compressor_Exit,M_air,T_PEM,T_ambient,p,P_ambient)
    R = 8.314; %Ideal Gas Constant (KJ/KmolK)
    Cp_Air = 1.04; %kJ/kg*K
    k_Air = 1.4;
%AIR HEAT EXCHANGER (CALCULATING HEAT INPUT)
    T_HeatExchanger_Air_Inlet  = T_Compressor_Exit; %Heat Exchanger Inlet Temperature
    Q_HeatExchanger_Air_In = M_air.*Cp_Air.*(T_PEM-T_HeatExchanger_Air_Inlet); %Heat
from enviroment into air heat exchanger
%%%%%%%%%%%%%%%%%%%%%%%%%%%%%%%%%%%%%%%%%%%%%%%%%%%%%%%%%%%%%%%%%%%%%%%%%%%%%%%
    %ENTROPY ANALYSIS
    %AIR HEAT EXCHANGER
    %0 = Q/T + Min*Sin - Mou*Sou + sigma
    %sigma = M(Sout-Sin)- Q/T
    Tb_Air = (T_HeatExchanger_Air_Inlet+T_PEM)./2;
    Sigma_Dot_Air_HE = (M_air.*((Cp_Air.*log(T_PEM./T_HeatExchanger_Air_Inlet))))-
(Q_HeatExchanger_Air_In/Tb_Air); %Entropy Generation in Water Pump (kW/kgK)
    dummy = 0;
if Q_HeatExchanger_Air_In < 0
    M_Cooling_Water = 1; %kg/s
    T_Cooling_Water_Out = (-1*Q_HeatExchanger_Air_In./(M_Cooling_Water*4.2))+T_ambient;
    Q_HeatExchanger_Air_In = 0;
    Sigma_Dot_Air_HE = (M_air.*((Cp_Air.*log(T_PEM./T_HeatExchanger_Air_Inlet)))) +
(M_Cooling_Water.*4.2.*log(T_Cooling_Water_Out./T_ambient));
    dummy = 1;
end
%%%%%%%%%%%%%%%%%%%%%%%%%%%%%%%%%%%%%%%%%%%%%%%%%%%%%%%%%%%%%%%%%%%%%%%%%%%%%%%
    %EXERGY ANALYSIS
    %AIR HEAT EXCHANGER
    %0 = (1-To/Tb)Qi + miefi - meefe - Ed
    %Ed = (1-To/Tb)Qi + miefi - meefe
    efi_Air_HE = (Cp_Air.*(T_Compressor_Exit-T_ambient))-(T_ambient.*(((Cp_Air.*log
(T_Compressor_Exit./T_ambient))-((R./29)*log(p./P_ambient)))));
    efe_Air_HE = (Cp_Air.*(T_PEM-T_ambient))-(T_ambient.*(((Cp_Air.*log(T_PEM.
/T_ambient))-((R./29)*log(p./P_ambient)))));
    Exergy_Destruction_Air_HE = ((1-(T_ambient./Tb_Air)).*Q_HeatExchanger_Air_In) +
M_air.*(efi_Air_HE-efe_Air_HE);
if dummy == 1
    C = 4.2;
    efi_Cooling_Water_HE = ((C.*(T_ambient-T_ambient))-(T_ambient.*C.*log(T_ambient.
/T_ambient)));
    efe_Cooling_Water_HE = ((C.*(T_Cooling_Water_Out-T_ambient))-(T_ambient.*C.*log
(T_Cooling_Water_Out./T_ambient)));
    M_Cooling_Water = 1; %kg/s
    Exergy_Destruction_Air_HE = M_air.*(efi_Air_HE-efe_Air_HE)+M_Cooling_Water.*
(efi_Cooling_Water_HE-efe_Cooling_Water_HE);
end
end
```

```
function [Sigma_Dot_Water_Pump,Exergy_Destruction_Water_Pump,W_Pump,T_Pump_Exit,↙
P_Pump_Exit] = Water_Pump(p,M_water,P_ambient,T_ambient)
   %CONSTANTS
    Specific_Vol_water = 0.001029; %m^3/kg
    C_Water = 4.2; %Specific heat of water, kJ/kg*K
    Pump_Efficiency = 0.85; %Isentropic efficiency of pump
    %Analysis
    P_Pump_Exit = p;
    W_Pump_s = M_water.*Specific_Vol_water.*(P_Pump_Exit-P_ambient)/1000;   %Ideal pump↙
work, kW
    W_Pump = W_Pump_s/Pump_Efficiency; %Actual pump work, kW
    T_Pump_Exit = (W_Pump-W_Pump_s)/(M_water*C_Water)+T_ambient;
%%%%%%%%%%%%%%%%%%%%%%%%%%%%%%%%%%%%%%%%%%%%%%%%%%%%%%%%%%%%%%%%%%%%%%%%%%%%
    %ENTROPY ANALYSIS
    %WATER PUMP
    %0 = Min*Sin - Mou*Sou + sigma
    %sigma = M(Sout-Sin)
    Sigma_Dot_Water_Pump = M_water.*C_Water.*log(T_Pump_Exit./T_ambient); %Entropy↙
Generation in Water Pump (kW/kgK)
%%%%%%%%%%%%%%%%%%%%%%%%%%%%%%%%%%%%%%%%%%%%%%%%%%%%%%%%%%%%%%%%%%%%%%%%%%%%
    %EXERGY ANALYSIS
    %WATER PUMP
    %0 = -W + miefi - meefe - Ed
    %Ed = -W + miefi - meefe
    efi_Water_Pump = ((C_Water.*(T_ambient-T_ambient))-(T_ambient.*C_Water.*log↙
(T_ambient./T_ambient)));
    efe_Water_Pump = ((C_Water.*(T_Pump_Exit-T_ambient))-(T_ambient.*C_Water.*log↙
(T_Pump_Exit./T_ambient)));
    Exergy_Destruction_Water_Pump = W_Pump + M_water.*(efi_Water_Pump-efe_Water_Pump);
end
```

```
function [Sigma_Dot_Water_HE,Q_HeatExchanger_Water_In,Exergy_Destruction_Water_HE] =↙
Water_HE(T_Pump_Exit,M_water,T_PEM,T_ambient)
    Specific_Vol_water = 0.001029; %m^3/kg
    C_Water = 4.2; %Specific heat of water, kJ/kg*K
    T_HeatExchanger_Water_Inlet  = T_Pump_Exit; %Heat Exchanger Inlet Temperature
    Q_HeatExchanger_Water_In = M_water.*C_Water.*(T_PEM-T_HeatExchanger_Water_Inlet); %↙
Heat from enviroment into air heat exchanger
%%%%%%%%%%%%%%%%%%%%%%%%%%%%%%%%%%%%%%%%%%%%%%%%%%%%%%%%%%%%%%%%%%%%%%%%%%%%%%%
%%%%%%%%%%%%%%%%%%%%%%%%%%%%%%%%%%%%%%%%%%%%%%%%%%%%%%%%%%%%%%%%%%%%%%%%%%%%%%%
    %ENTROPY ANALYSIS
    %WATER HEAT EXCHANGER
    %0 = Q/T + Min*Sin - Mou*Sou + sigma
    %sigma = M(Sout-Sin)- Q/T
    Tb_Water = (T_HeatExchanger_Water_Inlet+T_PEM)./2;
    Sigma_Dot_Water_HE = (M_water.*C_Water.*log(T_PEM./T_HeatExchanger_Water_Inlet))-↙
(Q_HeatExchanger_Water_In/Tb_Water); %Entropy Generation in Water Pump (kW/kgK)
%%%%%%%%%%%%%%%%%%%%%%%%%%%%%%%%%%%%%%%%%%%%%%%%%%%%%%%%%%%%%%%%%%%%%%%%%%%%%%%
    %EXERGY ANALYSIS
    %WATER HEAT EXCHANGER
    %0 = (1-To/Tb)Qi + miefi - meefe - Ed
    %Ed = (1-To/Tb)Qi + miefi - meefe
    efi_Water_HE = ((C_Water.*(T_Pump_Exit-T_ambient))-(T_ambient.*C_Water.*log↙
(T_Pump_Exit./T_ambient)));
    efe_Water_HE = ((C_Water.*(T_PEM-T_ambient))-(T_ambient.*C_Water.*log(T_PEM.↙
/T_ambient)));
    Exergy_Destruction_Water_HE = ((1-(T_ambient./Tb_Water)).*Q_HeatExchanger_Water_In)↙
+ M_water.*(efi_Water_HE-efe_Water_HE);
end
```

```
function [Q_heat_PEM] = HEAT_PEM( T_PEM,N2_mole,delS,Current_Need,V_drop)
    %0 = Q/T + miSi - meSe
    %Q = TdS - sigma
    F = 96485;
    mole = Current_Need./(6.*F);
    T_dS = T_PEM.*mole.*delS./1000;
    SIGMA_PEM = Current_Need.*V_drop./1000;
    Q_heat_PEM = T_dS - SIGMA_PEM;
end
```

REFERENCES

[1] J. W. McArthur and G. C. McCord, "Fertilizing growth: Agricultural inputs and their effects in economic development," *Journal of development economics*, vol. 127, pp. 133–152, 2017.

[2] AfricaFertilizer.org. (2020). Africa fertilizer production directory, (visited on 05/30/2020).

[3] R. Schlögl, "Catalytic synthesis of ammonia – a "never ending story"?" *Angewandte Chemie International*, vol. Edition 42, no. 52, pp. 2004–2008, 2003.

[4] G. Hochman, A. Goldman, F. A. Felder, J. Mayer, A. Miller, P. L. Holland, L. Goldman, P. Manocha, Z. Song, and S. Aleti, "The Potential Economic Feasibility of Direct Electrochemical Nitrogen Reduction as a Route to Ammonia," Oct. 2019.

[5] P. H. Pfromm, "Towards sustainable agriculture: Fossil-free ammonia," *Journal of Renewable and Sustainable Energy*, vol. 9, no. 3, p. 034 702, 2017.

[6] C. Smith, A. K. Hill, and L. Torrente-Murciano, "Current and future role of haber–bosch ammonia in a carbon-free energy landscape," *Energy Environ. Sci.*, vol. 13, pp. 331–344, 2 2020.

[7] Advanced Research Projects Agency—Energy—US Department of Energy, "Refuel.," *https://arpa-e.energy.gov/?q=arpa-e-programs/refuel.*, 2016.

[8] A. J. Martín, T. Shinagawa, and J. Pérez-Ramírez, "Electrocatalytic reduction of nitrogen: From haber-bosch to ammonia artificial leaf," *Chem*, vol. 5, no. 2, pp. 263–283, 2019.

[9] M. Zhang, M. Moore, J. Watson, T. Zawodzinski, and R. Counce, "Capital cost sensitivity analysis of an all-vanadium redox-flow battery," *Journal of the Electrochemical Society*, vol. 159, A1183–A1188, Jan. 2012.

[10] C. R. Soccol, V. Faraco, S. G. Karp, L. P. Vandenberghe, V. Thomaz-Soccol, A. L. Woiciechowski, and A. Pandey, "Chapter 14 - lignocellulosic bioethanol: Current status and future perspectives," in *Biofuels: Alternative Feedstocks and Conversion Processes for the Production of Liquid and Gaseous Biofuels (Second Edition)*, ser. Biomass, Biofuels, Biochemicals, A. Pandey, C. Larroche, C.-G. Dussap, E. Gnansounou, S. K. Khanal, and S. Ricke, Eds., Second Edition, Academic Press, 2019, pp. 331 –354, ISBN: 978-0-12-816856-1.

[11] J. Liu, L. You, M. Amini, M. Obersteiner, M. Herrero, A. J. B. Zehnder, and H. Yang, "A high-resolution assessment on global nitrogen flows in cropland," *Proceedings of the National Academy of Sciences*, vol. 107, no. 17, pp. 8035–8040, 2010. eprint: `https://www.pnas.org/content/107/17/8035.full.pdf`.

[12] P. A. Sanchez and M. Swaminathan, "Hunger in africa: The link between unhealthy people and unhealthy soils," *The Lancet*, vol. 365, no. 9457, pp. 442–444, 2005.

[13] P. A. Sanchez and M. S. Swaminathan, "Hunger in africa: The link between unhealthy people and unhealthy soils," *The Lancet*, vol. 365, no. 9457, pp. 442–444, 2005.

[14] Food and A. O. of the United Nations, "Faostat statistics database," 2016.

[15] N. P. Nitrogen, "Northern plains nitrogen, northern plains nitrogen to construct $1.5 billion nitrogen fertilizer production facility northwest of grand forks.," 2013.

[16] F. FAOSTAT, "Faostat data," 2016.

[17] B. M. Comer, P. Fuentes, C. O. Dimkpa, Y.-H. Liu, C. A. Fernandez, P. Arora, M. Realff, U. Singh, M. C. Hatzell, and A. J. Medford, "Prospects and challenges for solar fertilizers," *Joule*, 2019.

[18] W.-y. Huang, *Impact of rising natural gas prices on US ammonia supply*. DIANE Publishing, 2007.

[19] X. L. Etienne, A. Trujillo-Barrera, and S. Wiggins, "Price and volatility transmissions between natural gas, fertilizer, and corn markets," *Agricultural Finance Review*, 2016.

[20] T. Czuppon, C. TA, and B. LJ, "Which feedstock for ammonia.," 1979.

[21] M. Wanzala, R. Groot, *et al.*, "Fertiliser market development in sub-saharan africa.," in *Proceedings-International Fertiliser Society*, International Fertiliser Society, 2013.

[22] C. Smith, A. K. Hill, and L. Torrente-Murciano, "Current and future role of haber–bosch ammonia in a carbon-free energy landscape," *Energy & Environmental Science*, vol. 13, no. 2, pp. 331–344, 2020.

[23] J. Rostrup-Nielsen, L. Christiansen, and J.-H. B. Hansen, "Activity of steam reforming catalysts: Role and assessment," *Applied Catalysis*, vol. 43, no. 2, pp. 287–303, 1988.

[24] L. Wang, M. Xia, H. Wang, K. Huang, C. Qian, C. T. Maravelias, and G. A. Ozin, "Greening ammonia toward the solar ammonia refinery," *Joule*, vol. 2, no. 6, pp. 1055–1074, 2018.

[25] Z. J. Schiffer and K. Manthiram, "Electrification and decarbonization of the chemical industry," *Joule*, vol. 1, no. 52, pp. 10–14, 2017.

[26] Y. Bicer, I. Dincer, C. Zamfirescu, G. Vezina, and F. Raso, "Comparative life cycle assessment of various ammonia production methods," *Journal of Cleaner Production*, vol. 135, pp. 1379–1395, 2016.

[27] K Noelker and J Ruether, "Low energy consumption ammonia production: Baseline energy consumption, options for energy optimization," in *Nitrogen+ Syngas Conference*, 2011.

[28] I. Rafiqul, C. Weber, B. Lehmann, and A. Voss, "Energy efficiency improvements in ammonia production—perspectives and uncertainties," *Energy*, vol. 30, no. 13, pp. 2487–2504, 2005.

[29] J. N. Renner, L. F. Greenlee, K. E. Ayres, and A. M. Herring, "Electrochemical synthesis of ammonia: A low pressure, low temperature approach," *Electrochemical Society Interface*, vol. 24, no. 2, p. 51, 2015.

[30] S Giddey, S. Badwal, and A Kulkarni, "Review of electrochemical ammonia production technologies and materials," *International Journal of Hydrogen Energy*, vol. 38, no. 34, pp. 14 576–14 594, 2013.

[31] J. R. Bartels, "A feasibility study of implementing an ammonia economy.," *Iowa State University*, 2008.

[32] P. De Luna, C. Hahn, D. Higgins, S. A. Jaffer, T. F. Jaramillo, and E. H. Sargent, "What would it take for renewably powered electrosynthesis to displace petrochemical processes?" *Science*, vol. 364, no. 6438, eaav3506, 2019.

[33] O. of Energy Efficiency and R. Energy, "New solar opportunities for a new decade," *SunShot 2030*, 2020.

[34] K. Kugler, M. Luhn, J. A. Schramm, K. Rahimi, and M. Wessling, "Galvanic deposition of rh and ru on randomly structured ti felts for the electrochemical nh3 synthesis," *Phys. Chem. Chem. Phys.*, vol. 17, pp. 3768–3782, 5 2015.

[35] V. Kordali, G. Kyriacou, and C. Lambrou, "Electrochemical synthesis of ammonia at atmospheric pressure and low temperature in a solid polymer electrolyte cell," *Chem. Commun.*, pp. 1673–1674, 17 2000.

[36] D. Bao, Q. Zhang, F.-L. Meng, H.-X. Zhong, M.-M. Shi, Y. Zhang, J.-M. Yan, Q. Jiang, and X.-B. Zhang, "Electrochemical reduction of n2 under ambient conditions for artificial n2 fixation and renewable energy storage using n2/nh3 cycle," *Advanced Materials*, vol. 29, no. 3, p. 1 604 799, 2017. eprint: https://onlinelibrary.wiley.com/doi/pdf/10.1002/adma.201604799.

[37] S.-J. Li, D. Bao, M.-M. Shi, B.-R. Wulan, J.-M. Yan, and Q. Jiang, "Amorphizing of au nanoparticles by ceox–rgo hybrid support towards highly efficient electrocatalyst for n2 reduction under ambient conditions," *Advanced Materials*, vol. 29, no. 33, p. 1 700 001, 2017. eprint: https://onlinelibrary.wiley.com/doi/pdf/10.1002/adma.201700001.

[38] M.-M. Shi, D. Bao, B.-R. Wulan, Y.-H. Li, Y.-F. Zhang, J.-M. Yan, and Q. Jiang, "Au sub-nanoclusters on tio2 toward highly efficient and selective electrocatalyst for n2 conversion to nh3 at ambient conditions," *Advanced Materials*, vol. 29, no. 17, p. 1 606 550, 2017. eprint: https://onlinelibrary.wiley.com/doi/pdf/10.1002/adma.201606550.

[39] Y. Yao, S. Zhu, H. Wang, H. Li, and M. Shao, "A spectroscopic study on the nitrogen electrochemical reduction reaction on gold and platinum surfaces," *Journal of the American Chemical Society*, vol. 140, no. 4, pp. 1496–1501, 2018, PMID: 29320173. eprint: https://doi.org/10.1021/jacs.7b12101.

[40] H. K. Lee, C. S. L. Koh, Y. H. Lee, C. Liu, I. Y. Phang, X. Han, C.-K. Tsung, and X. Y. Ling, "Favoring the unfavored: Selective electrochemical nitrogen fixation using a reticular chemistry approach," *Science Advances*, vol. 4, no. 3, 2018. eprint: https://advances.sciencemag.org/content/4/3/eaar3208.full.pdf.

[41] Y. Hao, Y. Guo, L. Chen, and et al., "Promoting nitrogen electroreduction to ammonia with bismuth nanocrystals and potassium cations in water.," *Nature Catalysis*, vol. 2, 448–456, 2019.

[42] S. Chen, S. Perathoner, C. Ampelli, C. Mebrahtu, D. Su, and G. Centi, "Electrocatalytic synthesis of ammonia at room temperature and atmospheric pressure from water and nitrogen on a carbon-nanotube-based electrocatalyst," *Angewandte Chemie International Edition*, vol. 56, no. 10, pp. 2699–2703, 2017.

[43] R. Lan, J. Irvine, and S. Tao, "Synthesis of ammonia directly from air and water at ambient temperature and pressure.," *Science*, vol. 3, 1–7, 2013.

[44] A. Tsuneto, A. Kudo, and T. Sakata, "Efficient electrochemical reduction of n2 to nh3 catalyzed by lithium," *Chemistry Letters*, vol. 22, no. 5, pp. 851–854, 1993. eprint: https://doi.org/10.1246/cl.1993.851.

[45] J. Wang, L. Yu, Hu, L. et al., and et al., "Ambient ammonia synthesis via palladium-catalyzed electrohydrogenation of dinitrogen at low overpotential.," *Nature Communications*, vol. 9, p. 1795, 2018.

[46] H.-M. Liu, S.-H. Han, Y. Zhao, Y.-Y. Zhu, X.-L. Tian, J.-H. Zeng, J.-X. Jiang, B. Y. Xia, and Y. Chen, "Surfactant-free atomically ultrathin rhodium nanosheet nanoassemblies for efficient nitrogen electroreduction," *J. Mater. Chem. A*, vol. 6, pp. 3211–3217, 7 2018.

[47] R. Lan and S. Tao, "Electrochemical synthesis of ammonia directly from air and water using a li+/h+/nh4+ mixed conducting electrolyte," *RSC Adv.*, vol. 3, pp. 18 016–18 021, 39 2013.

[48] N. Furuya and H. Yoshiba, "Electroreduction of nitrogen to ammonia on gas-diffusion electrodes loaded with inorganic catalyst," *Journal of electroanalytical chemistry and interfacial electrochemistry*, vol. 291, no. 1-2, pp. 269–272, 1990.

[49] F. Zhou, L. M. Azofra, M. Ali, M. Kar, A. N. Simonov, C. McDonnell-Worth, C. Sun, X. Zhang, and D. R. MacFarlane, "Electro-synthesis of ammonia from nitrogen at ambient temperature and pressure in ionic liquids," *Energy Environ. Sci.*, vol. 10, pp. 2516–2520, 12 2017.

[50] D. Yang, T. Chen, and Z. Wang, "Electrochemical reduction of aqueous nitrogen (n2) at a low overpotential on (110)-oriented mo nanofilm," *J. Mater. Chem. A*, vol. 5, pp. 18 967–18 971, 36 2017.

[51] X. Zhao, F. Yin, N. Liu, G. Li, T. Fan, and B. Chen, "Highly efficient metal–organic-framework catalysts for electrochemical synthesis of ammonia from n2 (air) and water at low temperature and ambient pressure," *Journal of Materials Science*, vol. 52, pp. 1–11, Sep. 2017.

[52] C. Lv, C. Yan, G. Chen, Y. Ding, J. Sun, Y. Zhou, and G. Yu, "An amorphous noble-metal-free electrocatalyst that enables nitrogen fixation under ambient conditions," *Angewandte Chemie*, vol. 130, no. 21, pp. 6181–6184, 2018.

[53] N. Furuya and H. Yoshiba, "Electroreduction of nitrogen to ammonia on gas-diffusion electrodes modified by fe-phthalocyanine," *Journal of electroanalytical chemistry and interfacial electrochemistry*, vol. 263, no. 1, pp. 171–174, 1989.

[54] L. Zhang, X. Ji, X. Ren, Y. Ma, X. Shi, Z. Tian, A. M. Asiri, L. Chen, B. Tang, and X. Sun, "Electrochemical ammonia synthesis via nitrogen reduction reaction on a mos2 catalyst: Theoretical and experimental studies," *Advanced Materials*, vol. 30, no. 28, p. 1 800 191, 2018.

[55] D. Yang, T. Chen, and Z. Wang, "Electrochemical reduction of aqueous nitrogen (n 2) at a low overpotential on (110)-oriented mo nanofilm," *Journal of Materials Chemistry A*, vol. 5, no. 36, pp. 18 967–18 971, 2017.

[56] X. Ren, G. Cui, L. Chen, F. Xie, Q. Wei, Z. Tian, and X. Sun, "Electrochemical n 2 fixation to nh 3 under ambient conditions: Mo 2 n nanorod as a highly efficient and selective catalyst," *Chemical Communications*, vol. 54, no. 61, pp. 8474–8477, 2018.

[57] L. Hu, A. Khaniya, J. Wang, G. Chen, W. E. Kaden, and X. Feng, "Ambient electrochemical ammonia synthesis with high selectivity on fe/fe oxide catalyst," *ACS Catalysis*, vol. 8, no. 10, pp. 9312–9319, 2018.

[58] X. Cui, C. Tang, X.-M. Liu, C. Wang, W. Ma, and Q. Zhang, "Highly selective electrochemical reduction of dinitrogen to ammonia at ambient temperature and pressure over iron oxide catalysts," *Chem.-Eur. J*, vol. 24, no. 69, pp. 18 494–18 501, 2018.

[59] B. H. Suryanto, C. S. Kang, D. Wang, C. Xiao, F. Zhou, L. M. Azofra, L. Cavallo, X. Zhang, and D. R. MacFarlane, "Rational electrode–electrolyte design for efficient ammonia electrosynthesis under ambient conditions," *ACS Energy Letters*, vol. 3, no. 6, pp. 1219–1224, 2018.

[60] X. Zhang, R.-M. Kong, H. Du, L. Xia, and F. Qu, "Highly efficient electrochemical ammonia synthesis via nitrogen reduction reactions on a vn nanowire array under ambient conditions," *Chemical Communications*, vol. 54, no. 42, pp. 5323–5325, 2018.

[61] X. Yang, J. Nash, J. Anibal, M. Dunwell, S. Kattel, E. Stavitski, K. Attenkofer, J. G. Chen, Y. Yan, and B. Xu, "Mechanistic insights into electrochemical nitrogen reduction reaction on vanadium nitride nanoparticles," *Journal of the American Chemical Society*, vol. 140, no. 41, pp. 13 387–13 391, 2018.

[62] R. Zhang, X. Ren, X. Shi, F. Xie, B. Zheng, X. Guo, and X. Sun, "Enabling effective electrocatalytic n2 conversion to nh3 by the tio2 nanosheets array under ambient conditions," *ACS applied materials & interfaces*, vol. 10, no. 34, pp. 28 251–28 255, 2018.

[63] Y. Luo, G.-F. Chen, L. Ding, X. Chen, L.-X. Ding, and H. Wang, "Efficient electrocatalytic n2 fixation with mxene under ambient conditions," *Joule*, vol. 3, no. 1, pp. 279–289, 2019.

[64] J. Han, Z. Liu, Y. Ma, G. Cui, F. Xie, F. Wang, Y. Wu, S. Gao, Y. Xu, and X. Sun, "Ambient n2 fixation to nh3 at ambient conditions: Using nb2o5 nanofiber as a high-performance electrocatalyst," *Nano Energy*, vol. 52, pp. 264–270, 2018.

[65] W. Guo, Z. Liang, J. Zhao, B. Zhu, K. Cai, R. Zou, and Q. Xu, "Hierarchical cobalt phosphide hollow nanocages toward electrocatalytic ammonia synthesis under ambient pressure and room temperature," *Small Methods*, vol. 2, no. 12, p. 1 800 204, 2018.

[66] Y. Yao, Q. Feng, S. Zhu, J. Li, Y. Yao, Y. Wang, Q. Wang, M. Gu, H. Wang, H. Li, *et al.*, "Chromium oxynitride electrocatalysts for electrochemical synthesis of ammonia under ambient conditions," *Small Methods*, vol. 3, no. 6, p. 1 800 324, 2019.

[67] K. Kim, N. Lee, C.-Y. Yoo, J.-N. Kim, H. C. Yoon, and J.-I. Han, "Communication—electrochemical reduction of nitrogen to ammonia in 2-propanol under ambient temperature and pressure," *Journal of The Electrochemical Society*, vol. 163, no. 7, F610, 2016.

[68] G.-F. Chen, X. Cao, S. Wu, X. Zeng, L.-X. Ding, M. Zhu, and H. Wang, "Ammonia electrosynthesis with high selectivity under ambient conditions via a li+ incorporation strategy," *Journal of the American Chemical Society*, vol. 139, no. 29, pp. 9771–9774, 2017.

[69] Y. Liu, Y. Su, X. Quan, X. Fan, S. Chen, H. Yu, H. Zhao, Y. Zhang, and J. Zhao, "Facile ammonia synthesis from electrocatalytic n2 reduction under ambient conditions on n-doped porous carbon," *ACS Catalysis*, vol. 8, no. 2, pp. 1186–1191, 2018.

[70] Y. Song, D. Johnson, R. Peng, D. K. Hensley, P. V. Bonnesen, L. Liang, J. Huang, F. Yang, F. Zhang, R. Qiao, *et al.*, "A physical catalyst for the electrolysis of nitrogen to ammonia," *Science advances*, vol. 4, no. 4, e1700336, 2018.

[71] N. V. Plechkova and K. R. Seddon, "Applications of ionic liquids in the chemical industry," *Chemical Society Reviews*, vol. 37, no. 1, pp. 123–150, 2008.

[72] Z. J. Schiffer and K. Manthiram, "Electrification and decarbonization of the chemical industry," *Joule*, vol. 1, no. 1, pp. 10–14, 2017.

[73] M. J. Moran, H. N. Shapiro, D. D. Boettner, and M. B. Bailey, *Fundamentals of engineering thermodynamics*. John Wiley & Sons, 2010.

[74] M. Temkin, N. Morozow, and E. Shapatina, "The kinetics of the synthesis of ammonia under nonequilibrium conditions," *Kinet. Catal*, vol. 4, p. 565, 1963.

[75] D. Dyson and J. Simon, "Kinetic expression with diffusion correction for ammonia synthesis on industrial catalyst," *Industrial & engineering chemistry fundamentals*, vol. 7, no. 4, pp. 605–610, 1968.

[76] H. Cooper, "Fugacities for high p and t," *Hydrocarbon Processing*, vol. 46, no. 2, p. 159, 1967.

[77] R. H. Newton, "Activity coefficients of gases," *Industrial & Engineering Chemistry*, vol. 27, no. 3, pp. 302–306, 1935.

[78] H. R. Shaw and D. R. Wones, "Fugacity coefficients for hydrogen gas between o degrees and 1000 degrees c, for pressures to 3000 atm," *American Journal of Science*, vol. 262, no. 7, pp. 918–929, 1964.

[79] L. J. Gillespie and J. A. Beattie, "The thermodynamic treatment of chemical equilibria in systems composed of real gases. i. an approximate equation for the mass action function applied to the existing data on the haber equilibrium," *Physical review*, vol. 36, no. 4, p. 743, 1930.

[80] D. Satimurty, "Kinetic parameter estimation in ammonia synthesis reaction through nonlinear regression.," *A project dissertation submitted to the Chemical Engineering Programme Universiti Teknologi PETRONAS*, 2014.

[81] O. Schmidt, A. Gambhir, I. Staffell, A Hawkes, J. Nelson, and S. Few, "Future cost and performance of water electrolysis: An expert elicitation study," *International Journal of Hydrogen Energy*, vol. 42, no. 52, pp. 30 470–30 492, 2017.

[82] A. Hauch, S. D. Ebbesen, S. H. Jensen, and M. Mogensen, "Highly efficient high temperature electrolysis," *Journal of Materials Chemistry*, vol. 18, no. 20, pp. 2331–2340, 2008.

[83] C. C. McCrory, S. Jung, I. M. Ferrer, S. M. Chatman, J. C. Peters, and T. F. Jaramillo, "Benchmarking hydrogen evolving reaction and oxygen evolving reaction electrocatalysts for solar water splitting devices," *Journal of the American Chemical Society*, vol. 137, no. 13, pp. 4347–4357, 2015.

[84] A. J. Martín, T. Shinagawa, and J. Pérez-Ramírez, "Electrocatalytic Reduction of Nitrogen: From Haber-Bosch to Ammonia Artificial Leaf," *Chem*, vol. 5, no. 2, pp. 263–283, 2019.

[85] D. C. Dyson and J. M. Simon, "A kinetic expression with diffusion correction for ammonia synthesis on industrial catalyst," *Industrial engineering chemistry*, 1968.

[86] V. Gurau, F. Barbir, and H. Liu, "An analytical solution of a half-cell model for pem fuel cells.," *Journal of The Electrochemical Society*, vol. 147, no. 7, pp. 2468–2477, 2000.

[87] H. Darling, "Conductivity of Sulfuric Acid Solutions," *J. Chem. Eng. Data*, vol. 9, 421–426, 1964.

[88] R. Battino and H. Clever, "The Solubility of Gases in Liquids," 1965.

[89] G. C. Shane P.C. and J. P. Trusler, "Diffusion Coefficients of CO2 and N2 in Water at Temperatures between 298.15 K and 423.15 K at Pressures up to 45 MPa," *J. Chem. Eng. Data*, vol. 59, pp. 519–525, 2014.

[90] D. Bruggeman, *Ann. Phys.*, vol. 24, p. 636, 1935.

[91] W. P. Toray Carbon Paper 090, *https://www.fuelcellstore.com/toray-carbon-paper-090.*, 2020.

[92] I. Mostinsky, "Diffusion Coefficient," *Thermopedia*, 2011.

[93] D. A. Salvatore, D. M. Weekes, J. He, K. E. Dettelbach, Y. C. Li, T. E. Mallouk, and C. P. Berlinguette, "Electrolysis of gaseous co2 to co in a flow cell with a bipolar membrane," *ACS Energy Letters*, vol. 3, no. 1, pp. 149–154, 2017.

[94] Y. Guo, H. Yang, X. Zhou, K. Liu, C. Zhang, Z. Zhou, C. Wang, and W. Lin, "Electrocatalytic reduction of co 2 to co with 100% faradaic efficiency by using pyrolyzed zeolitic imidazolate frameworks supported on carbon nanotube networks," *Journal of Materials Chemistry A*, vol. 5, no. 47, pp. 24 867–24 873, 2017.

[95] C. Chen and G. Ma, "Proton conduction in bace1- xgdxo3- α at intermediate temperature and its application to synthesis of ammonia at atmospheric pressure," *Journal of alloys and compounds*, vol. 485, no. 1-2, pp. 69–72, 2009.

[96] D. Higgins, C. Hahn, C. Xiang, T. F. Jaramillo, and A. Z. Weber, "Gas-diffusion electrodes for carbon dioxide reduction: A new paradigm," *ACS Energy Letters*, vol. 4, no. 1, pp. 317–324, 2018.

[97] R. T. Balmer, "Modern Engineering Thermodynamics.," pp. 447–534, 2011.

[98] F. Tsuchiyaa and O. Kobayashib, "Mass Production Cost of PEM Fuel Cell by Learning Curve.," *International Journal of Hydrogen Energy*, vol. 29, no. 10, pp. 985–990, 2004.

[99] J. Armijo and C. Philibert, "Flexible Production of Hydrogen and Ammonia from Variable Solar and Wind Energy. Case Study of Chile and Argentina.," 2019.

[100] DOE, "Manufacturing Cost Analysis of 100 and 250 kW Fuel Cell Systems for Primary Power and Combined Heat and Power Applications.," 2016.

[101] N. Haegel, R. Margolis, T. Buonassisi, D. Feldman, A. Froitzheim, R. Garabedian, M. Green, S. Glunz, H. Henning, B. Holder, I. Kaizuka, B. Kroposki, K. Matsubara, S. Niki, K. Sakurai, R. Schindler, W. Tumas, E. Weber, G. Wilson, M. Wood-

house, and S. Kurtz, "Terawatt-scale photovoltaics: Trajectories and challenges.," *Science.*, vol. 356, pp. 141–143, 2017.

[102] M. Taniguchi, H. Asaoka, and T. Ayuhara, "Energy Saving Air-Separation Plant Based on Exergy Analysis.," *Kobelco Technology Review.*, vol. 33, pp. 34–38, 2015.

[103] M. Appl, "Ammonia, 1. introduction," *Ullmann's encyclopedia of industrial chemistry*, 2000.

[104] K. Zeng and D. Zhang, "Recent progress in alkaline water electrolysis for hydrogen production and applications," *Progress in Energy and Combustion Science*, vol. 36, pp. 307–326, Jun. 2010.